TECHNISCHE UNIVERSITÄT MÜNCHEN

Experimentelle Unfallchirurgie

Klinik und Poliklinik für Unfallchirurgie

des Klinikums rechts der Isar

Gender-independent miRNA expression profiles in bone homeostasis as potential cellular biomarkers and targets for osteoporosis diagnosis and treatment

Sarah Kelch

Vollständiger Abdruck der von der Fakultät für Medizin der Technischen Universität München

zur Erlangung des akademischen Grades eines Doktors der Medizin

genehmigten Dissertation.

Vorsitzende(r):   Prof. Dr. Ernst J. Rummeny

Prüfer der Dissertation:

1. apl. Prof. Dr. Dr. Martijn van Griensven

2. Prof. Dr. Marion B. Kiechle

3. Prof. Dr. Florian Bassermann

Die Dissertation wurde am 22.08.2017 bei der Technischen Universität München eingereicht und durch die Fakultät für Medizin am 02.05.2018 angenommen.

Dekan: Prof. Dr. Henningsen

Doktorvater: Prof. Dr. Dr. van Griensven

Für meine geliebte Familie.

Table of content

Abbreviations

AP	alkaline phosphatase
BMU	basic multicellular unit
BMD	bone mineral density
BMI	bone mass index
BMPR2	bone morphogenetic protein receptor type II
DALYs	disability-adjusted life years
cDNA	complementary deoxyribonucleic acid
COL1A1	collagen type I α1
DNA	deoxyribonucleic acid
dNTP(s)	deoxynucleosidetriphosphate(s)
D-MEM	Dulbecco's Modified Eagle Medium
D-PBS	Dulbecco's phosphate buffered saline
DVO	Dachverband Osteologie (German Umbrella Association for Osteology)
DXA	Dual X-ray absorptiometry
EDTA	ethylenediaminetetraacetic acid
EdU	5-ethynyl-2'-deoxyuridine
EtBr	ethidium bromide
FCS	fetal calf serum
HCC	hepatocellular carcinoma
HDL	high density lipoprotein

HEPES	4-(2-hydroxyethyl)-1-piperazineethanesulfonic acid
LNAs	locked nucleic acids
LSM	lymphocyte separation medium
MAFB	V-maf musculoaponeurotic fibrosarcoma oncogene homolog B
M-CSF	macrophage colony-stimulating factor
mRNA	messenger ribonucleic acid
MTT	3-(4,5-dimethylthiazol-2-yl)-2,5-diphenyltetrazoliumbromide
NF-κB	nuclear factor kappa-light-chain-enhancer of activated B cells
NIH	National Institutes of Health
NSE	neuron-specific enolase
OPG	osteoprotegerin
PBMC(s)	peripheral blood mononuclear cell(s)
pre-miRNAs	precursor miRNAs
pri-miRNAs	primary miRNAs
PTH	parathyroid hormone
qCT	quantitative computed tomography
RANK	receptor activator of nuclear factor κB
RANKL	receptor activator of nuclear factor κB ligand
RT-PCR	reverse transcription polymerase chain reaction
RISC	RNA induced silencing complex

RNA	ribonucleic acid
RUNX2	runt-related transcription factor II
SEM	standard error of the mean
SERM	selective estrogen receptor modulators
SVR	sustained viral response
Tcf-1	T-cell factor 1
TNF	tumor necrosis factor
TRAP	tartrate resistant acid phosphatase
3' UTR	3' untranslated region
Wnt	wingless type

1 Introduction

1.1 Bone homeostasis

Continuous bone formation and degradation reflect a bone remodeling balance, where bone-building anabolic activities of osteoblasts and bone-degrading catabolic activities of osteoclasts constitute the smallest functional unit. This unit is also known as the basic multicellular unit (BMU). Due to a dynamic balance in composition and depletion processes performed by paracrine signaling-coupled osteoblast and osteoclast cells, increased bone strength and decreased fracture susceptibility result. In cases of osteoporosis, the imbalance can also go in the other direction. Any disturbance of this bone cell remodeling interactions that exceeds osteoclastogenesis causes the disease pattern of osteoporosis, which is characterized by a reduction in bone mass and degradation in micro-architecture. The intercellular exchange of information in this case is generally mediated through mechanical signal transduction into chemical signals leading to controlling the release of numerous biological growth factors and hormones (Jilka 2003).

1.2 Transcriptional regulation of bone homeostasis

The amount of bone formation is determined by the celerity and efficiency of mesenchymal progenitor cells forming mature osteoblast cells. Mesenchymal progenitor cells primarily differentiate into pre-osteoblasts, before further differentiation into mature osteoblasts and osteocytes. The responsibility of osteoblasts is the production of collagen I, osteocalcin, osteonectin and bone mineralization with hydroxyapatite.

In turn, osteoblasts are controlled by reduced apoptosis via parathyroid hormone (PTH) and PTH-related proteins with anabolic consequences (Jilka, Weinstein et al. 1999, Lippuner 2012).

Osteocytes, conclusively differentiated osteoblast cells, are embedded in the bone matrix and are no longer capable of cell division. These cells have thin fibers and communicate among each other via small canaliculi. Their skills lie in the preservation of the bone matrix and calcium homeostasis by recording and converting mechanical stress into biological signals for an intercellular communication between osteoblasts and osteoclasts (Papachroni, Karatzas et al. 2009, Jing, Hao et al. 2015) (Figure 1).
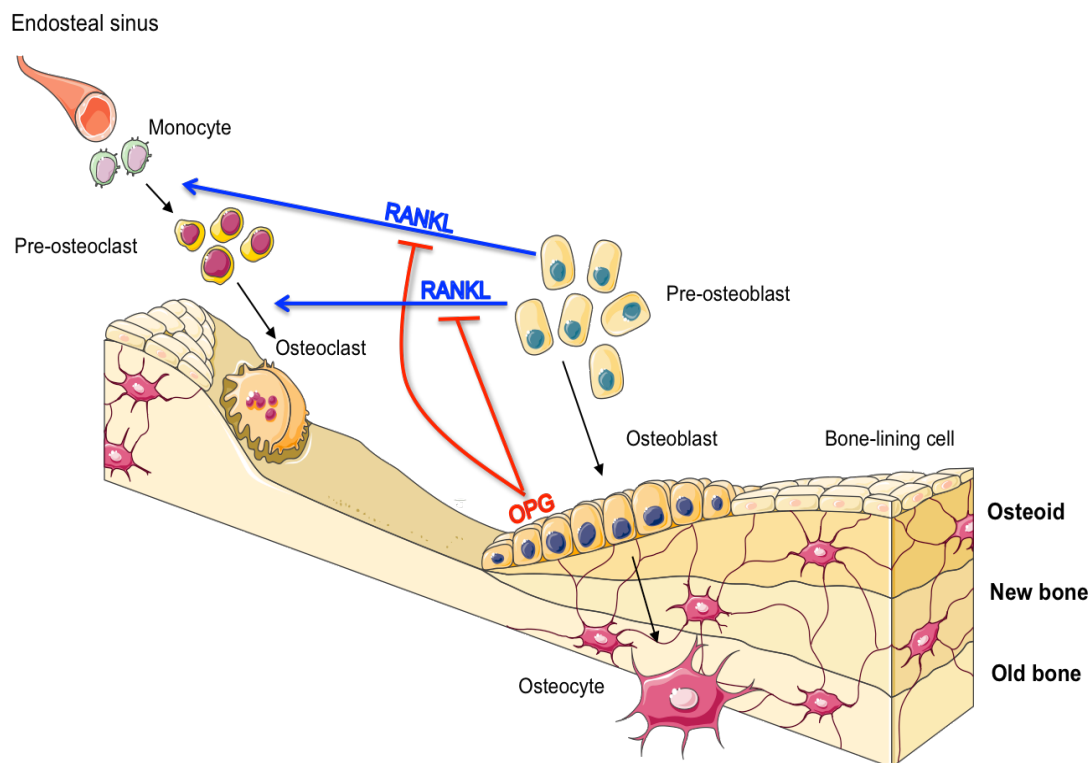
Figure 1 Schematic structure of bone homeostasis. Individual cells that are embedded in the bone matrix. Osteoblast and osteoclast cells inferentially regulate their activity intracellularly by alternate gene expressions. RANKL=receptor activator of nuclear factor κB ligand, distributed by precursor osteoblasts, stimulates the differentiation of osteoclasts. Mature osteoblasts in turn influence the differentiation of hematopoietic precursors into active osteoclasts by OPG=osteoprotegerin. *Designed elements were adapted from Servier Medical Art.*

By comparison, counter-regulating multinucleated osteoclasts are derived from hematopoietic stem cells through the consolidation of the monocyte/macrophage lineage. Monocytes merge to prokaryotic cells after initiation through osteoclast stimuli. The continuing osteoclast cell differentiation thereby depends on the presence of two specific growth factors: receptor activator of nuclear factor κB ligand (RANKL) and macrophage colony-stimulating factor (M-CSF). RANKL and its antagonist osteoprotegerin (OPG) itself are generated by osteoblasts, demonstrating an intercellular differentiation control (Figure 1). M-CSF is essential for the survival of osteoclasts, the precursors' cell migration and osteoclast proliferation. RANKL on the other hand initiates the ensuing differentiation steps. Creating an acidic milieu and releasing proteolytic enzymes, osteoclasts further degrade organic and inorganic bone substance (Lorenzo, Horowitz et al. 2008). In addition to the transcription factors already mentioned above, there are a number of other factors and key signaling pathways that play an essential role in bone homeostasis, such as the bone morphogenic protein (BMP), Notch- and Wnt-signaling pathway (Boyle, Simonet et al. 2003, Jing, Hao et al. 2015).

1.3 Osteoporosis

1.3.1 Definition

The enormous increase in the worldwide prevalence of osteoporosis over the past years has transduced this disease of the osseous system into a major public health disconcertment of the 21st century, whereas the definition of osteoporosis has constantly changed over decades. Before 1994, osteoporosis was referred as a syndrome with a slightly increased risk of fracture in the elderly population. The World Health Organization (WHO) introduced a definition that was based on a bone density test. After this time point, a bone mineral density measurement of more than or equal to two and one-half standard deviations compared to a reference group of thirty years old women confirmed the presence of osteoporosis

(World Health Organization: WHO scientific group on the assessment of osteoporosis at primary health care level. Summary Meeting report. Brussels , Horvath 2016). In 2000, the National Institutes of Health (NIH) Consensus Conference specified osteoporosis as a skeletal disorder designated by impaired bone strength as well as extended risk of fractures (Statement 2000). Nowadays, more than 200 million people worldwide are affected by osteoporosis, whereupon the WHO designated this condition as a silent epidemic with more than 8.9 million fractures per year (Johnell and Kanis 2006). For osteoporotic fractures, medical sociological estimates evaluated about 2.8 million disability-adjusted life years (DALYs) in America and Europe, which is astonishingly more than for hypertension and rheumatoid arthritis (The world health report 2004: changing history. Geneva , World Health Organization: WHO scientific group on the assessment of osteoporosis at primary health care level. Summary Meeting report. Brussels). By the year 2050, experts even consider an increase of hip fractures in men up to 310% and in women up to 240%, referenced to the year 1990 (Gullberg, Johnell et al. 1997).

1.3.2 Classification

Generally, there are two forms of osteoporosis: the primary form and the secondary form. The primary form includes senile osteoporosis, postmenopausal osteoporosis and idiopathic osteoporosis at a younger age. Secondary forms are caused by a long-term systemic therapy of glucocorticoids, proton pump inhibitors, antiepileptic drugs, aromatase inhibitors, immobilization and endocrine disorders such as hypercortisolism, hypogonadism, eating disorders as well as cadmium intoxications. Another additional classification exists based on the division in a high-turnover osteoporosis with increased bone resorption rates and a low-turnover osteoporosis with a generally decreased bone metabolism both resulting in an increased loss of bone (Behmann, Semler et al. 2008, Horvath 2016).

1.3.3 Diagnosis

As mentioned before, osteoporosis is radiologically determined by bone density measurements, called dual X-ray absorptiometry (DXA) or osteodensitometry, measuring the bone areal density in g/cm^2. In order to compare different measurement methods, the deviation of the age-corresponding end standard is used, which is represented by the T-value. In this way, osteopenia refers to a T-score between -1 and 2, representing a significant and facultative preliminary stage of osteoporosis. A T-score of -2.5 or below defines a diagnosis of osteoporosis. Examples are T-scores of -2.7, -3.5 and -3.9. Alternative measurement methods are represented by the quantitative computed tomography (qCT), quantifying the real physical density in g/cm^3. This method constitutes as inconvenient for patient health due to high doses of radiation. Also, quantitative ultrasound represents a way of bone densitometry procedures without finding a broad clinical application (Behmann, Semler et al. 2008, Philipot, Guerit et al. 2014, Horvath 2016).

1.3.4 Current therapy and side effects

Due to consequent disastrously pathological effects of osteoporosis, special attention should be called to the prevention of the disease and associated fractures to maintain the physical health, quality of life and independence in the elderly population. Because fracture prevention remains a challenge, most therapeutic substances reside in evolution. Ranges of presently available drug options fall into an anti-catabolic drug class and an anabolic drug class (Kim, Kim et al. 2002, Philipot, Guerit et al. 2014). A 10-year fracture risk of 30% formally indicates the initiation of a drug therapy in primary osteoporosis. Therefore, the 'Dachverband Osteologie' (German Umbrella Association for Osteology - DVO) guidelines recommend a drug administration scheme oriented to the T-value, age and gender, whereby certain risk factors indicate a precautious treatment already at T-values 0.5-1.0 higher than the normal limits (Philipot, Guerit et al. 2014). This means, for example, for a woman suffering from diabetes mellitus type 1 that the therapy

regime should start at a T-value of -3 rather than -4. In contrast, if this patient has a heart failure or a singular vertebral fracture 1st grade, therapy should start at a T-value of -3.5. Next to the prevention by nicotine and alcohol waiver, Vitamin D and calcium prophylaxis have a preventive character for osteoporotic fractures and are of high priority in each treatment protocol (Bhutani and Gupta 2013, Philipot, Guerit et al. 2014).

The medical gold standard includes preparations of the class of bisphosphonates such as alendronate. By inhibiting osteoclasts, these drugs work anti-catabolic and demonstrably reduce vertebral fractures. Estrogens may be administered only under careful individual consideration. In order to reduce cardiovascular side effects, estrogens are usually prescribed in combination with gestagenes. Raloxifene, a selective estrogen receptor modulator (SERM) approved for osteoporotic therapy, has a similar estrogen inhibitory effect on bone resorption and provides an alternative therapeutic option. Its selective agonistic and antagonistic effects on estrogen-sensitive tissues reduces bone resorption as well as renal calcium losses, which in turn leads to a positive calcium balance without effecting the female breast and endometrium (Rey, Cervino et al. 2009). Other anabolic medications include strontium ranelate, enhancing bone formation and inhibiting bone resorption by incorporation of strontium in the skeleton as well as parathyroid hormone analogs such as teriparatide, leading to an increase in calcium absorption, phosphate excretion in the kidneys and vitamin D3 synthesis. Additional medications include fluorides (stimulating osteoblasts), calcitonin (exerting antiresorptive effects on osteoclasts) and a monoclonal antibody called denosumab (directing against RANKL) (Bhutani and Gupta 2013).

However, since there are studies showing that current clinical used hormone therapy may result in increased breast-, ovary- and endometrium-cancer and the main osteoclast-inhibiting bisphosphonates causing accreted esophageal and gastrointestinal cancer as well as osteonecrosis, there is an urgent requirement to develop new potential treatment options for the further improvement of bone microarchitecture in order to avoid side-effects and limited efficacy (Kuehn 2009, Morrow, Deyhim et al. 2009). Comparing all treatment options, anabolic

substances are limited and hence the need for bone activating matters for the reconstruction of quantitative and qualitative healthy bone is eminently large.

1.4 miRNAs

1.4.1 Role in bone homeostasis

The discovery that miRNAs are not only extracellular circulating molecules, but are also intracellular players in many biological processes, has put them into the spotlight as possible biological markers for osteoporosis, osteoarthritis and skeletal dysplasia (Iliopoulos, Malizos et al. 2008, de Pontual, Yao et al. 2011, Seeliger, Balmayor et al. 2016). Among the mentioned regulatory factors that may affect the differentiation direction of mesenchymal stem cells in osteoblasts and monocyte cell lines in osteoclasts, miRNAs play a crucial role in various stages of cell differentiation, metabolism and apoptosis. In the recent past, several miRNAs have been identified that either induce or reduce the bone remodeling activity and its cohesive cells on a post-transcriptional level, offering new insights into bone pathophysiology and opening a gateway for future diagnostic and therapeutic options (Seeliger, Balmayor et al. 2016).

1.4.2 Biogenesis

miRNAs are 22 base pair-long single-stranded noncoding RNAs that regulate gene expression at a post-transcriptional level through a complementary binding and translation inhibition or even degradation of the miRNA. Following the transcription by a RNA polymerase II in the first step, the primary miRNAs (pri-miRNAs) are formed in the cell nucleus. The length of these pri-miRNAs extends to several kilobases, whereby the morphology comprises a 5' Cap structure and a poly-A tail. In the second intra-nuclear proceeding step, a protein complex containing RNase III-like endonuclease Drosha and DGCR8/Pasha splits the hairpin structure at its base. In the nucleus, generated precursor miRNAs (pre-

miRNAs) constitute typical hairpin structures and contain 70 nucleotides. Pre-miRNAs are afterwards funneled by exportin-5 in the cytoplasm, where the conversion of pre-miRNAs into the mature form takes place due to the impact of the essential enzyme Dicer, a ribonuclease III. The so emerged mature miRNAs finally bind the RNA-induced silencing complex (RISC) containing Argonaute proteins for further 3'-untranslated region (3'-UTR) binding and translational expression inhibition (Han, Lee et al. 2004, Papagiannakopoulos and Kosik 2008) (Figure 2).
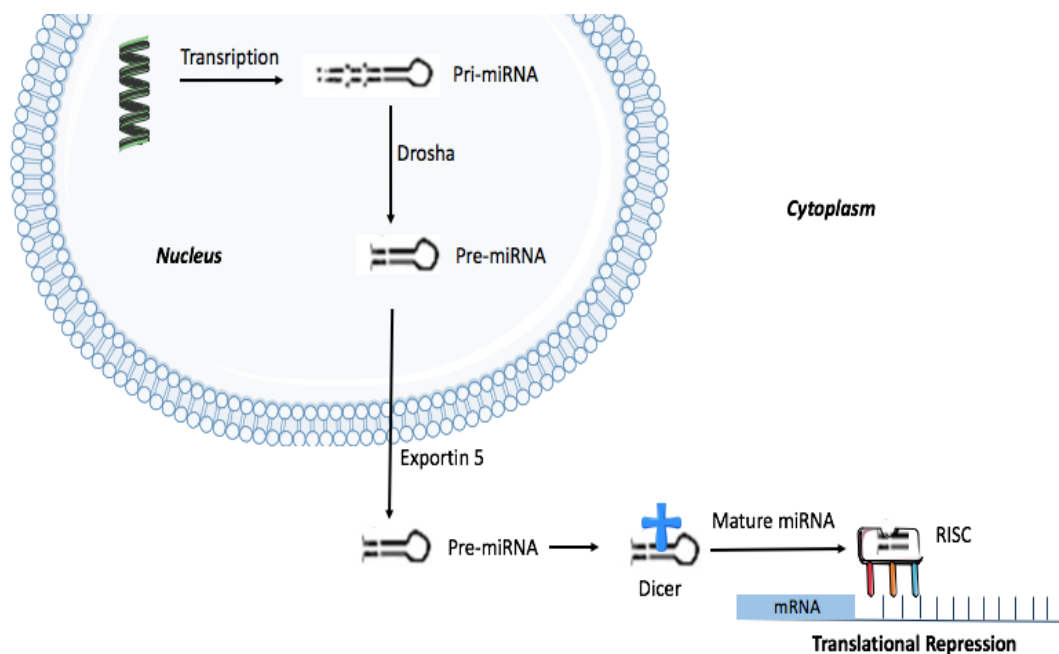
Figure 1 miRNA Biogenesis. After transcription, primary miRNAs (pri-miRNA) get processed by RNAse III Drosha to precursor miRNAs (pre-miRNAs). pre-miRNAs form typical hairpin structures and get funneled by exportin-5 into the cytoplasm. There, the conversion of pre-miRNAs into the mature form by a Dicer, a ribonuclease III is taking place. The mature miRNA ties the RNA inducing silencing complex (RISC) to bind the 3'-untranslated region (3'-UTR). *Designed elements were adapted from Servier Medical Art.*

In order to explore the importance of miRNAs, mouse experiments were conducted with a targeted deletion of the enzyme Dicer, leading to a consequently global mature miRNA deletion. Due to this deletion, mouse embryonic death and

a shortening of the limbs were observed (Harfe, McManus et al. 2005). Also, in osteoblasts of mice at an embryonal and neonatal stage, retarded bone development was observed due to the absence of this enzyme and consequently absent miRNA. Dicer deletion in osteoblasts of adult mice, in contrast, improved the bone development after 2 months observation, so that it can be estimated that miRNAs exert different effects on early and late development stages (Gaur, Hussain et al. 2010). Dicer deletion in osteoclasts, however, resulted in a cell reduction and a loss of function (Sugatani and Hruska 2009).

1.4.3 Circulating miRNAs as biomarkers

Altered miRNA expression is demonstrably associated with different diseases such as tumor diseases, cardiovascular diseases, infectious diseases and bone disorders (Kobayashi, Hornicek et al. 2012, van Rooij and Olson 2012, Janssen, Reesink et al. 2013, Moore and Xiao 2013). A number of studies has proven that donor cells are able to transmit miRNAs due to exocytic vesicles, apoptotic bodies or protein-high density lipoprotein (HDL)-binding complexes into the cytoplasm of receiving cells to regulate their expression of genes. Through these diverse transport mechanisms, miRNAs are detectable in serum, plasma, cells and tissues. miRNAs, that so to say circulate in any body fluid, thus provide a new class of suitable molecules for diagnosis (Moldovan, Batte et al. 2013, Rayner and Hennessy 2013). Stammet et al. for instance validated miRNA levels and neuron-specific enolase (NSE) in blood samples of patients at 48 hours after a cardiac arrest. In patients with poor neurological outcome, increased serum expression values of miR-21 and miR-122 were detected.

Also in an *in vitro* cell culture experiment, an increased expression could be detected in neural cells. Compared with the diagnostic marker NSE, miR-21 and miR-122 demonstrably represent two significant biomarkers for evaluating the neurological status and mortality after cardiac arrest (Stammet, Goretti et al. 2012). Another study examined the prognostic relevance of miRNAs as biomarkers for diseases concerning hepatocellular carcinoma (HCC). Köberle et

al. explored that miR-1 serum levels are significantly associated with prolonged survival in patients with HCC (Koberle, Kronenberger et al. 2013).

It is known from studies that the detection of miRNAs in plasma and serum can be reflected under physiological conditions and under pathological processes (Garzon, Calin et al. 2009, Xu, Dong et al. 2010). Findings of Farid et al. deliver decreased miR-148a serum levels as a sensitive marker of liver injury (Farid, Pan et al. 2012). In this sense, our research group published results about the identification of specific osteoporosis-associated circulating miRNAs in the serum of osteoporotic patients with femoral neck fractures and identified the miRNAs miR-21, miR-23a, miR-24, miR-93, miR-100, miR-122a, miR-124a, miR-125b and miR-148a as specificly upregulated (Seeliger, Karpinski et al. 2014). Various other studies displayed that miRNAs may also play a key role in osteoblast proliferation and differentiation (Guo, Ren et al. 2012, Hassan, Maeda et al. 2012, Seeliger, Karpinski et al. 2014).

Regarding osteoclastogenesis, for example the study of Mizoguchi et al. described an upregulation of miR-31 in osteoclasts under RANKL stimulation, controlling osteoclast formation and function (Mizoguchi, Murakami et al. 2013). Some authors additionally wrote about miR-155, miR-223, miR-503 and miR-637 regulating influences in osteoclastogenesis (Zhang, Zhao et al. 2012, Chen, Cheng et al. 2014, Xie, Zhang et al. 2015).

For diagnosis based on circulating miRNAs, it is yet not known whether they are gender-, age- and ethnicity-dependent or how many miRNAs are needed for a sufficient diagnosis. As in the study by Stammet et al., who put the miR-21 and miR-122 expression in relation to the NSE, a similar relation to BMD should be created for exploring the suitability of miRNAs as circulating biomarkers for osteoporosis. These mentioned facts and hypotheses were foundations of my thesis, in which we explored these mentioned miRNAs to their biomarker adequacy in relation to BMD and gender. In addition, it was the target to investigate the expression origin *in vitro* in bone tissue as well as intracellularly both in osteoblasts and osteoclasts (Figure 3).

1.4.4 miRNA targeting therapy

Various *in vitro* and *in vivo* animal models proved that miRNAs or their base-complementary counterpart can be used for therapeutic purposes. Generally, miRNA mimics increase the expression of miRNA, whereas antagomiRs, containing chemically engineered antisense oligonucleotides, reduce the expression of miRNAs by complementary strand blocking. According to the fact that miRNAs inhibit translation, the use of miRNA mimics results in a downregulation of messenger ribonucleic acid (mRNA), whereas the use of antagomiRs results in a mRNA upregulation. Both manipulations effect the cell phenotype of recipient cells (Krutzfeldt, Rajewsky et al. 2005, Czech 2006). In an *in vivo* mouse model, Krutzfeldt et al. for example injected antagomiRs against the miRNAs miR-16, miR-122, miR-192 and miR-194 via an intravenous line and could evidence an efficient, specific and lasting systemic miRNA silencing (Krutzfeldt, Rajewsky et al. 2005). An interesting study by Lee et al. observed increased miR-203 values in the hippocampus of mice suffering from epileptic convulsions. *In vitro* transfection with antagomiR-203 demonstrated the direct inhibition of the glycine receptor-β. The intranasal agent application with the antagomiR drug AM203 against miR-203 was studied in a clinical trial, showing a significant successful seizure reduction (Lee, Jeon et al. 2016).

To ensure stability, specificity, transmission capacity and repeatability, a variety of transfection methods based on chemical or physical methods exist to assure an applicable miRNA delivery system for cell cytoplasm transfection. Physical processes use e.g. electrically based transfection protocols while using antisense DNA oligomers containing Locked Nucleic Acids (LNAs) (Chabot, Orio et al. 2012). Another variant offers the Helios gene gun system of Bio-Rad (Hercules, CA), in which RNA-covered gold particles penetrate into the cytoplasm due to high modem speed (Aravindaram, Yin et al. 2013). Facing these physical methods, Dai et al. availed a vector-based plasmid-enclosed cationic liposome method to examine the anti-colon cancer properties of miR-15a and miR-16-1 mimics *in vivo* (Dai, Wang et al. 2012). Other methods are based on

nanospherical, exosomal and liposomal transfection (Cheng and Saltzman 2012, Moldovan, Batte et al. 2013).

The possibility to use miRNA-targeting therapy for gene enhancement in eukaryotic systems has become a current and popular subject of the miRNA research in recent years. The representative sector of anticancer research comprises various studies concentrating on antagomiR application. As a first example, Ge et al. modulated the gene FOXO3a by targeting miR-27a with an antagomiR-27a in human glioblastoma cells *in vitro* and demonstrated a significantly repressed tumor growth in mice *in vivo* (Ge, Sun et al. 2013). Ma et al. were able to demonstrate a reduced formation of lung metastases in breast cancer with a significant expression decrease of the gene Hoxd10 through the use of antagomiR-10b both *in vitro* and *in vivo* (Ma, Reinhardt et al. 2010). The group of Care et al. likewise treated mice with an antagomiR-133, leading to cardiac growth and the group of Engelhardt et al. displayed a decreased remodeling in cardiac fibrosis (Care, Catalucci et al. 2007, Thum, Gross et al. 2008). Mercatelli et al. as a final example, achieved reduced prostate cancer growth by antagomir-221/222 modulation of the gene P27 (Mercatelli, Coppola et al. 2008).

From the use of therapeutic antagomiR agents *in vitro*, it is a big step up for *in vivo* research. In this case, the liver research holds a big lead. miR-122, that represents a virus host factor for chronic hepatitis C (HCV), therefore provides a central point of attack for a targeted antagomiR therapy. At the International Liver Congress in Barcelona earlier this year, the latest results of the clinical Phase II study of a miR-122 antisense targeting therapeutic agent called RG-101 (Santaris Pharma, Copenhagen, Denmark) in chronic hepatitis C were presented, displaying the first effective clinical application example of RNA-targeted therapy. Santaris, as the only company worldwide, has the exclusive rights for the therapeutic application of the LNA technology. Since RNA-based therapeutics have a low degree of affinity and stability, the LNA technology provides a modified variant by introducing a ribose ring for a molecule stabilization against the influence of circulating nucleases as well as for an efficient analog binding capacity . RG-101, was given at a dose of 2 mg per kg for 4 weeks along with antiviral drugs. The

treatment response was measured by sustained viral response (SVR), which was achieved in the current study in 97% of patients and so far was only possible through the use of interferons.

According to studies, antagomiR agents directed against endogenous miRNA specific to bone, might selectively permit accelerated osteoblast differentiation and increased bone formation rate (van Rooij and Olson 2012). With the knowledge of all mentioned study results, our hypothesis was that overexpressed miRNAs in osteoporotic patients will offer suitable targets for miRNA-targeted therapy. Therefore, in the second part of this research work, we used a specific antagomiR sequence against the overexpressed miR-100 signature in osteoblast cells of osteoporotic patients based on a lipotransfection system to detect any influences on the osteogenic differentiation by miRNA silencing (Figure 3). At this stage, the role of miR-148a in the osteogenic differentiation is not fully explored. Since all encountered publications did not examine regulatory effects of miR-148a on the differentiation of human bone-building osteoblast and based on our results that miR-148a was indicated to be up-regulated in studies mentioned above, the thesis was additionally designed to explore the intracellular influence of miR-148a inhibition in the context of the clinical picture of osteoporosis.

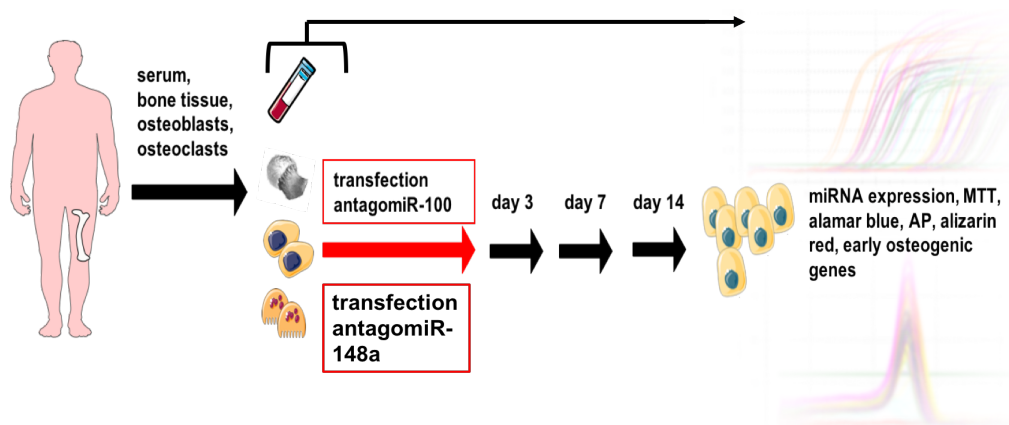**Figure 2** Illustrated overview of the experimental study procedure. miRNA and mRNA isolation from serum, bone tissue and cells. Due to a significant miR-100 and miR-148a overexpression, osteoblasts were transfected with antagomiR-100 as well as antagomiR-148a. Osteogenic gene expression changes were detected over 14-day cell culture (AP = alkaline phosphatase). *Designed elements were adapted from Servier Medical Art.*

2 Material and Methods

2.1 Material

2.1.1 Cell culture

Material	Type	Company
Machines	Bone Mill - Mixer Mill MM 400	Retsch, Haan, Germany
	Centrifuge	Eppendorf, Hamburg, Germany
	Cell counter	Eppendorf, Hamburg, Germany
	Incubator HERAcell 150	Taylor-Wharton, Theodore, Germany
	Lab bench, MSC Advantage	BioRad, Munich, Germany
	Nitrogen tank LS 3000	Taylor-Wharton, Theodore, Germany
	q-CT	Philips iCT, Austin, TX, USA
Materials	Cell scraper, 20 mm	Sarstedt, Nümbrecht, Germany
	Counting chamber	Carl Roth GmbH&CO. KG, Karlsruhe, Germany
	Culture flasks 175 cm^2	Sarstedt, Nümbrecht, Germany
	Forceps	Sklarcorp, West Chester, USA
	Monovette-S® Serum 7.5 ml, EDTA K$_3$ 9 ml	Sarstedt, Nümbrecht, Germany
	Multiwell-plates	PAA GmbH, Pasching, Austria
	Petri dishes 100 mm ∅	PAA GmbH, Pasching, Austria

	Pipettes + pipette tips	Sarstedt, Nümbrecht, Germany
	Polypropyl falcon tubes 50 ml	Sarstedt, Nümbrecht, Germany
	Sterile scalpel	Sklarcorp, West Chester, USA
	Stille-Luer bone rongeur	Sklarcorp, West Chester, USA
	Syringe 20 ml	B. Braun, Melsungen, Germany
	Syringe filter 0.2 μm	Sartorius Biotech, Göttingen, Germany
	Transmitted light microscope Axiovert 40C	Zeiss, Oberkochen, Germany
	Tubes 2 ml, 1.5 ml	Eppendorf, Hamburg, Germany
Basal media	D-MEM low glucose with L-Glutamine	Sigma-Aldrich, Munich, Germany
Supplemental	All protect	Qiagen, Hilden, Germany
	AntagomiR-100	Qiagen, Hilden, Germany
	β-glycerol phosphate	Sigma-Aldrich, Munich, Germany
	CaCl	Roth, Karlsruhe, Germany
	Dexamethasone 100nM	Roth, Karlsruhe, Germany
	EDTA	PAA GmbH, Pasching, Austria
	FCS	Sigma-Aldrich, Munich, Germany
	HEPES	Sigma-Aldrich, Munich, Germany
	HIPerfect HTS Reagent	Qiagen, Hilden, Germany
	L-ascorbate-2-phosphate	Sigma-Aldrich, Munich, Germany
	M-CSF	PeproTech, Hamburg, Germany
	Penicillin/ Streptomycin	Sigma-Aldrich, Munich, Germany
	RANKL	PeproTech, Hamburg, Germany
	Negative Control siRNA	Qiagen, Hilden, Germany

	Trypsin	PAA GmbH, Pasching, Austria
Solutions	DMSO	Sigma-Aldrich, Munich, Germany
	D-PBS	Sigma-Aldrich, Munich, Germany
	LSM-1077	Biowest, Nuaillé, France
	Tri Reagent	Sigma-Aldrich, Munich, Germany
	Trypan Blue 0.5%	Biochrom, Berlin, Germany

2.1.2 miRNA isolation, transcription and quantitative RT-PCR

2.1.2.1 Material for miRNA isolation

Material	Type	Company
Machines	INTAS Gel iX20 Doc System	Intas, Göttingen, Germany
	HellmaTrayCell Photometer	Eppendorf, Hamburg, Germany
	Mastercycler® pro	Eppendorf, Hamburg, Germany
Solutions	Aqua delta select	Roth, Karlsruhe, Germany
	Agarose gel 1.5%	Sigma-Aldrich, Munich, Germany
	Boric Acid	Roth, Karlsruhe, Germany
	Bromophenol blue	Roth, Karlsruhe, Germany
	Chloroform	Roth, Karlsruhe, Germany
	Ethanol 100%	Roth, Karlsruhe, Germany
	Glycerol	Sigma-Aldrich, Munich, Germany

	Isopropanol	Roth, Karlsruhe, Deutschland
	miRNAeasy Serum/Plasma Kit	Qiagen, Hilden, Germany
	NaOH solution	Roth, Karlsruhe, Germany
	pUC 19 marker	Roth, Karlsruhe, Germany
	QIAzol Lysis Reagent	Qiagen, Hilden, Germany
	RNeasy MinElute spin columns	Qiagen, Hilden, Germany
	Spike-In Control dilution	Qiagen, Hilden, Germany
	TriReagent	Sigma-Aldrich, Munich, Germany
	TRIS aminomethane	Roth, Karlsruhe, Germany
	Ultra-pure RNAse-free water	Qiagen, Hilden, Germany

2.1.2.2 Material for transcription and quantitative RT-PCR to evaluate miRNA expressions

Material	Type	Company
Machines	Bio-Rad CFX Manager	BioRad, Munich, Germany
	Mastercycler® pro	Eppendorf, Hamburg, Germany
	Q-PCR CFX 96 Touch	BioRad, Munich, Germany
Solutions	Deoxynucleotide triphosphates	Qiagen, Hilden, Germany
	Deoxynucleotide triphosphates	Fermentas, St. Leon-Rot, Germany
	First Strand cDNA Synthesis Kit	Fermentas, St. Leon-Rot, Germany
	HiSpec Buffer	Qiagen, Hilden, Germany
	miScript SYBR Green PCR Kit	Qiagen, Hilden, Germany

miScript II RT Kit	Qiagen, Hilden, Germany
Oligo (dT)18 Primer	Fermentas, St. Leon-Rot, Germany
PCR 96-well plates	BioRad, Munich, Germany
Random Hexamer	Fermentas, St. Leon-Rot, Germany
Reverse transcriptase	Qiagen, Hilden, Germany
Reverse transcriptase	Fermentas, St. Leon-Rot, Germany
SsoFast EvaGreen	BioRad, Munich, Deutschland
Transcription tubes 0.2 ml	Eppendorf, Hamburg, Germany

2.1.2.3 Material for quantitative RT-PCR to evaluate miRNA expressions

Target gene	Forward Primer	Accession No.	Company
miR-21	5´- UAGCUUAUCAGACUGAUGUUGA - 3´	MS00009079	Qiagen, Hilden, Germany
miR-23a	5´- AUCACAUUGCCAGGGAUUUCC -3´	MS00031633	Qiagen, Hilden, Germany
miR-24	5´- UGGCUCAGUUCAGCAGGAACAG -3´	MS00006552	Qiagen, Hilden, Germany
miR-93	5- CAAAGUGCUGUUCGUGCAGGUAG -3´	MS00003346	Qiagen, Hilden, Germany
miR-100	5´- AACCCGUAGAUCCGAACUUGUG - 3´	MS00003388	Qiagen, Hilden, Germany
miR-122	5´- UGGAGUGUGACAAUGGUGUUUG -3´	MS00003416	Qiagen, Hilden, Germany
miR-124	5´- UAAGGCACGCGGUGAAUGCC -3´	MS00006622	Qiagen, Hilden, Germany
miR-125	5- UCCCUGAGACCCUAACUUGUGA -3´	MS00006629	Qiagen, Hilden, Germany
miR-148a	5- UCAGUGCACUACAGAACUUUGU -3´	MS00003556	Qiagen, Hilden, Germany
Snord-96	5- UAGCUUAUCAGACUGAUGUUGA -3´	MS00033733	Qiagen, Hilden, Germany

2.1.2.4 Material for quantitative RT-PCR to evaluate early gene expressions

Target gene Acc. No.	Forward Primer	Reversed Primer	Company
AP NM_001204.6	5´- UAGCUUAUCAGACUGAUGUUGA - 3´	5´- AACCCGUAGAUCCGAACUUG UG - 3´	Qiagen, Hilden, Germany
BMPR2 NM_001204.6	5´- AUCACAUUGCCAGGGAUUUCC -3´	5´- AACCCGUAGAUCCGAACUUG UG - 3´	Qiagen, Hilden, Germany
COL1A1 NM_000088.3	5´- UGGCUCAGUUCAGCAGGAACAG -3´	5´- AACCCGUAGAUCCGAACUUG UG - 3´	Qiagen, Hilden, Germany
RUNX2 NM_004348	5- CAAAGUGCUGUUCGUGCAGGUAG -3´	5´- AACCCGUAGAUCCGAACUUG UG - 3´	Qiagen, Hilden, Germany
β-Tubulin NM_001069.2	5´- AACCCGUAGAUCCGAACUUGUG - 3´	5´- AACCCGUAGAUCCGAACUUG UG - 3´	Qiagen, Hilden, Germany

2.1.3 Activity assay, viability assay and staining

Material	Type	Company
Machines	FLUOstar Omega	BMG labtech, Ortenberg, Germany
	Fluorescence microscope BZ-9000	Keyence, Osaka, Japan
Solutions	Triton-X-100	Merck, Darmstadt, Germany
	Acetic acid	Roth, Karlsruhe, Germany
	Alamar Blue reagent	Biozol, Eching, Germany
	Alizarin RedS Sigma	Sigma-Aldrich, Munich, Germany
	Dimethylformamide	Merck, Darmstadt, Germany

DMSO	Roth, Karlsruhe, Germany
Double distilled water	Sigma-Aldrich, Munich, Germany
Ethanol 96%	Sigma-Aldrich, Munich, Germany
Fast Blue B Salt	Sigma-Aldrich, Munich, Germany
Fast Red Violet LB Salt	Sigma-Aldrich, Munich, Germany
Formaldehyde solution 37%	Roth, Karlsruhe, Germany
Glycine	Sigma-Aldrich, Munich, Germany
Hexadecylpyridiniumchloride	Sigma-Aldrich, Munich, Germany
HCl	Roth, Karlsruhe, Germany
MgCl2	Sigma-Aldrich, Munich, Germany
NaOH	Roth, Karlsruhe, Germany
Naphtol-AS-MX-Phosphate	Sigma-Aldrich, Munich, Germany
4-Nitrophenyl phosphate di-sodium salt hexahydrate	Sigma-Aldrich, Munich, Germany
4-Nitrophenol solution 10mM	Sigma-Aldrich, Munich, Germany
pH indicator paper litmus	Macherey-Nagel, Düren, Germany
SDS	Roth, Karlsruhe, Germany
Sodium acetate	Sigma-Aldrich, Munich, Germany
Sodium tartrate dibasic dihydrate	Sigma-Aldrich, Munich, Germany
Sodium phosphate	Sigma-Aldrich, Munich, Germany
Thiazolylblue	Roth, Karlsruhe, Germany

Tris-Base		Sigma-Aldrich, Munich, Germany

2.1.4 Software

Material	Type	Company
Statistical Software	GraphPadPrism 6.0	GraphPad Software La Jolla, USA
Literature Software	EndNote X6	Thomas Reuters, San Francisco

2.2   Methods

2.2.1 Sample collection

After a positive approval from the ethical committee of the hospital Klinikum rechts der Isar, Technical University of Munich and in equivalence to the declaration of Helsinki, patient consent was obtained prior collecting bone tissue, femoral heads and blood samples of osteoporotic and non-osteoporotic patients. The inclusion criteria included female and male patients who have reached the age of 18, patients with a hip or shoulder fracture requiring the indication for prosthesis and osteoporosis diagnosis. Patients enrolled in this study were primarily accurately classified by clinical, radiographic examinations into the osteoporotic and non-osteoporotic collective. DXA measurements with T-values of 1 and above were rated as healthy, T-values between -1 and -2.5 were rated as osteopenia and T-values of -2.5 and below were rated as osteoporosis. Radiological assessment was performed by inspection of radiographs. Admitted non-osteoporotic patients underwent total hip replacement surgery due to coxarthrosis Kellgren-Lawrence grade 3 and 4. There was no osteoarthritis in healthy patients with coxarthrosis. Admitted osteoporotic patients underwent total hip replacement surgery due to hip fractures (type AO 31-A/B) based on osteoporosis disease. The selected patients were treated in the Department of Trauma Surgery of the university hospital Klinikum rechts der Isar. Afterwards, femoral heads, which were obtained during hip replacement surgery, were evaluated via q-CT bone density measurements (Philips iCT, Best, The Netherlands and Mindways calibration phantom and software, Austin, TX, USA) into non-osteoporotic, osteopenic and osteoporotic groups. The advantage of this measurement was that volumetric BMD values could be obtained. A BMD value of $\geq 120 \text{g/cm}^3$ was considered normal, a BMD value between 80 and 120 was considered osteopenia and a BMD value of $\leq 80 \text{g/cm}^3$ was considered osteoporotic, suggested by the International Society for Clinical Densitometry (ISCD) and by the American College of Radiology (ACR) (Engelke, Adams et al.

2008, Ma, Zhang et al. 2015). Blood was collected at least 2 hours after fracture from osteoporotic patients and after operation from non-osteoporotic patients. We determined malignancy, inflammation, benign ovarian cysts except endometrioma, known chronic, systemic, metabolic and endocrine disease including polycystic ovarian syndrome, chronic liver disease, viral hepatitis, HIV infection, hormone therapy as well as vitamin D medication in the previous three months and any medical history of other inflammatory or infectious diseases as relevant criteria for exclusion. Further exclusion criteria were patients who have not yet reached the age of 18, patients who are incapable of consent, patients receiving immunomodulating medication, patients treated with bone metabolism-affecting medicines such as cortisone, osteoarthritis, RANKL antibodies, PTH and strontium ranelate as well as patients with osteologic primary disease, such as hyperparathyroidism, Paget's disease or osteomalacia.

2.2.1.1 Demographic data

Samples for miRNA expression in serum		
	Female osteoporotic patients	**Female non-osteoporotic patients**
Patients Number (N)	4	4
Age (y), (mean)	79.1 (67-91)	74.8 (66-83)
Diagnosis	Femoral neck fracture, osteoporosis	Coxarthrosis
BMD (mg/dl) ± SD	75.1 ± 12.3	237.5 ± 38.6
BMI ± SD	24.6 ± 1.7	26.1 ± 5.4
	Male osteoporotic patients	**Male non-osteoporotic patients**
Patients Number (N)	4	4
Age (y), (mean)	78.0 (72-89)	68.6 (51-85)
Diagnosis	Femoral neck fracture, osteoporosis	Coxarthrosis
BMD (mg/dl) ± SD	32.0 ± 37.3	235.6 ± 39.7

BMI ± SD	25.4 ± 4.2	28.0 ± 4.2

Samples for miRNA expression in osteoblast cells and bone tissue		
	osteoporotic patients	**non-osteoporotic patients**
Male: Female	2:4	6:0
Patients Number (N)	6	6
Age (y), (mean)	81.3 (74-87)	73.7 (61-86)
Diagnosis	Femoral neck fracture, osteoporosis	Coxarthrosis
BMI ± SD	60.5 ± 13.5	223.4 ± 28.2

Samples for miRNA expression in osteoclast cells		
	osteoporotic patients	**non-osteoporotic patients**
Male: Female	1:2	3:0
Patients Number (N)	3	3
Age (y), (mean)	85.3 (63-73)	73.7 (61-86)
Diagnosis	Femoral neck fracture, osteoporosis	Coxarthrosis
BMI ± SD	24.6 ± 1.7	26.1 ± 5.4

Samples for antagomiR-100 transfection of osteoblast cells		
	osteoporotic patients	**non-osteoporotic patients**
Male: Female	0:6	5:1
Patients Number (N)	6	6
Age (y), (mean)	81.3 (74-87)	73.7 (61-86)
Diagnosis	Femoral neck fracture, osteoporosis	Coxarthrosis
BMI ± SD	24.2 ± 3.0	27.1 ± 2.7

BMD (mg/dl) ± SD	60.5 ± 13.5	223.4 ± 28.2

Samples for antagomiR-148a transfection of osteoblast cells		
	osteoporotic patients	**non-osteoporotic patients**
Male: Female	0:6	5:1
Patients Number (N)	6	6
Age (y), (mean)	75.5 (74-87)	73.7 (61-86)
Diagnosis	Femoral neck fracture, osteoporosis	Coxarthrosis
BMI ± SD	25.2 ± 3.3	26.0 ± 3.7
BMD (mg/dl) ± SD	60.5 ± 13.5	198.0 ± 93.2

2.2.2 Bone tissue and bone cell culture

2.2.2.1 Serum

Serum was collected using 7.5 ml polypropylene tubes S-Monovette® (Sarstedt AG) from venous blood. S-Monovette® serum tubes including clotting factor was used for serum prearrangement. The S-Monovette® serum tubes were stored for 30 minutes at room temperature and centrifuged for 10 minutes at 1900 g. The clear serum supernatant was then transferred into 2 ml Eppendorf tubes and a part of this was examined by clinical chemistry in order to rule out any hemolysis that can alter miRNA contents in serum (spectrophotometrically Harboe method, 315/380/450 nm) (Kirschner, Edelman et al. 2013). The other part was frozen at -80 °C for further miRNA expression analysis described in chapter 2.2.3.1.

2.2.2.2 Bone tissue

From femoral heads that were collected about 8 hours after fracture from osteoporotic patients and about 30 minutes after operation from non-osteoporotic patients directly after qCT measurements, bone and cancellous bone fragments were collected using a Luer forceps from the middle part of the femur head after removing solid tissue from the bone. The tissue was removed using sterile scalpels and sterile gauzes. Then, the bone fragments were washed twice with Dulbecco's phosphate buffered saline (D-PBS). Afterwards, 1.0-1.5 mg bone tissue pieces (1.0-1.5 mm^3) were inserted in 2 x 2 ml Eppendorf tubes and covered with TriReagent from Sigma-Aldrich. All samples were afterwards stored at -80 °C for further procedure.

2.2.2.3 Osteoblasts

2.2.2.3.1 Osteoblast isolation and culture

Femoral heads for the isolation of primary human osteoblast cells were collected in sterile containers from patients with hip fractures type A0 31-A/B and following endoprosthetic hip replacement surgery. To restrict the risk of contamination, cancellous bone from the collected femoral heads was contemporarily mechanically shredded to small bone fragments using a Stille-Luer bone rongeur under sterile conditions. The osteoblast isolation was carried out according to an established protocol of Gallagher et al. (Gallagher 2003). In 50 ml falcons, deposited bone fragments were repetitively washed five times with D-PBS. After the bone had been freed from the remnants of blood and fat, the 10 ml bone fragments were transferred into a sterile 175 cm^2 culture flask. In each culture bottle, 20 ml osteoblast culture medium (500 ml low glucose Dulbecco's Modified Eagle Medium (D-MEM), 10% fetal calf serum (FCS), 1% penicillin/streptomycin, 50 µg L-ascorbate-2-phosphate) was filled and the bone fragments were distributed evenly on the bottom of the bottle prior seven days of incubation at 37 °C, 5% CO_2. During this week of incubation, the culture bottles were not dislodged in order to not disturb the cell outgrowth and cell proliferation.

On day 7, the first media replacement occurred with 20 ml fresh osteoblast medium and under extreme caution to prevent any fragment dislocation. The new medium was then left again for 7 days. All following media replacements were carried out twice a week. Observing the osteoblast cell outgrowth, a satisfactory confluence could be achieved after roughly 2 to 3 weeks. At this time, cell passaging was started by aspirating the medium, removing the bone fragments and washing the cells with 20 ml of D-PBS to remove any residuals. To reach the cell detachment from the flask bottom, 3 ml trypsin-ethylenediaminetetraacetic acid (EDTA) solution was added for 7 to 10 minutes at 37 °C incubation and afterwards checked under the inverse light microscope. Adding 10 ml osteoblast medium afterwards inactivated the trypsin/EDTA solution. The osteoblasts brought into solution were then transferred to a 50 ml polypropylene falcon tube and centrifuged at 650 g for 10 minutes. The resulting pellet was then resuspended with 30 ml medium. Cell count (also for osteoclasts in 2.2.2.3) afterwards was carried out using a hemocytometer counting chamber. Therefore, 50 µl of 0.5% Trypan Blue were mixed with 50 µl cell suspension. 10 µl mixture was then transferred into the counting chamber. The average cell number was determined and cells were divided into three 175 cm^2 culture flasks at passage 1 (Gallagher 2003).

For osteoblast miRNA expression analysis, in cell passage three, the experimental setup was reached. The cells were plated at 1×10^4 cells/cm^2 and the cell culture medium was replaced by osteoblast expansion medium (500 ml low glucose D-MEM, 5% FCS, 1% penicillin/streptomycin, 10 mM β-glycerol phosphate, 1.56 mM calcium chloride, 0.025 M 4-(2-hydroxyethyl)-1-piperazineethanesulfonic acid (HEPES) buffer, 100 nM dexamethasone, 0.2 mM L-ascorbic acid). Day 3, 7 and 14 were set time points for harvesting the cells and performing miRNA isolation as mentioned above.

2.2.2.3.2 AntagomiR-100 and AntagomiR-148a transfection

The transfection with antagomiR-100 or antagomiR-148a was carried out according to the protocol of the manufacturer Qiagen. Also for transfection experiments, the experimental setup was reached in cell passage three. Therefore, we used HIPerfect HTS Reagent and antagomiR-100 or antagomiR-148a (Qiagen, Hilden, Germany), operating as lipotransfection reagents due to electrostatic interactions (Figure 4).

At the start, osteoblasts were plated at a cell density of 1.0×10^4 cells/cm^2 on 6-well plates for miRNA isolation and on 48-well plates for further assays. After 24-hour incubation and a washing step with D-PBS, the cells were covered with supplement-free culture medium: 2.3 ml for 6-well plates and 230 µl for 48-well plates. Transfection solution containing 300 ng antagomiR-100 or antagomiR-148a, supplement-free culture medium (100 µl for 6-well plates and 10 µl for 48-well plates) and HIPerFect HTS Reagent (12 µl for 6-well plates and 1.2 µl for 48-well plates) were vortexed in conjunction in the next step. Afterwards, the solution was incubated for 10 minutes at room temperature and diligently pipetted into the cell medium. Then, the plate was driven in eights for mingling. In addition, one well each was used as a negative control using 0.3 µl miScript Negative Control (Qiagen, Hilden, Germany). A four-hour incubation at 37 °C, 5% CO$_2$ was followed by a medium replacement with 500 ml low glucose D-MEM, 5% FCS, 1% penicillin/streptomycin, 10 mM β-glycerol phosphate, 1.56 mM calcium chloride, 0.025 M HEPES buffer, 100 nM dexamethasone and 0.2 mM L-ascorbic acid. Then, on day 1, 3 and 7, miRNA of the transfected osteoblasts was isolated as well as viability tests, activity assays and staining were performed (Gallagher 2003, Stammet, Goretti et al. 2012).
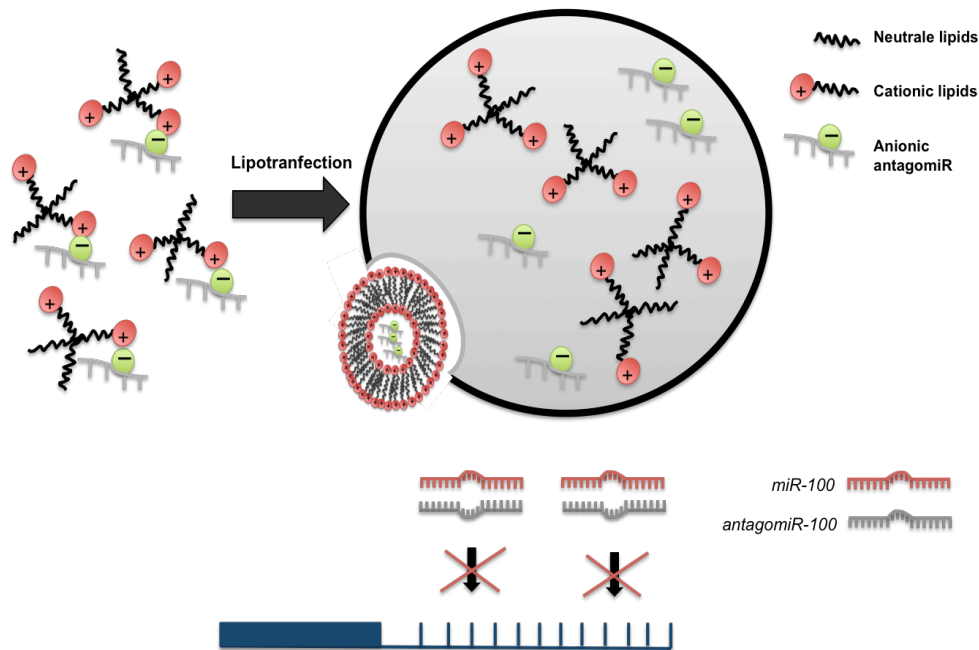
Figure 3 Depicting the principle of lipotransfection. Anionically charged antagomiR-100 and cationically charged HiPerFect HTS Reagent enter an electrostatic interaction enabling antagomiR-100 to enter the nucleus via endocytosis. AntagomiR-100, as a chemically single-stranded RNA complementary inhibits endogenous miR-100 intracellularly in osteoblasts.

2.2.2.4 Osteoclasts

The implementation of the osteoclast isolation was based on the manufacturer's protocol from Biowest. For the generation of osteoclasts, 40 ml of blood per patient were taken in S-Monovette® EDTA K$_3$ tubes from osteoporotic and non-osteoporotic donors. Blood was carefully layered on top of 20 ml of lymphocyte separation medium (LSM) (Biowest, Nuaillé, France) in a 50 ml falcon tube, before 20 minutes of centrifugation at 1,000 g at 22 °C. LSM with a density of 1.077 g/ml again composes a density gradient for cell separation. Thereafter, the resulted interphase containing rich amounts of peripheral blood mononuclear cells (PBMCs) was transferred into a fresh falcon tube. After additional 40 ml D-PBS for cell purification were added, the falcon tube was centrifuged at 650 g for 10 minutes at 22 °C. Furthermore, supernatant was aspirated and the pellet was resuspended with osteoclast culture medium. The osteoclast isolation medium comprised of 500 ml α-modification minimum essential medium, 10% FCS,

100 U/ml penicillin and 10 μg/ml streptomycin. After osteoclast cell count was carried out with Trypan Blue, the osteoclast cells were plated at a density of 3x10^6 cells/cm^2 on 48-well plates. For further cultivation steps, an M-CSF stock solution was prepared with 400 μl sterile DMEM, 5% FCS, 1% penicillin/streptomycin and 10 μg M-CSF. Secondly, a RANKL stock solution was blended with 500 μl sterile DMEM, 5% FCS, 1% penicillin/streptomycin and 10 μg RANKL. After a following 24-hours incubation in isolation medium, the first medium change was performed with freshly prepared differentiation medium made from 50 ml isolation medium and 50 μl M-CSF stock solution to induce the differentiation of isolated hematopoietic stem cells into macrophages. This medium change was repeated on day 4. On day 6, half of the de-differentiation medium on the cells was replaced with freshly prepared differentiation medium consisting of 50 ml isolation medium and 50 μl RANKL stock solution. Further media replacements were fully performed with the RANKL supplemented medium until day 21 and day 28, when miRNA isolation was initiated (Koberle, Kronenberger et al. 2013).

2.2.3 Nucleic Acid expression analysis

To understand interindividual variances, it was a crucial step not to pool our samples (serum, bone tissue, osteoblasts, osteoclasts). Therefore, miRNA was separately isolated and measured for each individual patient.

2.2.3.1 miRNA isolation from serum

The miRNA isolation from serum was performed according to the miRNAeasy Serum/Plasma Handbook February 2012 from Qiagen. For miRNA expression analysis in osteoporotic and non-osteoporotic patients, serum of each patient was thawed on ice. Afterwards, clear serum supernatant was shortly vortexed with 1000 µl QIAzol Lysis Reagent, which is part of the utilized miRNAeasy Serum/Plasma Kit from Qiagen (Hilden, Germany). The solution was afterwards vortexed to ensure a sufficient mixture. Spike-In control solution was used to monitor RNA extraction efficiency. Therefore, after 5 minutes' incubation at

room temperature, 3.5 µl Spike-In Control dilution (part of the miRNAeasy Serum/Plasma Kit with 1.6 x 10^8 copies/µl C. elegans miR-39-3p miRNA mimic from Qiagen) and 200 µl chloroform were added and the suspension was incubated for further 2 minutes. Transmitting the superior aqueous layer into a new 2 ml Eppendorf tube without damaging the interphase followed the addition of 900 µl of 96% ethanol. In the next step, 700 µl sample was immediately transferred via RNeasy MinElute spin columns and buffer supplementation into 2 ml Eppendorf tubes at 8,000 g. Using 15 µl ultra-pure RNAse-free water and one-minute centrifuging at full speed, miRNA was directly dropped into a new 1.5 ml Eppendorf tube. Afterwards, obtained samples were consequently stored at -80 °C.

2.2.3.2 miRNA and mRNA co-isolation from bone tissue and cells

For quantitative miRNA expression analysis, it was necessary to isolate RNA from the collected samples for subsequent reverse transcription polymerase chain reaction (RT-PCR). Therefore, the extraction of miRNA of bone tissue, osteoblasts and osteoclasts from osteoporotic and non-osteoporotic donors was performed using TriReagent as mentioned before.

For the isolation of miRNA from bone tissue, 2 x 1.5 ml bone and cancellous bone fragments of femoral heads were inserted in 2 x 2 ml Eppendorf tubes and covered with AllProtect/RNA-later directly after qCT measurements. The filled Eppendorf tubes were then stored at -80 °C until the use of a Mixer Mill MM 400 bone mill (Retch, Haan, Germany). Before the first use, the grinding container and grinding ball were cleaned with NaOH solution to prevent inactivation by RNAse. The bone and cancellous bone fragments were placed directly from -80 °C into the grinding container and sealed airtight together with the grinding ball. The container was then placed in prepared liquid nitrogen for 2 minutes for snap freezing (Nitrogen tank LS 3000, Taylor-Wharton, Mildstedt, Germany). Subsequently, the grinding container was inserted into the holder of the bone mill and the bone mill was adjusted for 40 seconds at 30 Hz/sec. Then, 0.5 ml of

grounded bone powder was transferred to a new 2 ml Eppendorf tube using a spoon cleaned with 10 mM NaOH. Prior to grinding of each further sample, the grinding container, grinding ball and spoon were again cleaned with 10 mM NaOH. The 0.5 ml grounded bone samples were then incubated for 5 minutes on ice before adding 2 ml TriReagent.

Whereas in regard to the gained bone tissue powder, 1 ml TriReagent was added to 0.5 ml grounded bone in a 2 ml Eppendorf tube, miRNA isolation from osteoblast and osteoclast cells started with replacing the differentiation medium with TriReagent on culture plates. For osteoblasts, 2 ml/well for 6-well plates and for osteoclasts, 250 µl/well for 48-well plates were used. After 3 minutes, the cells were detached using a cell scraper and collected in 2 ml Eppendorf tubes.

Final miRNA extraction of bone tissue powder, osteoblasts and osteoclasts started by adding 100 µl chloroform per 500 µl TriReagent to each sample and incubating the vortexed samples on ice for 10 minutes. Afterwards, the samples were centrifuged at 14,000 g for 10 minutes at 4 °C, the upper aqueous layer was transferred into new 1.5 ml Eppendorf tubes prepared with 500 µl isopropanol. It was a crucial step to gently sway the samples and to wait for the end of 10 minutes of incubation on ice before a repetitive centrifugation at 14,000 g for 10 minutes at 4 °C. The recovered pellet was washed twice with 100% ethanol and centrifuged at 14,000 g for 10 minutes at 4 °C. After 5 minutes of ethanol evaporation, the miRNA pellet was re-suspended in 15 µl ultra-pure RNAse-free water and stored at -80 °C until further procedure.

2.2.3.3 RNA measurement

Using a Hellma Traycell UV spectrophotometer from Eppendorf (Hamburg, Germany), the amount and purity of the isolated miRNA and mRNA was determined at 260 and 280 nm. The ratio A260/A280 was determinate to assess the purity and value ranges from 1.8 to 2.0 were defined as pure. Results obtained outside the area were not included in the evaluation. A blank measurement with 2 µl ultra-pure water was done in the first step. Subsequently, samples were

thawed and 2 µl of each sample were measured in a dilution of 1:49 µl with a 0.2 mm lid according to the manufacturers' recommendation. Between each measurement, the apparatus was cleaned with ethanol.

2.2.3.4 RNA Integrity check

To verify the integrity of the nucleic acids, a RNA Integrity check was assessed running aliquots of the isolated miRNA and mRNA samples on a denaturing 1.5% agarose gel containing 7 µl ethidium bromide (EtBr) (Chomczynski 1993). Therefore, the agarose was dissolved in the microwave until the solution appeared without any agarose remains. Of each sample, 0.3 µg miRNA/mRNA was brought into solution with 15 µl RNAse-free ultra-pure water and 5 µl loading buffer. Afterwards 3 µl pUC 19 marker and the prepared samples were placed in the gel. Subsequently, 90 volts were applied for 40 minutes and pictures were taken using INTAS Gel iX20 Doc System (Intas Science Imaging Instruments GmBH, Göttingen, Germany).

2.2.3.5 Transcription of miRNA into cDNA

The miRNA transcription into complementary deoxyribonucleic acid (cDNA) was carried out using the specific miScript II RT Kit (Qiagen, Hilden, Germany). The transcription was performed according to consolidated and standardized protocols. miRNA transcription with the miScript II RT Kit started with transferring 1.5 µl miRNA sample for transcription in 0.2 ml transcription tubes and subjoining a calculated Master Mix containing HiSpec Buffer, mix of deoxynucleotidetriphosphates (dNTPs), Aqua ad iniectabilia and reverse transcriptase. Initially, the samples were incubated for 60 minutes at 37 °C followed by 5 minutes of incubation at 95 °C before finally cooling down to 4 °C. The completed transcription products afterwards were diluted with 200 µl RNAse-free ultra-pure water and frozen at -20 °C.

2.2.3.6 Transcription of mRNA into cDNA

For early osteogenic gene expression analysis after osteoblast transfection with antagomiR-100 and antagomiR-148a, a further portion of the extracted RNA was converted into cDNA by means of the First Strand cDNA Synthesis Kit from Fermentas (St. Leon-Rot, Germany). For the transcription with Fermentas First Strand cDNA Synthesis Kit, 9 µl mRNA were transferred into transcription tubes under the presence of a 2 µl mix containing Oligo(dT)18 Primer and Random Hexamer Primer. Samples were denatured at 65 °C for 5 minutes, which allowed an initial primer hybridization. After these 5 minutes, a range of deoxynucleotidetriphosphates (5x Reaction Buffer, 20 U/ µl RiboLock^{TM} RNase Inhibitor and 10mM dNTP Mix) as well as reverse transcriptase with a total volume of 9 µl was enclosed to guarantee an adequate lengthening of the annealed primers before continuing the transcription cycles for 60 minutes at 37 °C. In the final cycles, the reaction terminated by heating up 5 minutes to 70 °C and stopped cooling down to 4 °C. Each transcribed sample was afterwards attenuated in 10 ng/µl RNAse-free ultra-pure water and stored at -20 °C.

2.2.4 Quantitative RT-PCR

2.2.4.1 miRNA in serum, bone tissue, osteoblasts and osteoclasts

For the quantification of mature miR-21, miR-23a, miR-24, miR-93, miR-100, miR-122a, miR-124a, miR-125b and miR-148a in serum, bone tissue, osteoblasts (3d, 7d, 14d) and osteoclasts (21d, 28d), we used a CFX 96 Touch Real-Time PCR System (Bio-Rad, Munich, Germany) and the miScript SYBR Green PCR Kit (Qiagen, Hilden, Germany). The mentioned equipment was also used for the miRNA quantification of miR-100 and miR-148a after transfection experiments. PCR, as a technique allowing the synthesis of copies of specific miRNA sequences goes through various steps including denaturation, annealing and extension shown in the executed protocol (Bonora, Wieckowsk et al. 2015). Therefore, 96-well PCR plates with a total volume of 25 µl per well were

designed on the computer using Bio-Rad CFX Manager. Melting temperatures as well as time frames were adjusted. For ruling out incorrect quantifications of miRNA ratios, the guidelines of Minimum Information for Publication of Quantitative Real-Time PCR Experiments (MIQE) were taken into account (Bustin, Benes et al. 2009). qPCR process was controlled using cel-miR-39-3p Spike-In control (Qiagen). Snord96a was used for the normalization of serum data, as well later in tissue and cellular expression. After merging QuantiTect SYBR Green PCR Master Mix, miScript Universal Primer, miScript Primer Assay and RNase-free water on ice, the mix was added to 3 µl previously generated template cDNA (miRNA primer sequences are illustrated in the referred research article). The 96-well plate was sealed and centrifuged for 60 seconds at 1,000 g at room temperature on a Rotor-Disc before starting the initial 40 PCR cycles for 15 minutes at 95 °C. The denaturation process lasted 15 seconds at 94 °C, the annealing process 30 seconds at 55 °C and the extension process 30 seconds at 70 °C at least. The PCR expression quantifications with SYBR Green were normalized to the mean value of the small-sized RNA standard control molecule Snord-96a comparatively to $2^{-\Delta CT}$.

2.2.4.2 Early osteogenic genes in osteoblasts

For early osteogenic gene expression quantifications (runt-related transcription factor II (RUNX2), collagen type I α1-chain (COL1A1), alkaline phosphatase (AP) and bone morphogenetic protein receptor type II (BMPR2)), SsoFast Eva Green (Bio-Rad, Munich, Germany) was used according to an established standard operating procedure (Wiame, Remy et al. 2000). Individual forward/reverse primers (MWG Eurofins, Ebersberg, Germany) and dNTPs contained in SsoFast Eva Green adjusted to our cDNA samples permitted the enzyme Taq deoxyribonucleic acid (DNA) polymerase to elongate the primers (for individually used primer sequences, please reference to the research article). All stated and utilized PCR reagents were acquired from Axon Labortechnik (Kaiserslautern, Germany). The 40 cycles were set prior starting. Therefore, double-stranded DNA segments separation was set for 40 seconds at 95 °C. Then,

the DNA polymerase tied to the specific primer and elongated the DNA complementary to its cDNA counter strand during 40 seconds at 72 °C. After the last cycle of the real-time PCR and a short denaturation step, a melt curve analysis was carried out by slowly raising the temperature under continuous measurement of the fluorescence Eva Green to obtain information about the specificity of the PCR reaction. β-tubulin served as the housekeeper gene using the $2^{-\Delta CT}$ method in order to normalize the mean level of the relatively early osteogenic gene expression levels.

2.2.5 Viability assays

2.2.5.1 MTT assay

To rule out any toxic effects on the osteoblast cells by lipotransfection, a 3-(4,5-dimethylthiazol-2-yl)-2,5-diphenyltetrazolium bromide (MTT) assay was carried out, based on a yellow tetrazolium salt reduction into a purple formazan color change in unaffected cells (Mosmann 1983). Therefore, osteoblasts were washed twice with D-PBS for non-adherent cell removal before adding 250 µl MTT solution (1.2 mM thiazolylblue solved in D-PBS) on each 48-well plate sample of transfected/non-transfected cells and the negative transfection control. As a positive MTT control, we used 1% triton-treated cells and as a negative MTT control, we used untreated cells. In the next step, the plates were incubated for 1.5 hours at 37 °C and 5% CO_2. Afterwards, the MTT solution was replaced with 250 µl of 5 g sodium dodecyl sulfate (w/v), 49.7 ml dimethyl sulfoxide and 0.3 ml acetic acid acetic solubilisation solution before incubating the plates for 10 minutes at room temperature until the stain was completely solved in the added solution. Subsequently, the plate was photometrical measured and quantified with a Fluostar Omega plate reader (Labtech, Ortenburg, Germany) at 570/690 nm (Mosmann 1983).

39

2.2.5.2 Alamar blue assay

In order to confirm any lipotransfection-induced cytotoxicity in osteoblasts and to measure the cell proliferation, Alamar blue assay was performed. Transfected and non-transfected osteoblasts were cultured in 48-well plates enabling measurements in triplicates. As a positive MTT control, 1% triton-treated cells and as a negative MTT control, untreated cells were used. Moreover, medium without cells served as a blank control. Afterwards cell medium was covered with 1/10 Alamar blue reagent (Biozol, Eching, Germany). The exposure time was 60 minutes prior fluorescence (544/590 nm) and absorption measurements (570/600 nm) with the Fluostar Omega plate reader (Lin, Schyschka et al. 2012).

2.2.6 Osteoblast-specific assays

2.2.6.1 Alkaline phosphatase activity measurement

For osteoblast characterization, typical alkaline phosphatase (AP) enzyme activity was used to display the calcium deposition of osteoblasts based on a protocol as described by Ehnert et al. (Ehnert S. 2011). AP enzyme is capable to initiate a color change by phosphorylating para-nitrophenylphosphate to para-nitrophenol that is measurable in a spectrophotometer. Cell culture medium was aspirated and 250 µl AP substrate solution was added after washing the cells once with D-PBS. In addition, a blank control was prepared of AP substrate solution. After one hour of incubation at 37 °C, a color change to yellow was visible and a standard curve was prepared for further calculation of p-nitrophenol concentration. Furthermore, triplicates of each sample were transferred into 96-well plates and the absorbance was finally measured at 405 nm with the Fluostar Omega plate reader.

2.2.6.2 Alkaline phosphatase staining

The alkaline phosphatase staining was performed according to an established protocol described by Wildemann et al. (Wildemann, Burkhardt et al. 2007) for phenotypical analysis of osteoblasts. Alkaline phosphatase as an enzyme produced

by osteoblasts can be illustrated as a staining to mark osteoblasts microscopically. First, a fresh AP staining solution was prepared. Therefore, 6 mg 0.06% Fast Blue B Salt was diluted in 1 mg Naphtol-AS-MX-Phosphate and 10 ml 0.01% AP-Staining Buffer. In a prior step, the AP-Staining Buffer was prepared using 2.5 ml 99.9% Dimethylformamide, 203.5 mg $MgCl_2$ and 500 ml 0.1 M Tris Buffer. In turn, the Tris Buffer is made from 6.05 g of Tris base, 450 ml of double distilled water and an adjustment with NaOH to a pH of 8.5. After the culture medium was aspirated, the cells were accurately purified with D-PBS from the cell culture medium. Since the cells had first to be fixed, they were covered with 3.7% formaldehyde and the plates were left at room temperature of 10 minutes. The formaldehyde was then aspirated again after ten minutes and the osteoblast cells were incubated with 100 µl Staining Solution per well for 96-well plates. After a following incubation time of 30 minutes at 37 °C, the osteoblast cells colored violet. The osteoblasts were again accurately washed with D-PBS and photos were taken under the microscope Axiovert by Zeiss (Oberkochen, Germany).

2.2.6.3 Alizarin red staining

The staining of the osteoblast cells using alizarin red staining was carried out according to the protocol of Stanford et al. (Stanford, Jacobson et al. 1995). Alizarin red staining demonstrates the mineralization of cultivated osteoblasts due to visualization of present calcium ions. This was realized using alizarin as a chelating agent forming a connection with calcium. Therefore, osteoblasts in a 48-well plate were fixed with ice-cold 96% ethanol for 30 minutes. As a negative blank control, we used hexadecylpyridiniumchloride solution. Two washing steps with distilled water were followed by adding 200 µl 0.5% alizarin red staining solution and a 10 minutes of incubation at room temperature. After another four washing steps with distilled water, 200 µl 10% hexadecylpyridiniumchloride were added and the plates were incubated for further 10 minutes. Through photometric measurements (Fluostar Omega plate reader) of 100 µl transferred solution into 96-well plates, quantitative analysis of the alizarin red concentration could be performed and photos were taken with the microscope.

2.2.7 Osteoclast-specific assays

2.2.7.1 TRAP activity assay

Tartrate-resistant acid phosphatase (TRAP) activity is expressed as a cytochemical marker of osteoclast cells. Generally, expression could be elevated by osteoclasts as well as in activated macrophages (Kadow-Romacker, Hoffmann et al. 2009). Trap activity assay was referred to the protocol of Kadow-Romacker et al. (Kadow-Romacker, Hoffmann et al. 2009). To investigate the TRAP activity, triplicates of 50 µl cell culture supernatant were transferred to a 96-well culture plate. A well with non-conditioned culture medium was used as a blank control. To the transferred medium, 150 µl substrate buffer per well were added, containing 5 mM 4-nitrophenyl phosphate di-sodium salt hexahydrate in a buffer of sodium acetate, sodium tartrate dibasic dehydrate and doubly distilled H_2O. The plates were then incubated for 1 hour at 37 °C and 5% CO_2, meanwhile a standard curve was prepared according to a defined scheme. Therefore, 1800 µl TRAP Assay Buffer (8.2 g Sodium acetate, 11.5 g Na_2-tartrate and double distilled water adjusted to pH 5.5) and 200 µl of 10 mM 4-nitrophenol solution were diluted to final a concentration of 0.139 mg/ml. Afterwards, 1000 µl were transferred to a second Eppendorf tube and mixed before transferring another 1000 µl. This step was repeated until a concentration of 0.001 mg/ml was reached in Eppendorf tube 7. TRAP Assay buffer without medium served as a blank control. In the next step, 200 µl of each dilution was transferred in triplicates on a 96-well plate and in a final step, 50 µl 3M NaOH were added before measurement. For calculation, the mean value of all triplicates was used to determine the standard curve. At the end of the hour, the reaction was terminated by adding 50 µl 3 M NaOH per well and quantified through photometrical detection of the dephosphorylated product formation at 405 nm with the FLUOStar Omega plate reader.

2.2.7.2 TRAP staining

Trap staining from osteoclasts was carried out according to the working protocol of Greiner et al. (Greiner, Kadow-Romacker et al. 2007). After aspirating the culture medium, osteoclasts were incubated with 500 µl of the fixation buffer for 5 minutes at room temperature. The fixation buffer itself was prepared from 10 ml 10x D-PBS, 11.1 ml 37% formaldehyde, 0.2 ml Triton-X-100 and 78.7 ml double distilled water. Subsequently, the fixation buffer was removed and the cells were dried at room temperature for a period of 2 minutes. In order to carry out the next dyeing step, the TRAP Staining Buffer was prepared with a pH of 5.0 from 3.28 g of sodium acetate, 2.3 g of sodium tartrate dihydrate, 1 liter of double distilled water and adjusted HCl. The cells were then covered with 1000 µl/24-well plate TRAP staining solution, which in turn contains 1 mg of Naphtol AS-MX phosphate, 6 mg Fast Red Violet LB Salt, 100 µl of 99.9% N-N dimethylformamide and 10 ml of TRAP staining buffer. The osteoclasts were afterwards incubated for 20 minutes at 37 °C and 5% CO_2. After examination of a red cell color change, the osteoclasts were carefully washed with D-PBS before microscopy.

2.2.8 Statistical analysis

To determine the relative expression of miRNAs in serum, bone tissue, osteoblasts and osteoclasts, the ΔCq was calculated. Therefore, the Cq value of the target miRNA was normalized to the Cq value of the reference gene Snord-96a (ΔCq = Cq $_{(Target)}$ − Cq $_{(Reference=Snord96a)}$). Then, ΔCq expression was determined by the following formula ΔCq-Expression = $2^{-ΔCq}$ before the replicates were averaged and the standard deviation was calculated (Haimes 2014). This method was chosen to compare the real values from the osteoporotic and the non-osteoporotic group. The results are illustrated on the y-axis as the relative expression. For calculating the normalized expression ratio ΔΔCq of the miRNA and osteogenic genes in osteoblast cells after transfection, the ΔCq expression was normalized to the non-transfected treatment control and the replicates were

averaged. These results are illustrated on the y- axis as the normalized expression ratio. All results were evaluated and analyzed using GraphPad Prism version 6.0 for Mac OS X (GraphPad Software, San Diego, USA). The gathered results were depicted as mean values ± standard error of the mean (SEM). After testing for normal distribution, to determine the significance of miRNA expression in serum, bone tissue and cells of osteoporotic and non-osteoporotic patients, we used the two-tailed Mann-Whitney U test. In contrast, for the determination of the significance for miRNA expression transfected osteoblasts, we used the non-parametric Kruskal-Wallis (one-way ANOVA) test with Dunn's multiple comparison tests. Because we set the measured BMD values in relationship to the respective miRNA expression values, we used a linear regression analysis. Therefore, the coefficient of correlation (r) values $(-1 \leq r \leq +1)$ and the coefficient of determination (r^2) values (defined as $0 \leq r^2 \leq 1$) designated the strength of the linear association. Pursuant, positive values indicated a positive linear correlation and negative values indicated a negative linear correlation, whereas an optimal linear fit was indicated by $r = \pm 1$ and $r^2 = 1$. To compare two groups at different time points and to calculate TRAP activity, t-test corrected for multiple comparisons using Holm-Sidak method was utilized. To calculate AR absorbance and AP activity, data was tested by D'Agostino Pearson test and the statistical analysis was carried out by means of one-way ANOVA. The minimum level of significance was specified as $*p < 0.05$. Significant differences were indicated by $**p < 0.01$, $***p < 0.001$, $****p < 0.0001$. All results are given as box plots showing 25th, 50th and 75th percentiles (horizontal bars), and minimum to maximum ranges (error bars). The band inside the box marks the median.

3 Results

3.1 miRNA levels in serum

3.1.1 miRNA levels in serum

To initially explore the role of miR-21, miR-23a, miR-24, miR-93, miR-100, miR-122a, miR-124a, miR-125b and miR-148a in osteoporosis genesis, we determined the expression level of mature miRNA in serum of 4 males and 4 females with osteoporosis as well as 4 males and 4 females without osteoporosis. The expression levels of mature miR-21, miR-23a, miR-24, miR-93, miR-100, miR-122a, miR-124a, miR-125b and miR-148a were significantly up-regulated in serum of osteoporotic patients compared to non-osteoporotic patients in males and in females (Figure 5). qPCR process controlled using cel-miR-39-3p Spike-In control resulted in a 94.4 ± 4.6 % miRNA recovery.

miRNA	p-value females	p-value males
miR-21	< 0.0001	0.0341
miR-23a	0.0003	0.0062
miR-24	0.0001	0.0014
miR-93	0.0023	(0.1203)
miR-100	0.0001	0.0020
miR-122	0.0016	< 0.0001
miR-124	0.0066	0.0027
miR-125b	0.0132	(0.6750)
miR-148a	0.0020	0.0296

Figure 4 P-values. Illustrating a significant increase of miRNA expression in osteoporotic females and males compared to non-osteoporotic females and males.

In respect to these results, the gender-specific analysis in female and male osteoporotic patients showed no significant difference in miRNA relative expressions for mature miR-21 (p=0.745), miR-23a (p=0.723), miR-24 (p=0.701), miR-93 (p=0.630), miR-100 (p=0.464), miR-122a (p=0.06), miR-124a (p=0.9) and miR-148a (p=0.648). Among these miRNAs listed, the only gender-specific expression pattern was detected for miR-125b (p=0.0358) showing up-regulated expression values in osteoporotic females (Figure 6).
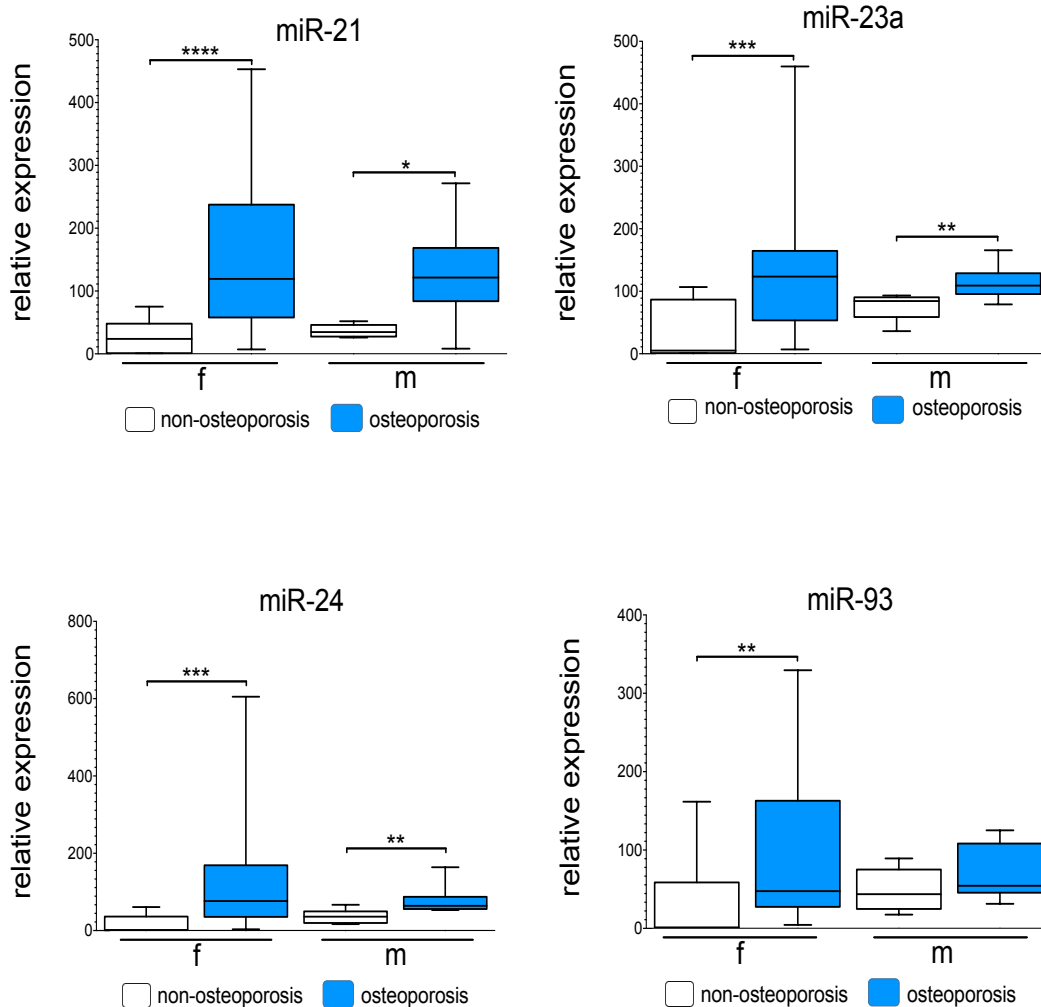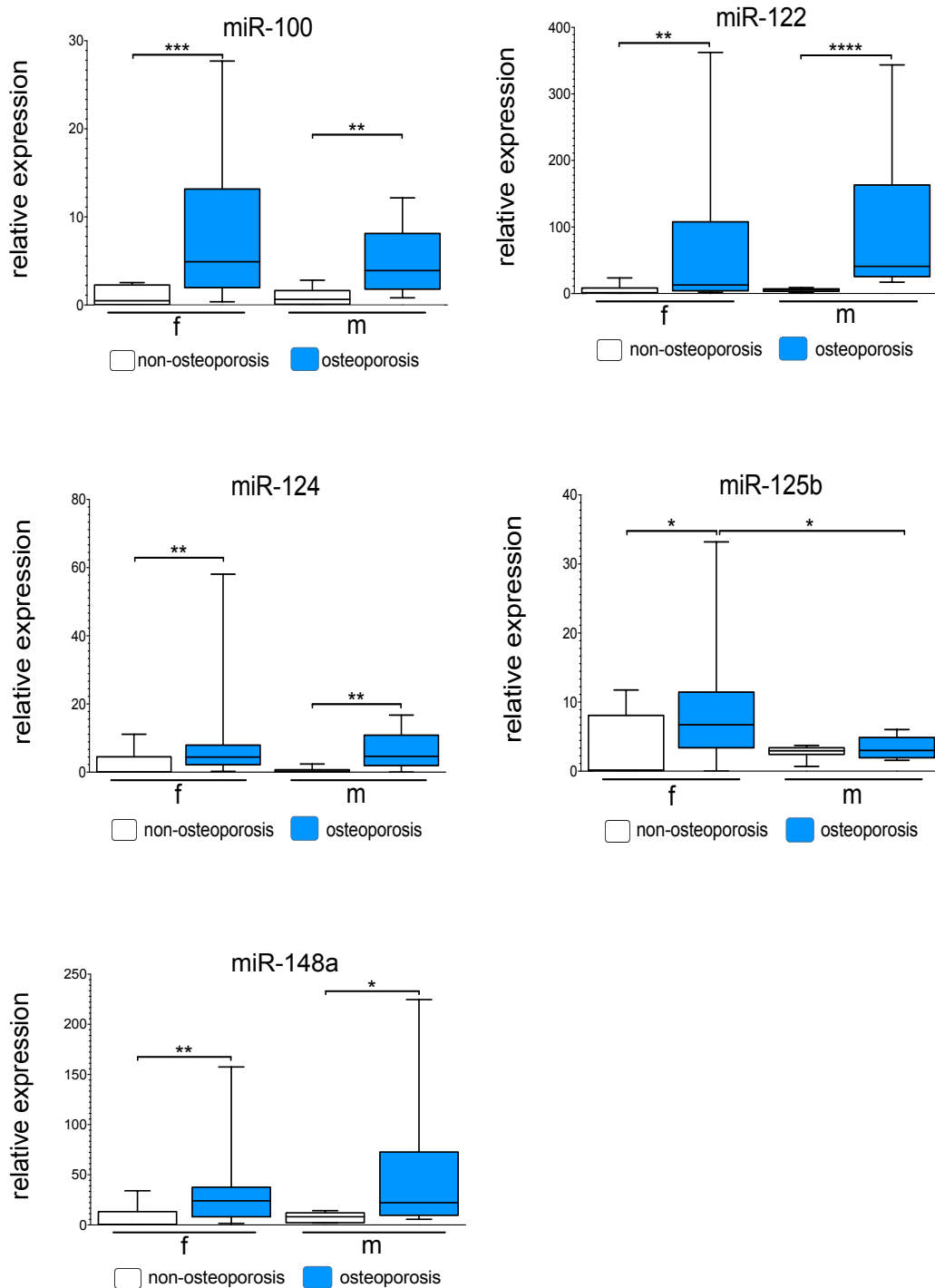
Figure 5 Relative miRNA expression levels in serum normalized to Snord-96a. The illustrated plots consist of a box bounded by the 25% quantile below and the 75% quantile above. The median is shown as an extra line in the box. The whiskers represent the value of maximum and minimum. Significant differences are indicated by *p <0.05, **p <0.01, ***p <0.001, ****p <0.0001. y-axis: relative expression, x-axis: female patients (f) and male (m) patients.

3.1.2 miRNA levels in bone tissue

Overall, the mature miRNA expressions of miR-21 (p=0.0143), miR-24 (p=0.0227), miR-93 (0.0317), miR-100 (p= 0.0397) and miR-125b (p=0.0071) in bone tissue were significantly up-regulated in osteoporotic patients compared to non-osteoporotic patients. These six miRNAs significantly showed a linear increased correlation to the measured BMD values (Figure 7).

miRNA	coefficient of determination (r^2)	deviation
miR-21	0.9403	0.0012
miR-23a	0.9220	0.0058
miR-24	0.8831	0.0016
miR-93	0.8741	0.0016
miR-100	0.8851	0.0211
miR-122	0.0338	0.4379
miR-124	0.0979	0.9884
miR-125b	0.8417	0.0012
miR-148a	0.6090	0.1327

Figure 6 Demonstrated coefficient of determination (r^2) and deviation for miRNA correlation with BMD.

Particularly for classification of the disease stages from healthy, osteopenia and osteoporosis, miRNA-21 shows a significant and linear correlation suggesting an association with osteopenia (p= 0.0476) and osteoporosis (p= 0.0143) (Figure 8). Averaging the deviation results leads to p-values less than 0.001. The calculated coefficient of determination (r^2) ranged between values from 0.84 to 0.94 for miR-21, miR-23a, miR-24, miR-100, miR-125b. Despite the illustrated trend of a linear increase of miR-23 (p=0.1017), miR-24 (p=0.1714), miR-93 (p= 0.0667), miR-100 (0.0952), miR-125b (p= 0.0714) and miR-148a (p= 0.1569), no linear correlation to the BMD value was detectable. An association with osteopenia or osteoporosis cannot be established with these miRNA (p>0.05). However, two

miRNAs, miR-122 (p= 0.0586) and miR-124 (0.4400) did not show any significant correlation neither to BMD, nor to osteopenia and osteoporosis.
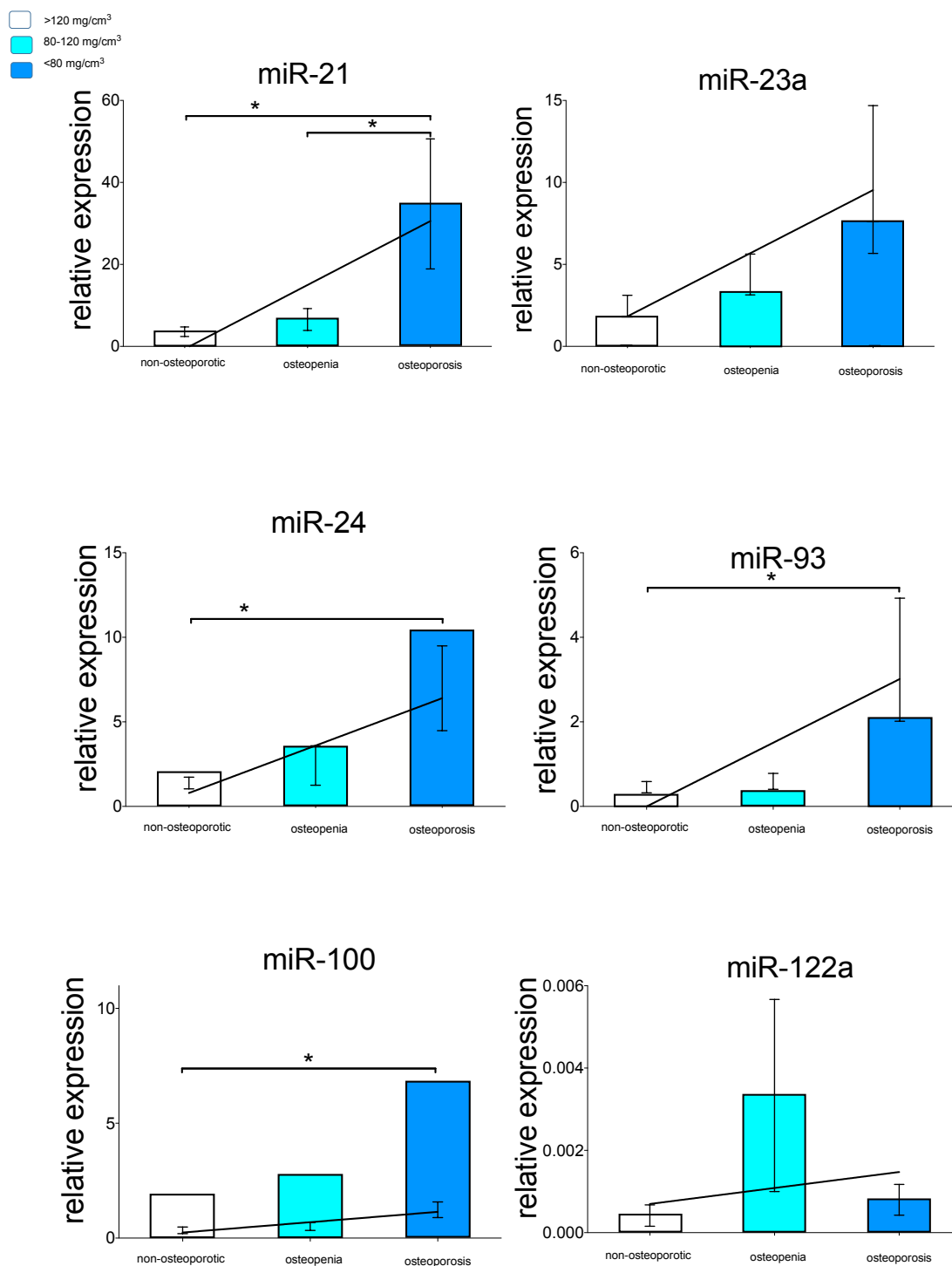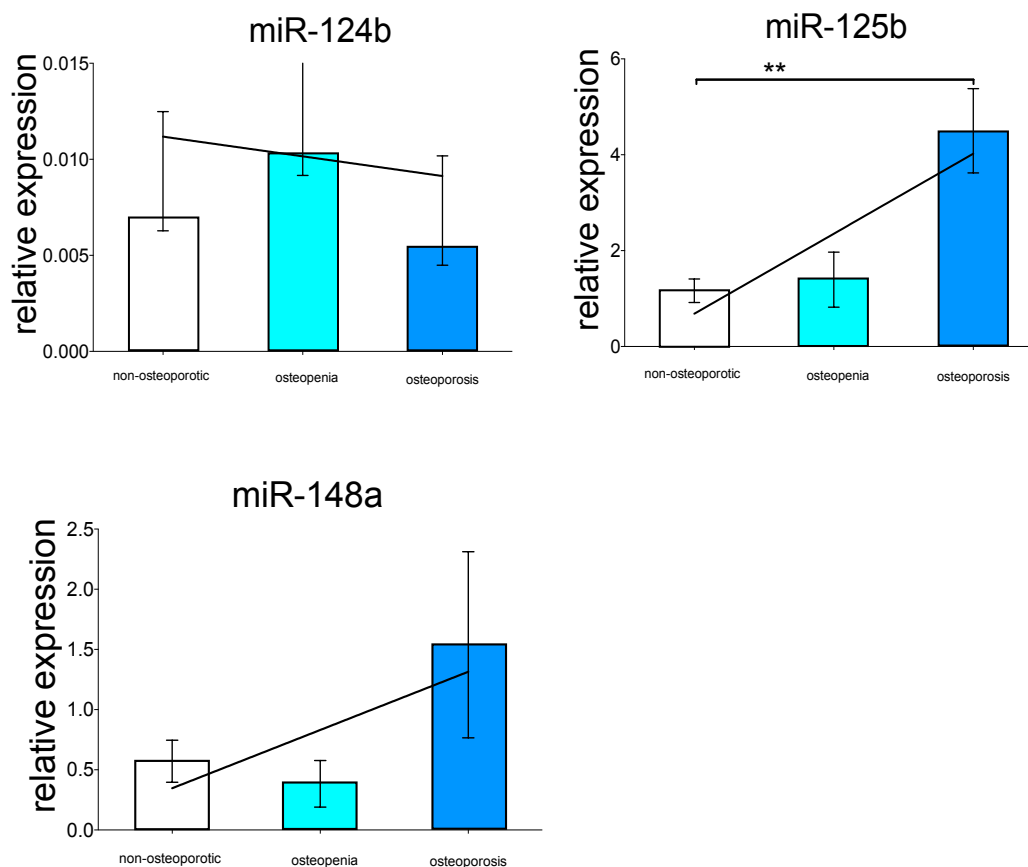
Figure 7 Illustration of a linearly increased correlation between relative miRNA expression normalized to Snord-96a and bone density measurements characterizing disease stages of osteoporosis. Column diagrams are illustrated comparing non-osteoporotic patients, patients with osteopenia and osteoporotic patients. Significant differences are indicated by *p <0.05, **p <0.01, ***p <0.001, ****p <0.0001. y-axis: relative expression, x-axis: patient groups.

3.1.3 miRNA levels in osteoblast cells

For evaluating the intracellular expression diversification of miR-21, miR-23a, miR-24, miR-93, miR-100, miR-122a, miR-124a, miR-125b and miR-148a during osteogenic differentiation, quantitative RT-PCR assay was performed to evaluate expression levels in primary human osteoblast cells of osteoporotic and non-osteoporotic patients after a differentiation period of 14 days. To assess the RNA integrity of osteoblasts, a prior RNA integrity check was evaluated, showing no

degradation or additional unattended bands. The overall distribution of the levels of these miRNAs in osteoblast cells between samples of osteoporotic patients and samples of non-osteoporotic patients are shown in Figure 10a. During osteogenic differentiation in cell culture, miRNA expression levels of miR-24 (p=0.040) and miR-93 (p=0.0390) increased in osteoblast cells of osteoporotic patients in comparison to non-osteoporotic patients already after 3 days (Figure 9).
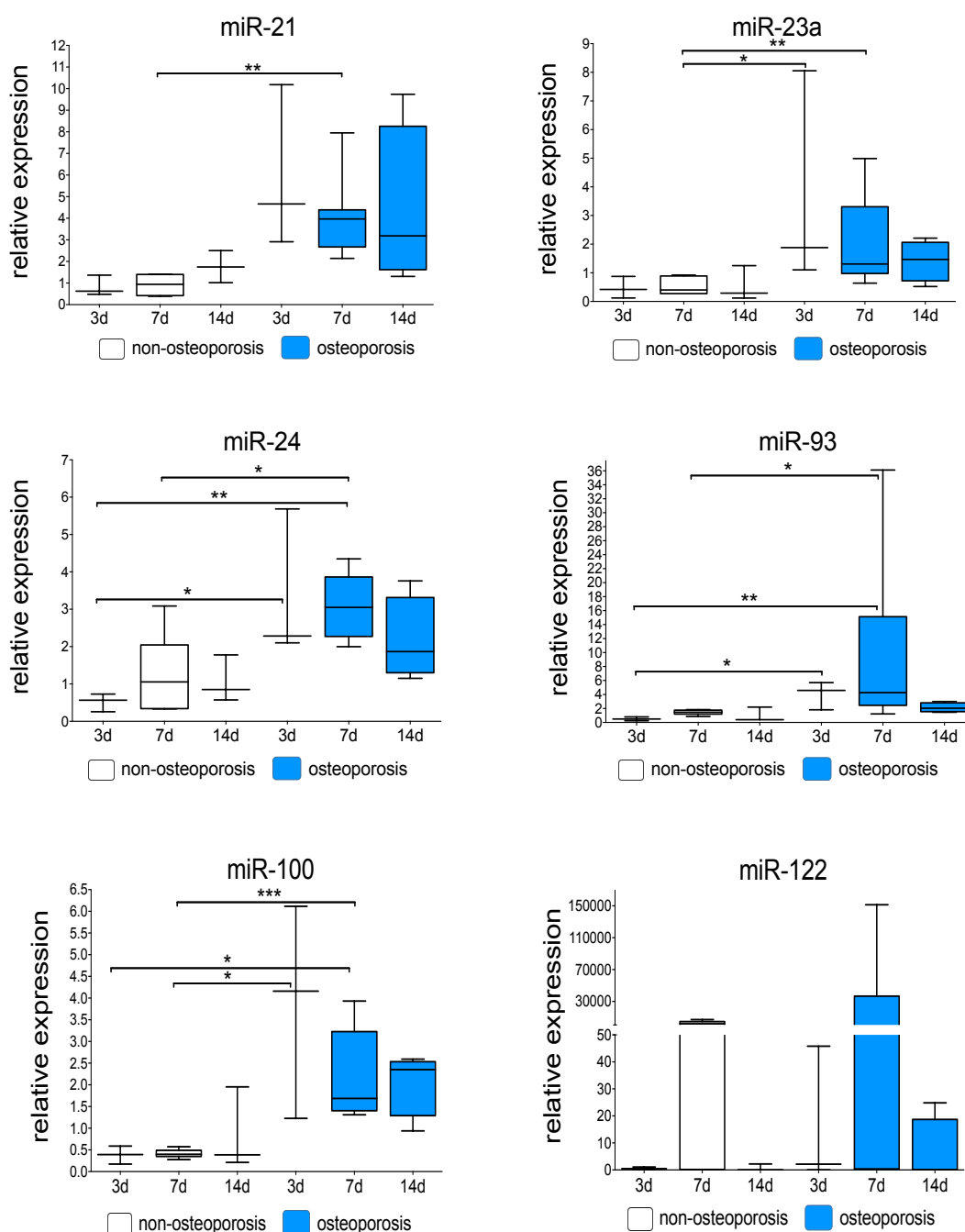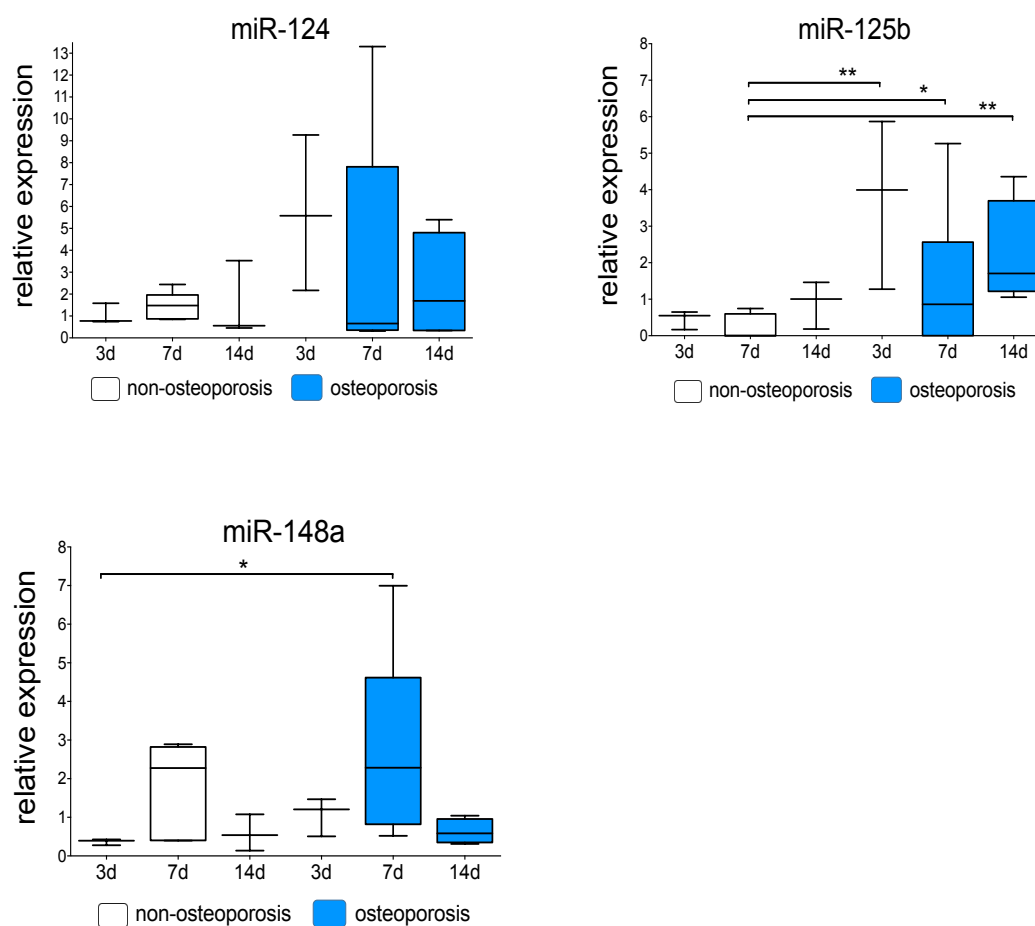
Figure 8 Relative miRNA expression levels in osteoblast cells normalized to Snord-96a. The different examination times are set at day 3, 7 and 14. Presented plots consist of a box bounded by the 25% quantile below and the 75% quantile above. The median is shown as an extra line in the box, whiskers represent the value of maximum and minimum. Significant differences are indicated by *p <0.05, **p <0.01, ***p <0.001, ****p <0.0001. y-axis: relative expression, x-axis: non-osteoporotic patients, patients with osteoporosis.

As illustrated, we could evidence a partly significant overexpression of miR-21 (p=0.0040), miR-23a (p=0.0027), miR-24 (p=0.0303), miR-93 (p=0.0256), miR-100 (p=0.0007) and miR-125b (p=0.0360) in primary human osteoblasts of osteoporotic patients on day 7 in osteoblasts of osteoporotic patients in contrast to osteoblasts of non-osteoporotic patients. miR-122a and miR-124a show a tending overexpression without signification (p>0.5). miR-148a demonstrates a significant increase on day 7 in osteoporotic cells compared to day 3 in non-osteoporotic cells (p=0.0121). Considering the osteoporotic group, during osteogenic-differentiation

miRNA expression levels of miR-23a, miR-24, miR-93, miR-100, miR-122, miR-124 and miR148a seem to decrease. The main rise is mainly reflected on day 7.

Furthermore, an alkaline phosphatase activity measurement of the osteoblasts on day 3, day 7 and day 14 showed that non-osteoporotic cells have a higher activity than cells of osteoporotic patients. The p-nitrophenol concentration in mg / ml was calculated and illustrated as y coordinate. Significantly lower values are observed on day 3 ($p<0.0001$), day 7 ($p<0.0001$) and day 14 ($p <0.05$). Both groups are presented by similar activity levels ($p<0.05$) and a falling activity over differentiation is observable (Figure 10).
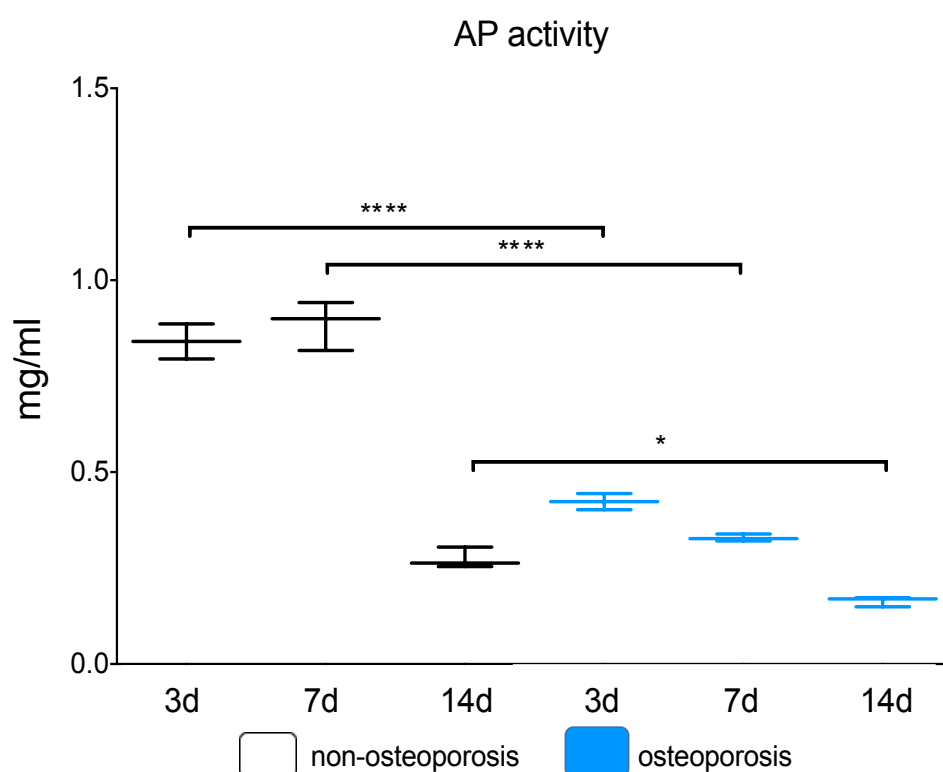
Figure 9 Alkaline phosphatase activity (AP) of osteoblast cells in osteoporotic and non-osteoporotic cells on day 3, day 7 and day 14 after differentiation (y-coordinate axis: p-Nitrophenol in mg/ml). The illustrated plots consist of a box bounded by the 25% quantile below and the 75% quantile above, median is shown as an extra line in the box, whiskers represent the value of maximum and minimum. Alkaline phosphatase activity is higher in the non-osteoporotic group. Significant differences are indicated by *p <0.05, **p <0.01, ***p <0.001, ****p <0.0001. y-axis: AP activity in mg/ml, x-axis: non-osteoporotic patients and osteoporotic patients

In addition to the AP activity, where significantly higher activity values could be shown, AP staining was carried out at all differentiation times points in both cell groups to illustrate the osteoblast phenotype microscopically (Figure 11). Here, no difference on osteoblast cell number or proliferation after isolation between osteoporotic and non-osteoporotic bone samples could be observed.
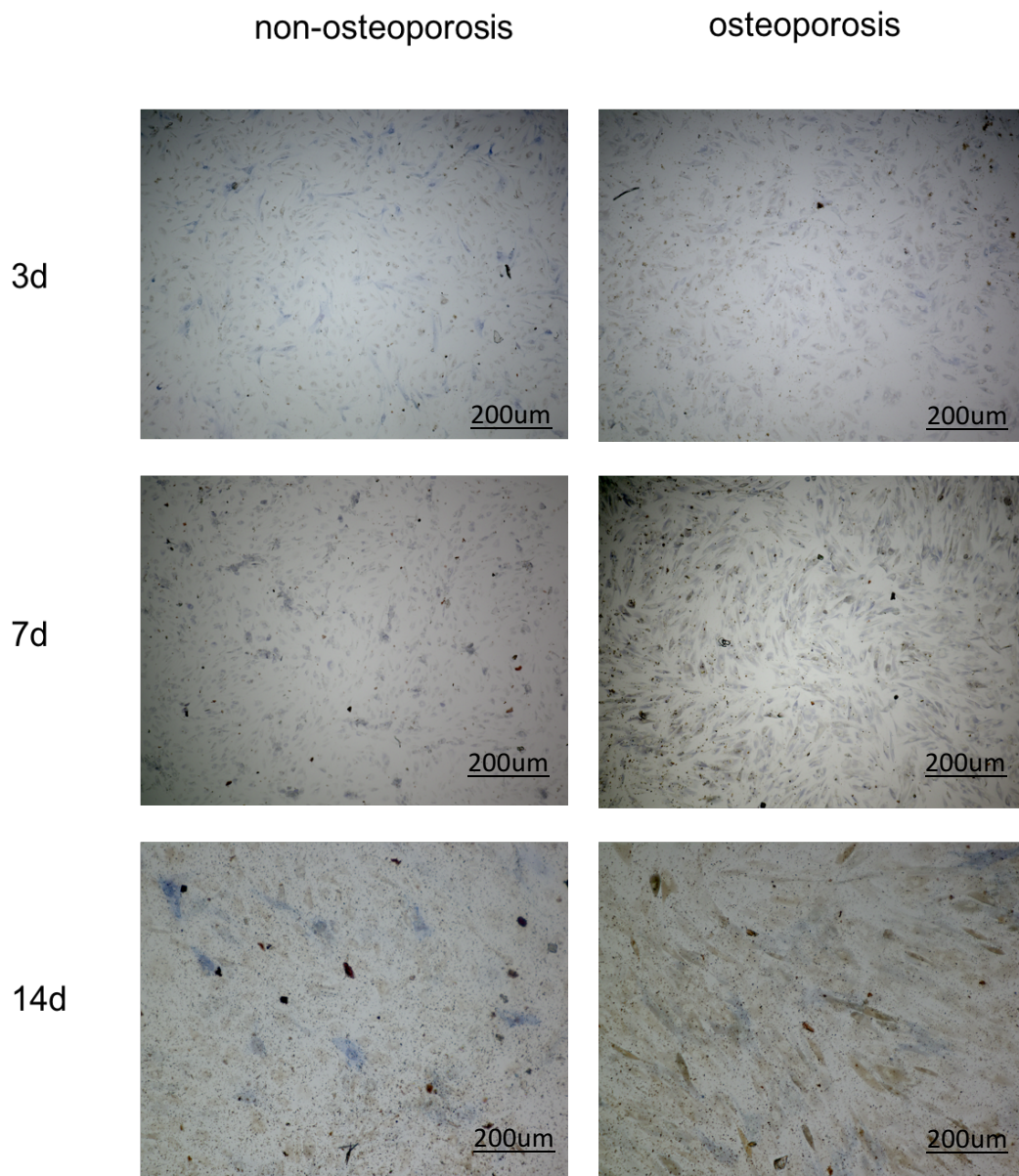
Figure 10 Alkaline phosphatase staining (AP) of mononucleotide osteoblast cells in osteoporotic and non-osteoporotic cells on day 3, day 7 and day 14 after differentiation. Original magnification was 20x for all photomicrographs.

Alizarin staining was performed for a secondary detection of the mineralization degree. Therefore, the absorbance after dissolving the dye was measured on the same days 3, 7 and 14 showing no difference between the osteoporotic and non-osteoporotic group (Figure 12). Alizarin was then photometrically recorded via light microscopy, illustrated in Figure 13, showing no significant difference between both groups. Only at day 14, both cell groups tend to show higher mineralization quantifications.
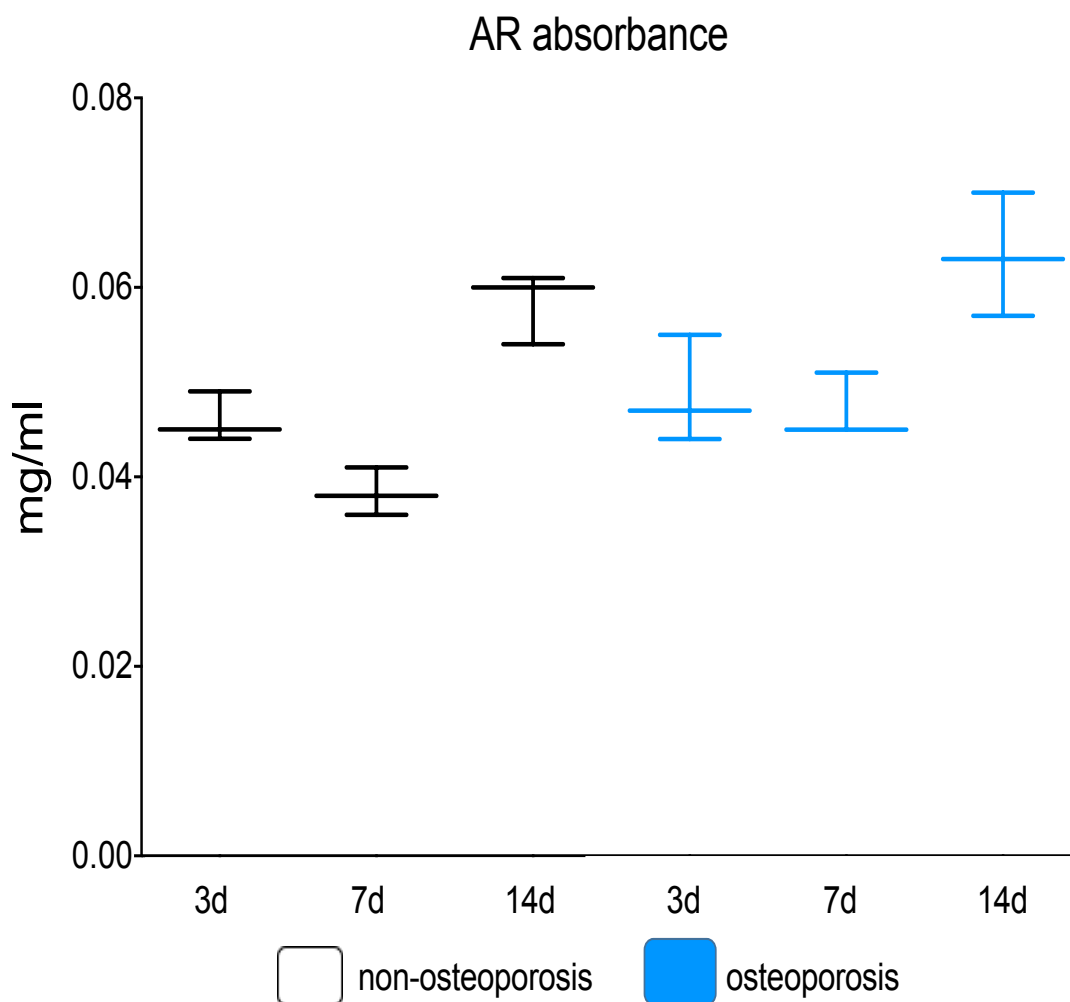
Figure 12 Alizarin red absorbance (AR) in mg/ml in osteoporotic and non-osteoporotic cells on day 3, day 7 and day 14 after differentiation. The presented plots consist of a box bounded by the 25% quantile below and the 75% quantile above, median is shown as an extra line in the box, whiskers represent the value of maximum and minimum. Alizarin red activity is similar in both

groups. Significant differences are indicated by *p <0.05, **p <0.01, ***p <0.001, ****p <0.0001.
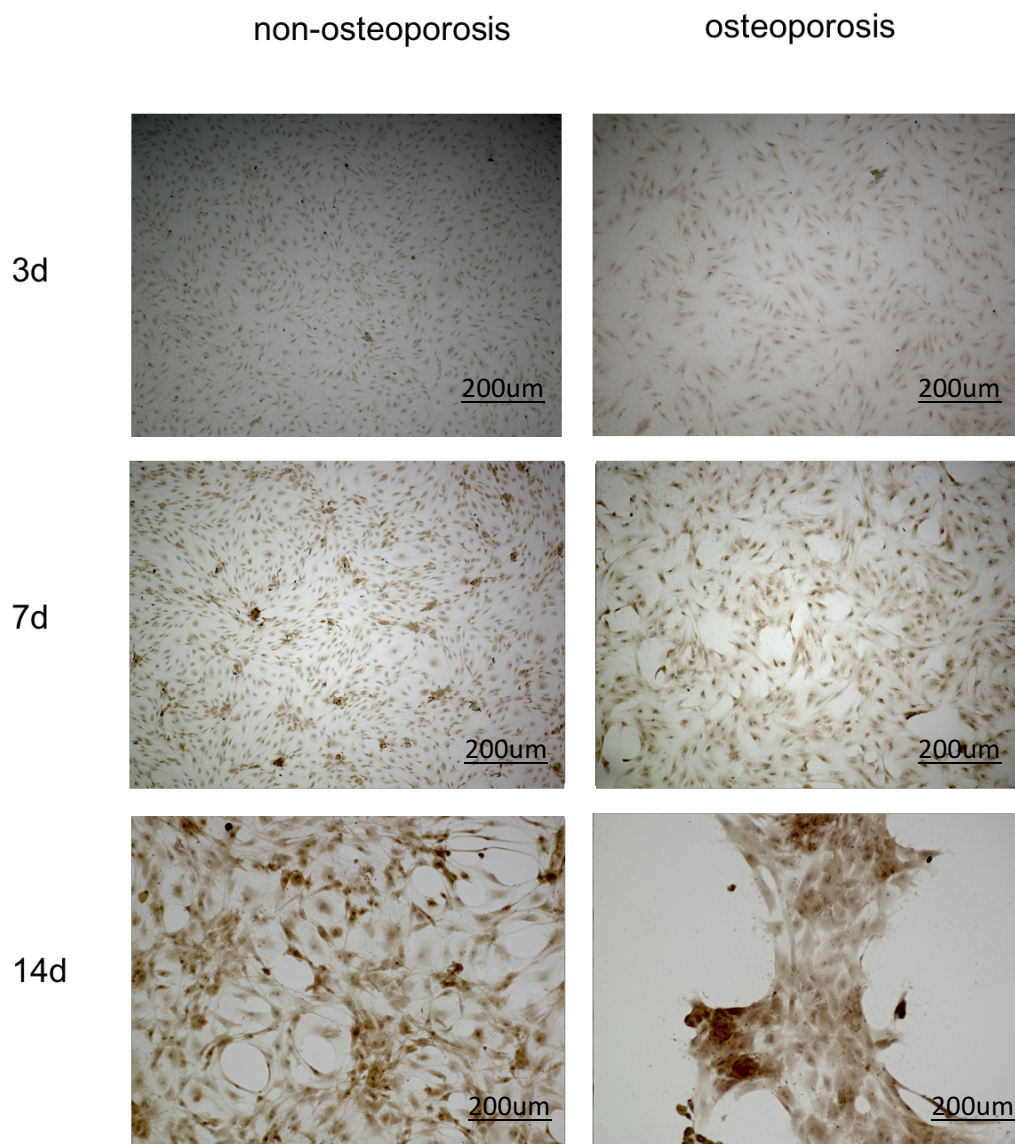
Figure 11 Alizarin res staining (AR) of mononucleotide osteoblast cells in osteoporotic and non-osteoporotic cells on day 3, 7 and 14 after differentiation. Original magnification was 20x for all photomicrographs.

3.1.4 miRNA levels in osteoclast cells

To assess the RNA integrity isolated from osteoclasts, a prior RNA integrity check was evaluated, showing no degradation or additional unattended bands. Focusing on the expression patterns of the osteoclasts in osteoporotic patients in contrast to non-osteoporotic patients, miR-21 (p=0.0245), miR-122a (p=0.0190), miR-125b (p=0.0476) and miR-148a (p=0.0159) presented a significant up-regulation on day 21. After 28 days, also miR-93 (p=0.0043), miR-122 (p=0.0073) and miR-124 (p=0.0411) attained a significant up-regulation (Figure 14). The results show a constant and significant increase of the miR-122 expression over the differentiation period. miR-125b, miR-100 and miR-148a display a tending increase on day 28 in both groups without confirming a significance between osteoporotic and non-osteoporotic specimens (p>0.05). Regarding miR-124, the results show a significant increase in expression during osteoclastogenesis in non-osteoporotic patients (p=0.0095), whereas the expression decreases in the osteoporotic group reaching the significant level.
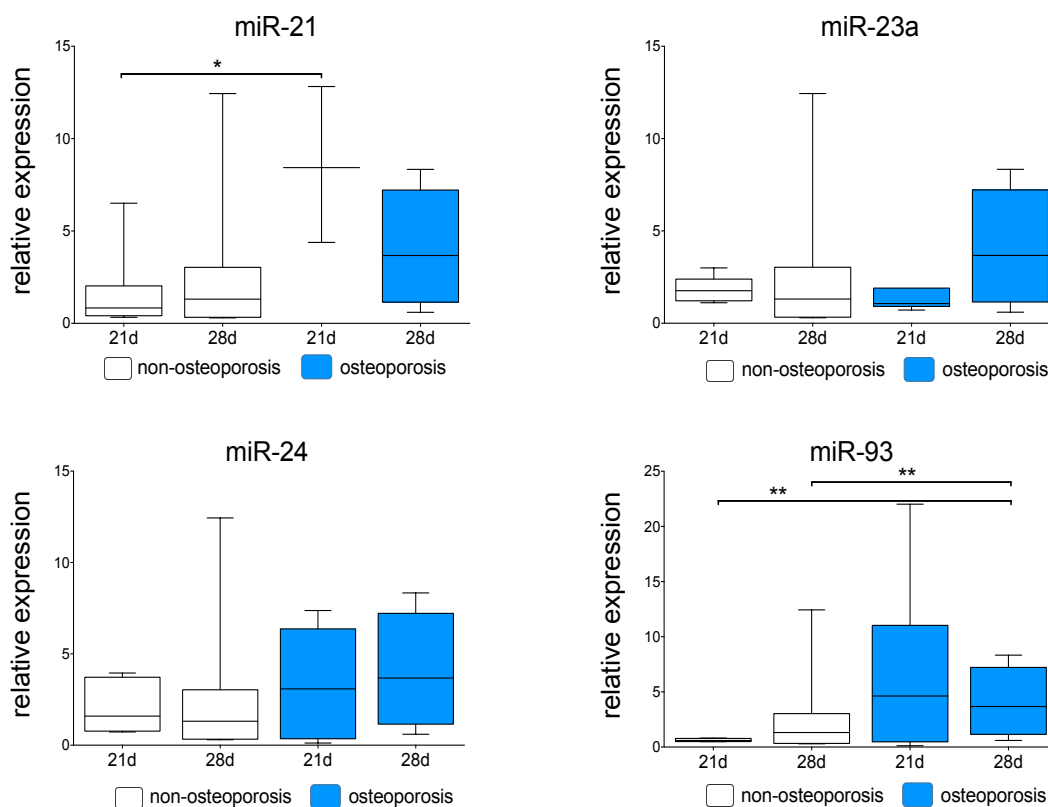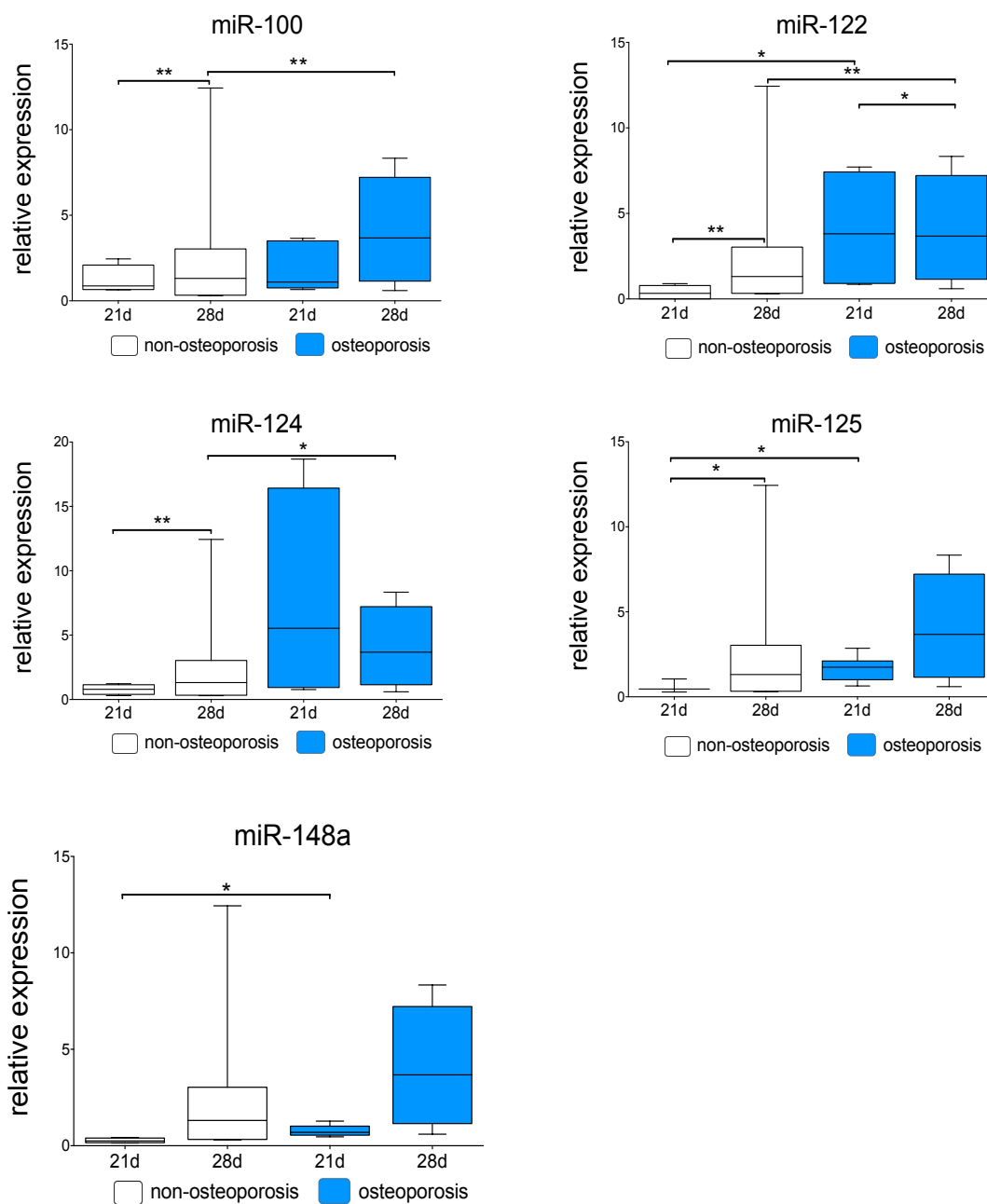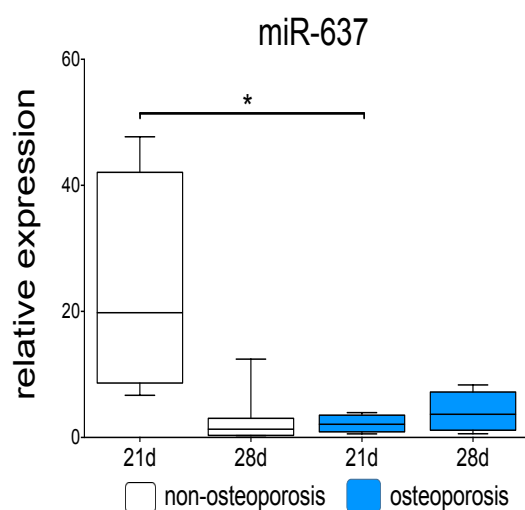
Figure 12 Relative miRNA expression in osteoclast cells normalized to Snord-96a. The presented plots consist of a box bounded by the 25% quantile below and the 75% quantile above, median is shown as an extra line in the box, whiskers show the value of maximum and minimum. Significant differences are indicated by *p <0.05, **p <0.01, ***p <0.001, ****p <0.0001.

In addition, the expression of some miRNAs described in the literature, which may play a role in osteoclastogenesis, were investigated (Figure 15). For this purpose, methodological and statistical procedures were applied in the same way

for miR-31, miR155, miR-223, miR-503 and miR-637. miR-155 showed a significant increase of expression on day 21 (p=0.0095) and on day 28 (p=0.0043) in osteoporotic patients compared to non-osteoporotic patients. miR-503 in turn showed a significant increase in non-osteoporotic patients from day 21 to 28 (p=0.0043) and on day 21 a significant increase in osteoporotic patients compared to non-osteoporotic patients with a p value of 0.0095. The only two miRNAs that showed no significant increase were miR-31 and miR-223 (p>0.05). miR-637 illustrated a significant decrease in osteoporotic patients compared to non-osteoporotic patients on day 21 with a p value of 0.0286.
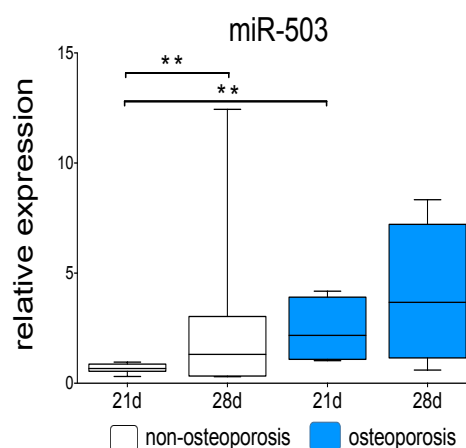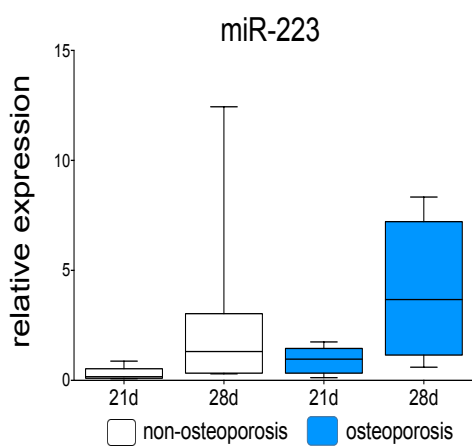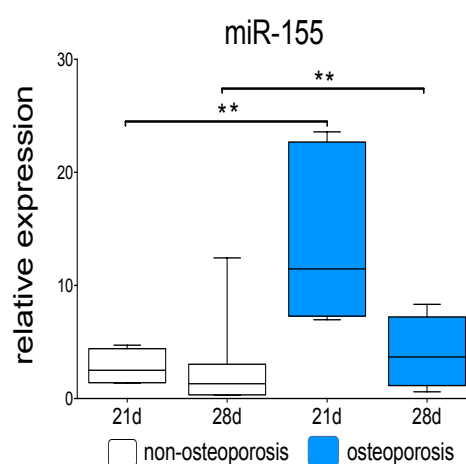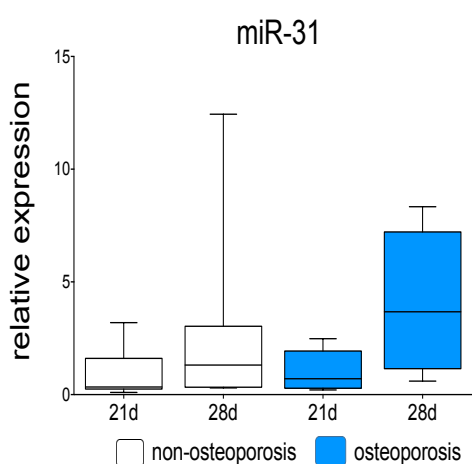
Figure 13 Relative miRNA expressions in osteoclast cells normalized to Snord-96a. The plots consist of a box bounded by the 25% quantile below and the 75% quantile above. The median is shown as an extra line in the box. Additional whiskers show the value of maximum and minimum. Significant differences are defined by *p <0.05, **p <0.01, ***p <0.001, ****p <0.0001. As illustrated, miR-155 and miR-503 show increased values with a p<0.001. miR-637 displays a significant decrease with a p<0.05. y-axis: relative expression, x-axis: examination day 21 and day 28.

To strengthen the characterization of functional osteoclasts, TRAP activity assay was performed. The assay was assessed on day 6, day 21 and day 28. After an initial differentiation, a significantly higher TRAP activity in the osteoporotic group was observed on day 6 (p=0.0256). On day 21, the TRAP activity significantly increased in both groups, while presenting the highest TRAP activity values in the osteoporotic group (p<0.0001). Here on day 21, the TRAP activity is significantly higher in the osteoporotic group compared to the non-osteoporotic group (p<0.001). Considering the differentiation progress, the TRAP activity also increases in the non-osteoporotic group displayed by a significant increase (p<0.01). These presented results are illustrated in Figure 16. Overall, the TRAP activity was higher in osteoporotic cells compared to non-osteoporotic cells.
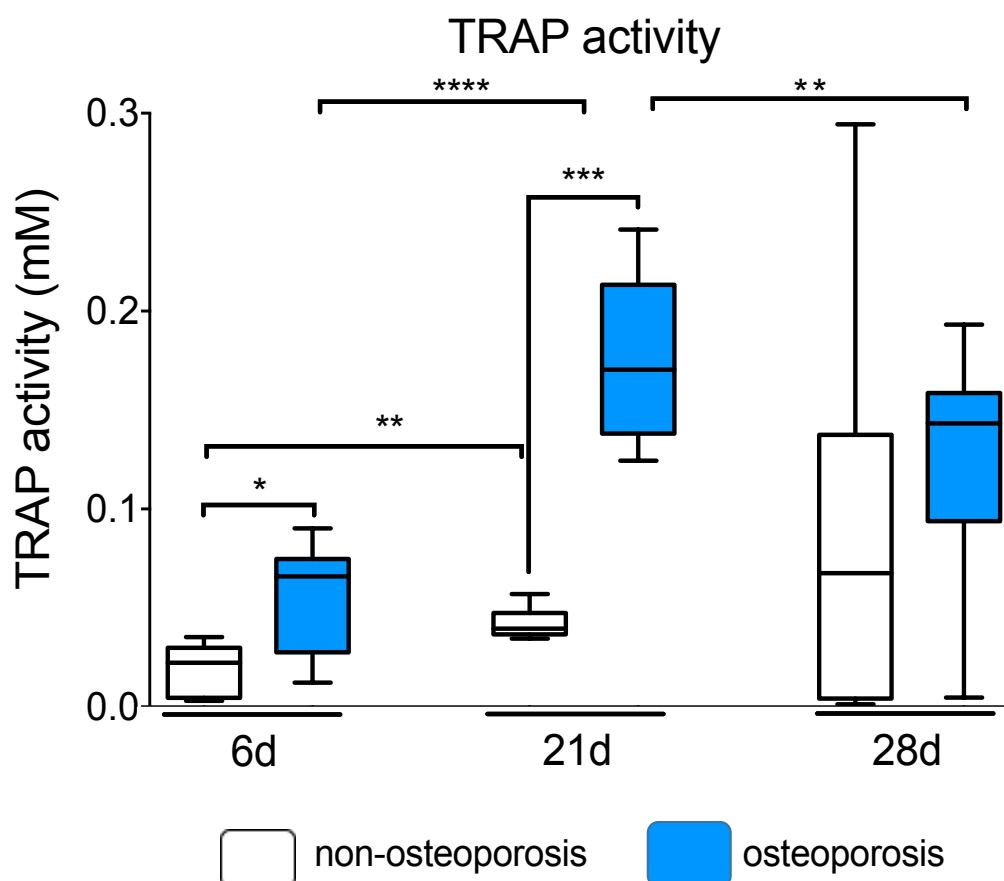
Figure 14 Depicted are three representative fields of view of TRAP-stained samples on day 6, day 7 and day 8 after differentiation. The plots contain a box bounded by the 25% quantile below and the 75% quantile above, median is illustrated as an extra line in the box, whiskers present the value of maximum and minimum. Significant differences are defined by *p <0.05, **p <0.01, ***p <0.001, ****p <0.0001. y-axis: TRAP activity in mM, x-axis: examination day 6, 21 and 28.

To visualize this calculated presence and resorptive activity of osteoclasts, additional TRAP staining was carried out on day 6, day 21 and day 28 after differentiation (Figure 17). Multinucleated osteoclasts are visible. The images show that the cell density and cell size increased macroscopically in the course of differentiation. Monocytes were also found, which at this time had not developed into osteoclasts. The imaged accumulation of TRAP stain implies a successful cell differentiation. Regarding these results, we did not observe any difference in the ability of monocytes to form osteoclasts comparing both groups.

non-osteoporosis   osteoporosis
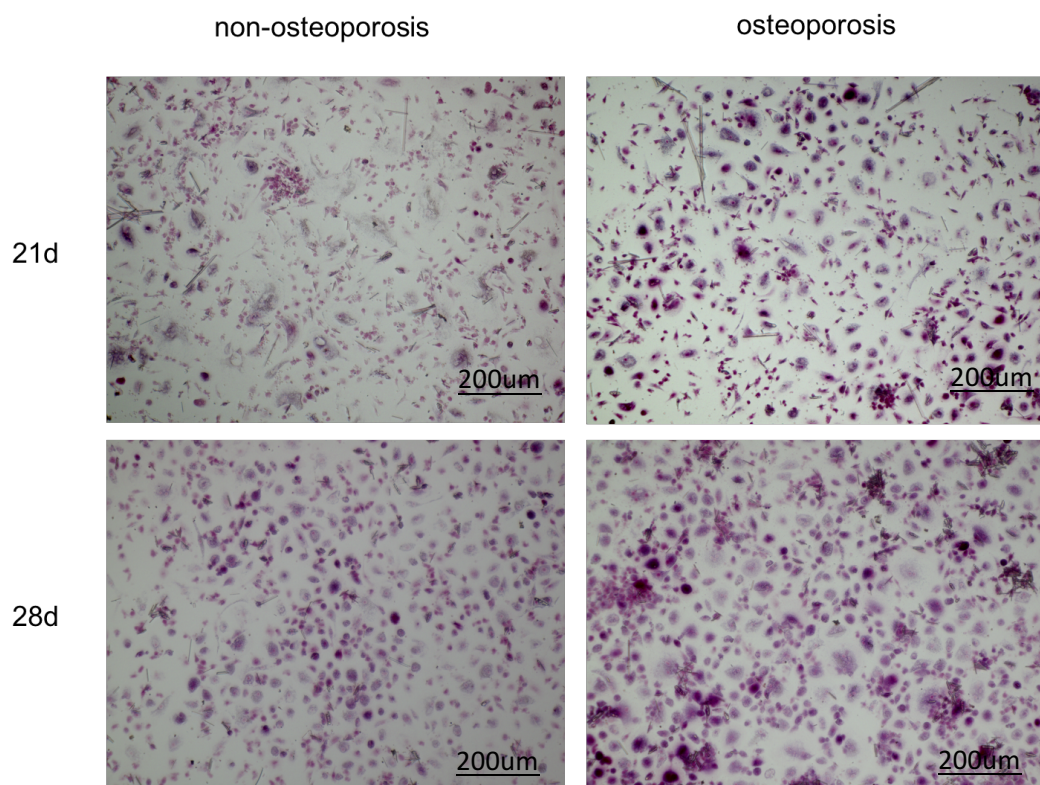
Figure 15 TRAP staining of multinucleated osteoclast cells in osteoporotic and non-osteoporotic cells on day 21 and day 28 after differentiation. Original magnification was 20x for all photomicrographs.

3.2   miRNA inhibition

3.2.1 AntagomiR-100 transfection

The intracellular miR-100 expression during osteogenic differentiation of primary human osteoblasts of osteoporotic and non-osteoporotic patients was ascertained in the preliminary test illustrated in Figure 9. On day 1, 3 and 7, the osteoblast differentiation was terminated to investigate intracellular expression changes. In order to better understand the role of miR-100 on the activity of osteoblasts, miR-100 was suppressed through antagomiR-100 transfection. In Figure 18, the verification of the transfection success displayed similar miR-100 expression

ratios in untreated osteoporotic osteoblast cells and cells treated with a negative control miRNA from Qiagen (Hilden, Germany) (=negative control). miR-100 was significantly suppressed up to 50% (($p<0.0015$)) compared to non-transfected cells and compared to negative control siRNA from Qiagen.
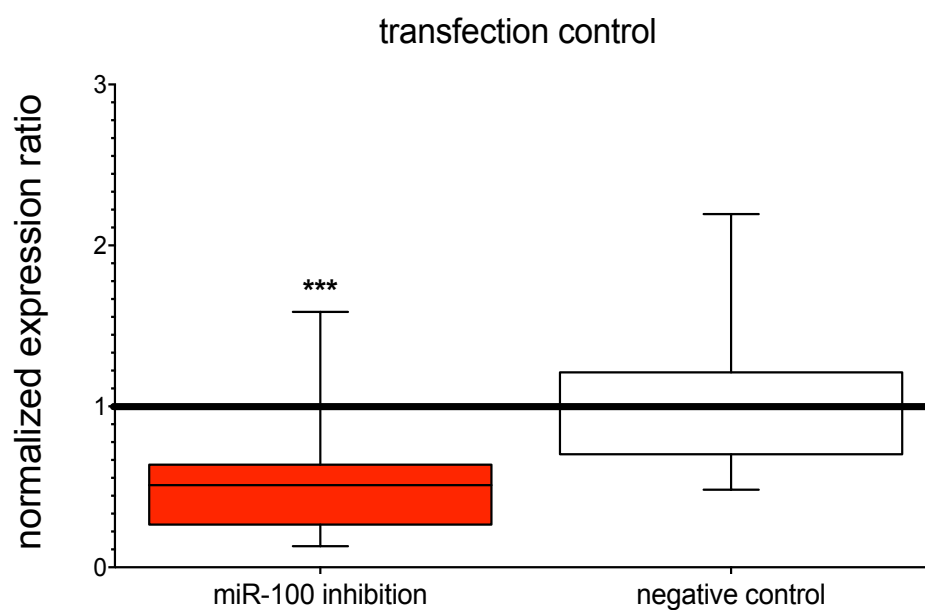
Figure 16 Transfection control with non-transfected osteoporotic osteoblast cells and negative control miRNA from Qiagen after miR-100 inhibition. The plots contain a box bounded by the 25% quantile below and the 75% quantile above, median is illustrated as an extra line in the box, whiskers present the value of maximum and minimum. Significant differences are defined by *p <0.05, **p <0.01, ***p <0.001, ****p <0.0001. y-axis: miR-100 expression, x-axis: antagomiR-100 transfected cells and transfection negative control. The black line represents non-transfected cells.

As shown in Figure 19, the transfection resulted in a suppression of miR-100 in both osteoporotic and non-osteoporotic cells showing a successful down-regulation compared to non-transfected cells. On day 1 ($p<0.0001$) and on day 3 ($p<0.0017$), a significant inhibition was achieved in non-osteoporotic osteoblasts. Osteoblasts of osteoporotic patients significantly decrease on day 3 ($p<0.0033$) and day 7 ($p<0.0001$). A difference in the suppression of both groups could not be shown ($p<0.05$).
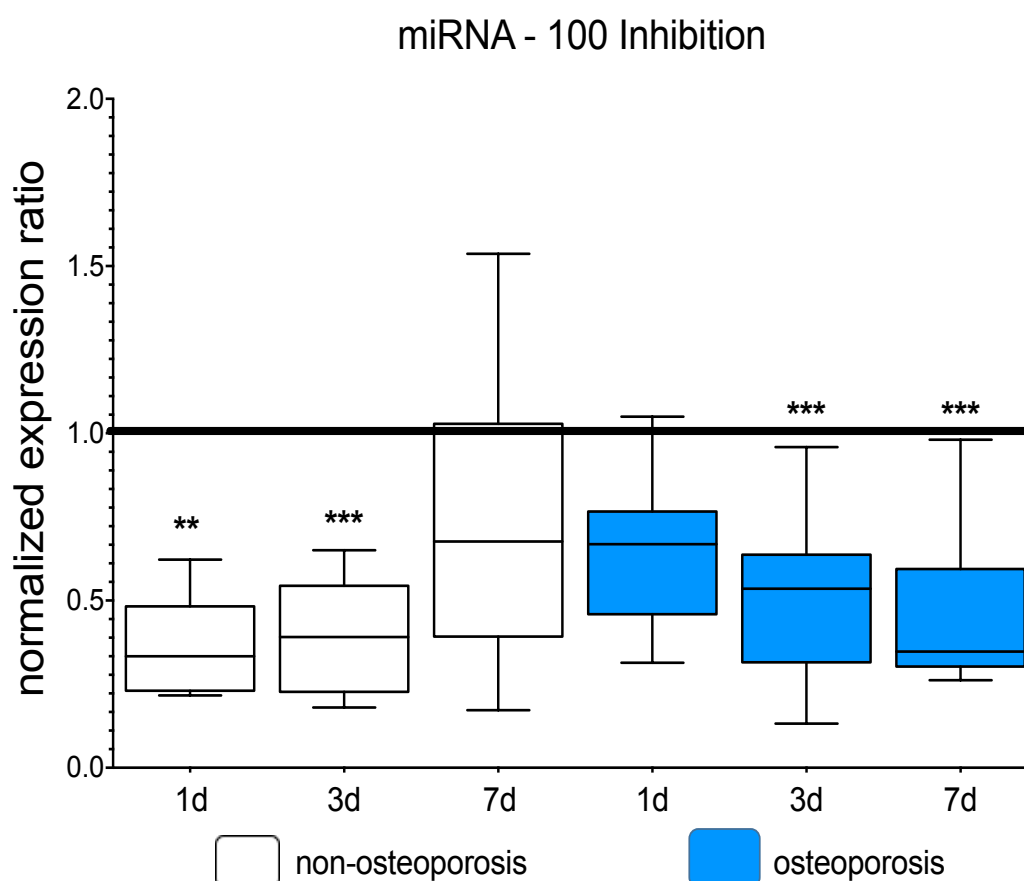
Figure 17 Normalized expression ratio of miR-100 after miR-100 inhibition in osteoporotic and non-osteoporotic osteoblasts. The plots contain a box bounded by the 25% quantile below and the 75% quantile above, median is illustrated as an extra line in the box, whiskers present the value of maximum and minimum. Significant differences are defined by *p <0.05, **p <0.01, ***p <0.001, ****p <0.0001. y-axis: miR-100 expression, x-axis: osteoblasts from non-osteoporotic patients and osteoblasts from osteoporotic patients on day 1, 3 and 7. The black line represents non-transfected cells.

3.2.2 Viability and activity assays after miR-100 transfection

In Figure 20, two independent tests were conducted to investigate cytotoxic side effects after transfection. Both MTT and Alamar Blue assay showed no toxic effects on the cell viability of primary human osteoblast cells in both groups. Regarding the Alamar Blue assay, no reduced cell viability was detectable. In both viability tests, the utilized 1% triton-treated cells that served as a positive

control presented radically minimized values. The negatively transfected control showed similar values as non-transfected cells.
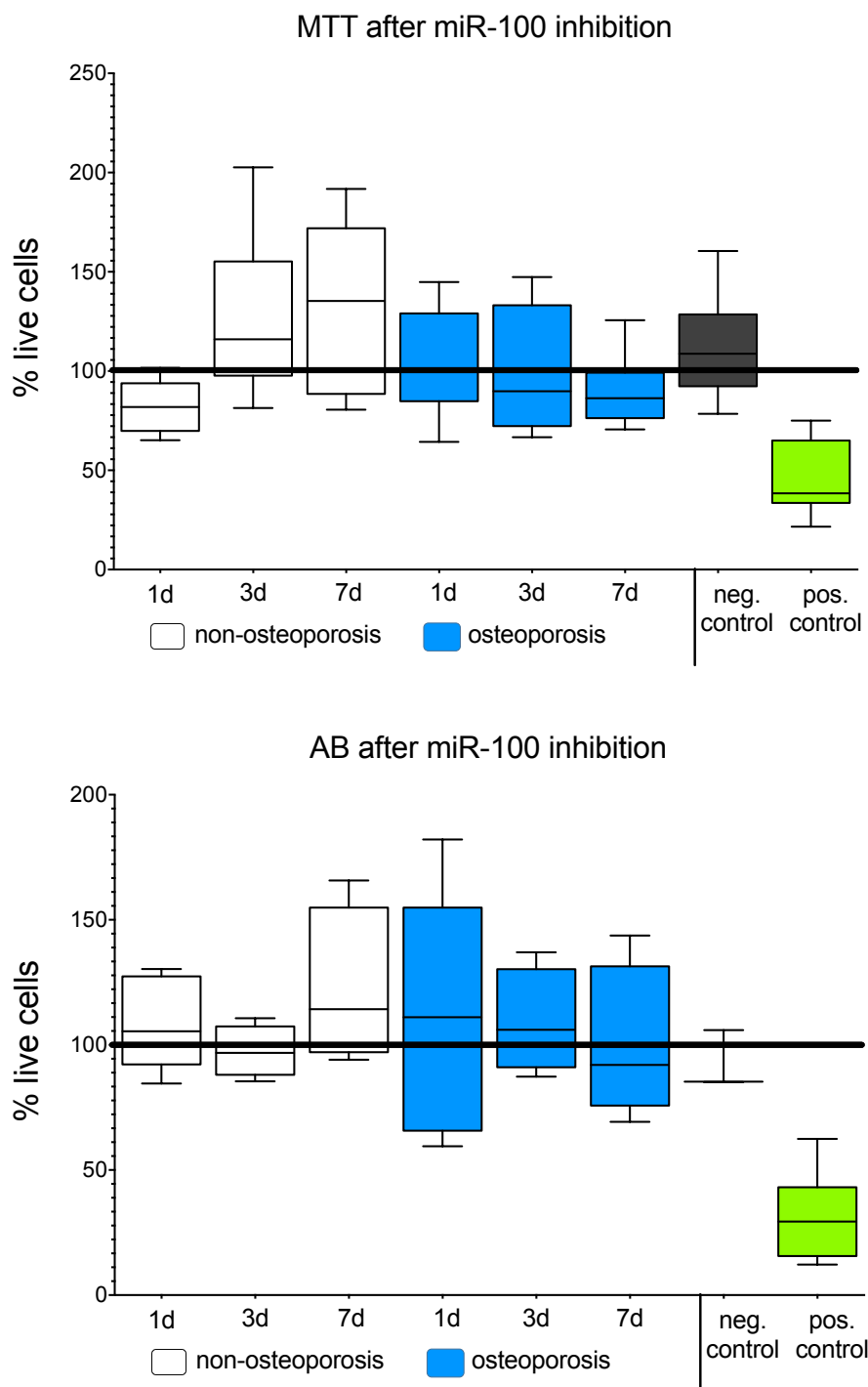
Figure 18 MTT and Alamar Blue (AB) viability tests after miR-100 transfection (percentile of live cells was calculated to control). The black line represents non-transfected cells.

AP activity was executed for osteoblast phenotype analysis after transfection with antagomiR-100. In Figure 21, the AP activity assay indicates no significant differences in transfected and non-transfected cells of both cell groups. There is just a slightly notable increase on day 3 in the osteoporotic group detectable.
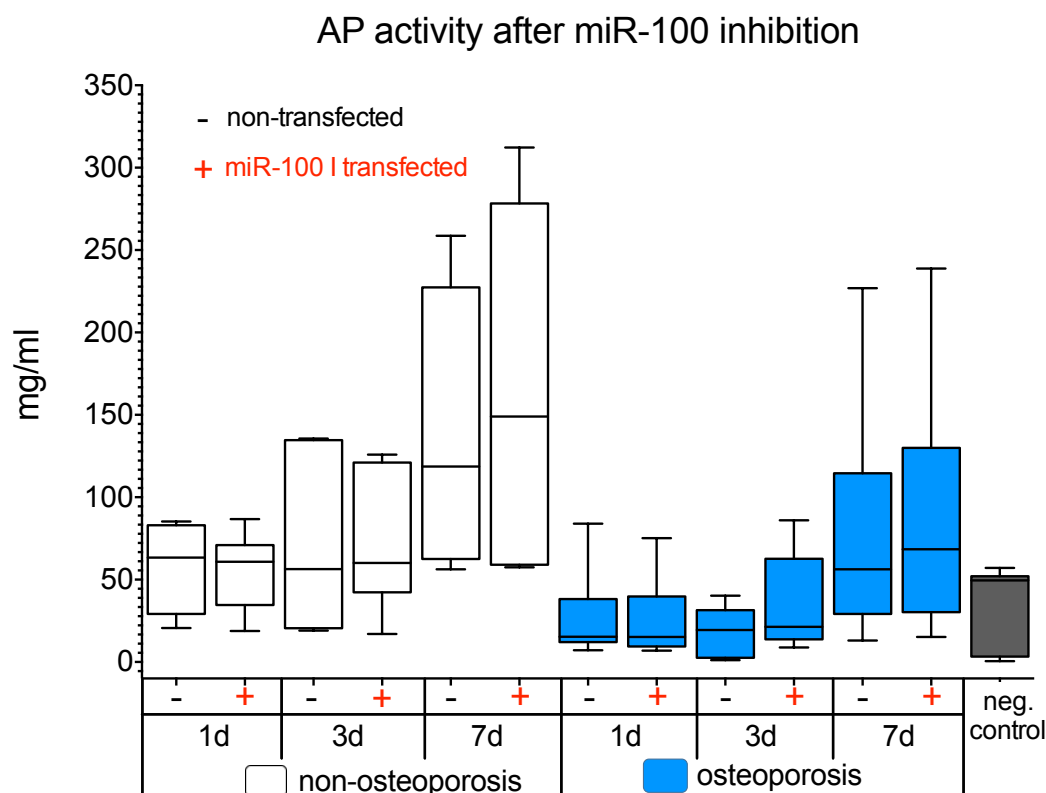
Figure 19 Alkaline phosphatase activity (AP). y-axis: p-Nitrophenol in mg/ml, x-axis: - non transfected osteoblasts, + antagomiR-100 (miR-100 I) transfected osteoblasts of osteoporotic and non-osteoporotic patients on day 1, 3, 7 and negative control. Significant differences are defined by *$p <0.05$, **$p <0.01$, ***$p <0.001$, ****$p <0.0001$.

To evaluate the mineralization capacity by the examination of calcium deposits via ultraviolet light, we accessed alizarin red staining. Figure 22 illustrates AR staining that also shows an increasing mineralization status after the inhibition of miR-100 over 7 days of differentiation in both the osteoporotic and the non-osteoporotic group. No significant differences could be detected in transfected and non-transfected cells of both groups.
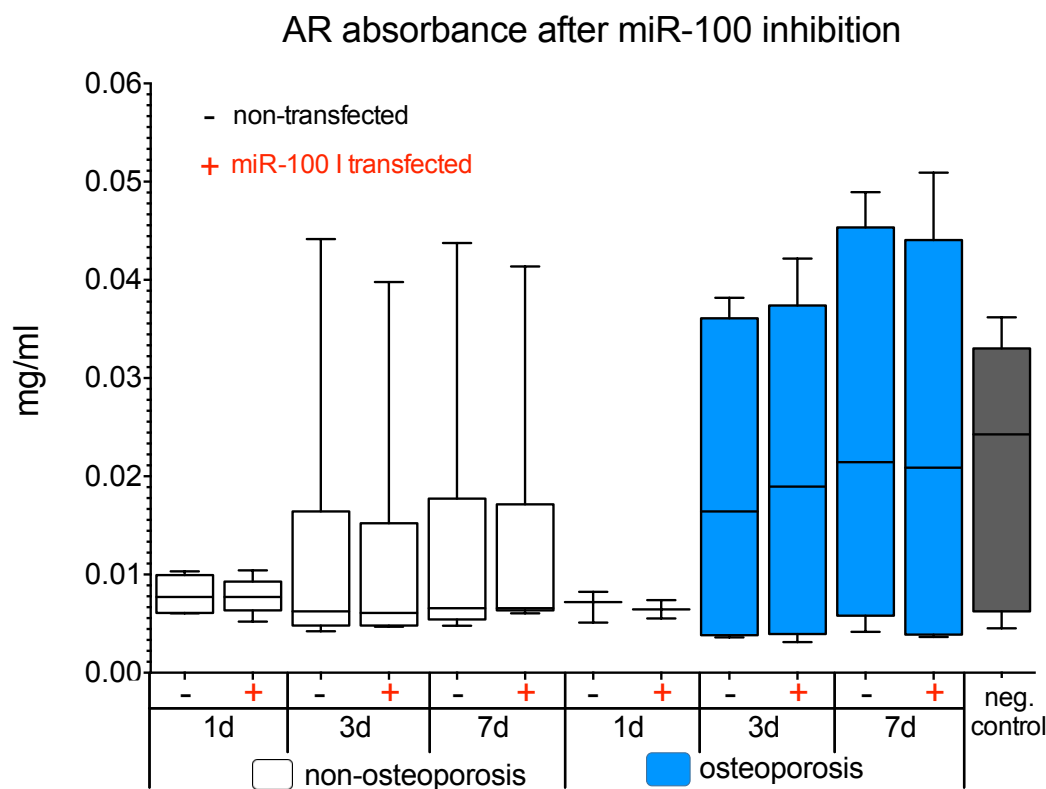
Figure 20 Alizarin red absorbance (AR). y-axis: AR in mg/ml, x-axis: - non transfected osteoblasts, + antagomiR-100 (miR-100 I) transfected osteoblasts of osteoporotic and non-osteoporotic patients on day 1, 3, 7 and negative control. Significant differences are defined by *p <0.05, **p <0.01, ***p <0.001, ****p <0.0001.

3.2.3 Osteogenic gene expression after miR-100 inhibition

Figure 23 and 24 illustrate the influence of miR-100 inhibition on RUNX2, Col1A1, AP and BMPR2 gene expression. All negative transfection controls showed similar values as non-transfected cells.

The normalized expression ratio of osteoblast transcription factor RUNX2 is significantly increased on day 3 in osteoporotic cells compared to non-osteoporotic cells ($p<0.0099$) after miR-100 inhibition. Reduction in the RUNX2 expression level appeared on day 3 in non-osteoporotic cells in comparison to

non-transfected cells. Regarding the COL1A1 gene, the values displayed a steady increase of COL1A1 expression in comparison to un-transfected cells in both groups (Figure 23). Notably, this increasing expression was more pronounced in the non-osteoporotic group, whereas on day 7 we detected a 75% decreased expression ($p < 0.0069$).
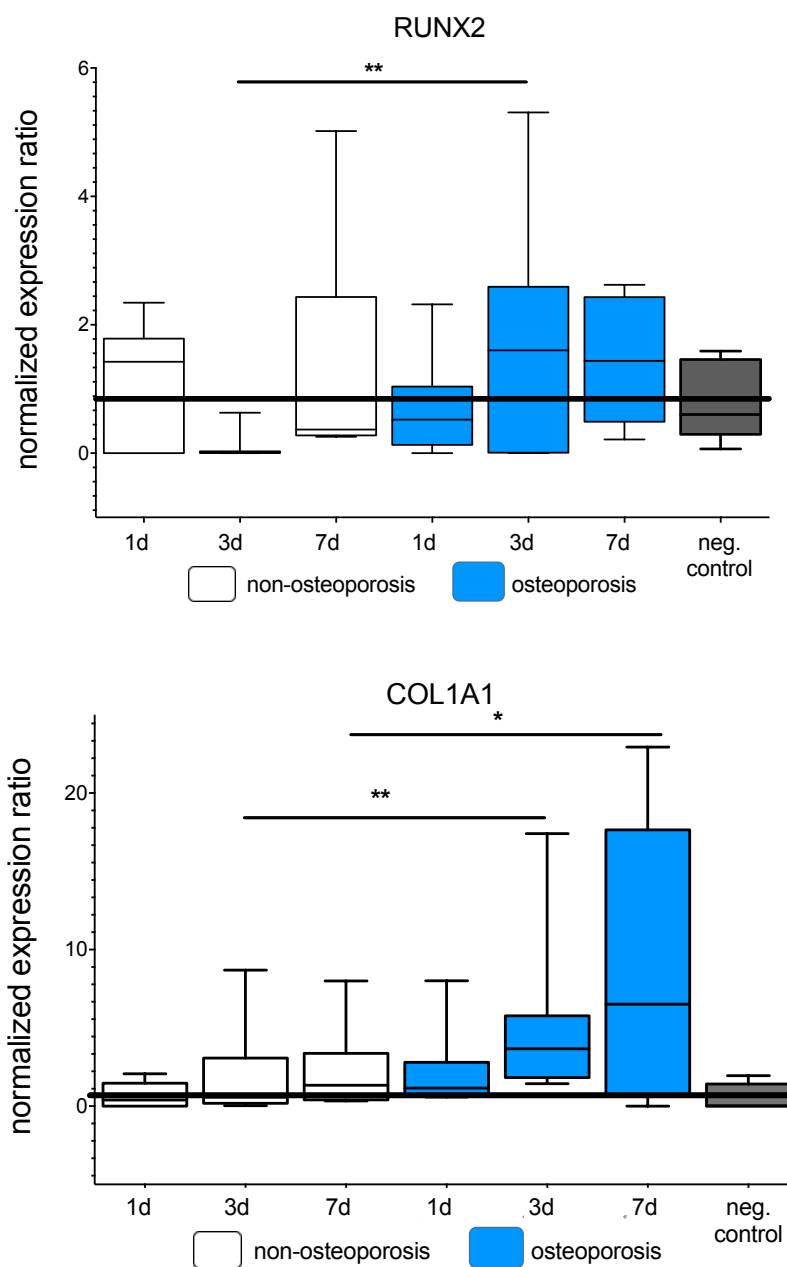

Figure 21 Normalized expression ratio of RUNX2 and COL1A1 after miR-100 inhibition. y-axis: RUNX2 and COL1A1 expression, x-axis: transfected osteoblasts of non-osteoporotic osteoblasts,

osteoporotic osteoblasts and negative control. Significant differences are defined by *p* <0.05, **p* <0.01, ***p* <0.001, ****p* <0.0001. The black line represents non-transfected cells.

Regarding the gene AP, a similar effect after miR-100 inhibition was seen. On day 3 (p=0.0051), a significant increase in osteoporotic osteoblasts could be detected compared to non-osteoporotic osteoblasts after miR-100 inhibition. Even an increasing trend is calculated and illustrated. The investigated gene BMPR2, however, showed no significant expression changes after miR-100 inhibition in both groups.
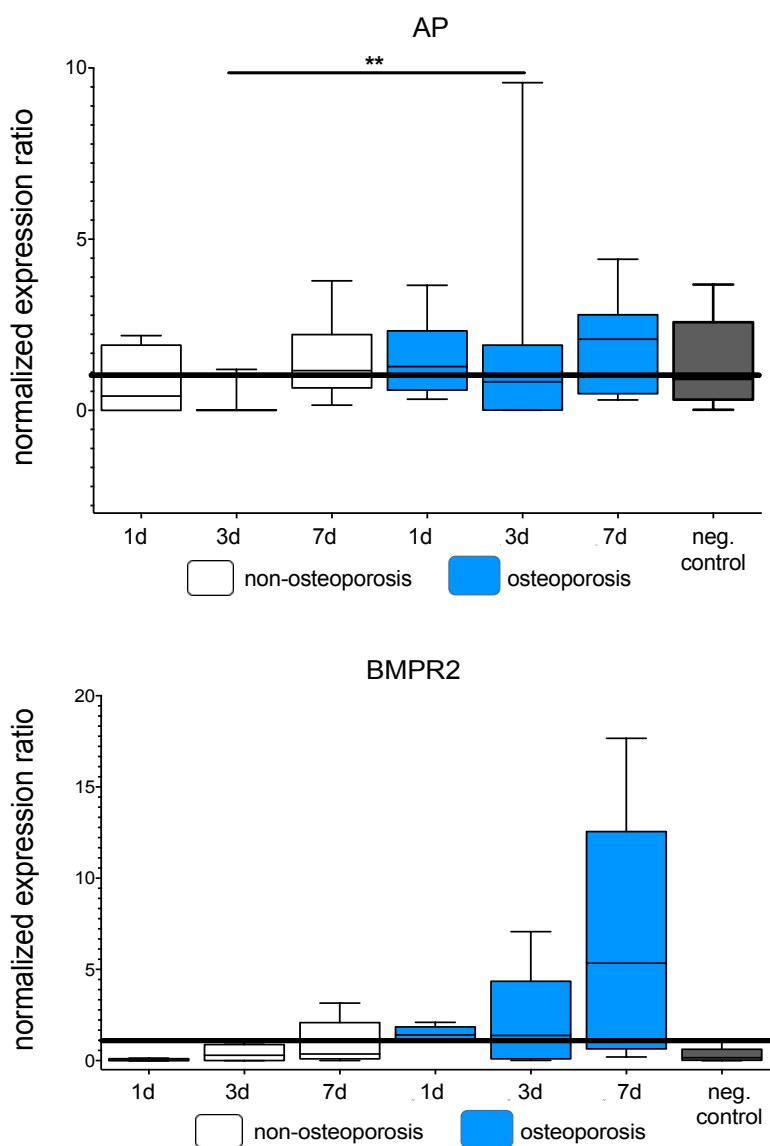
Figure 22 Normalized expression ratio of AP and BMPR2 after miR-100 inhibition. y-axis: AP and BMPR2 expression, x-axis: transfected osteoblasts of non-osteoporotic osteoblasts,

osteoporotic osteoblasts and negative control. Significant differences are defined by *p <0.05, **p <0.01, ***p <0.001, ****p <0.0001. The black line represents non-transfected cells.

3.2.4 AntagomiR-148a transfection

An increased intracellular concentration of miR-148a during osteoblastogenesis in osteoporotic cells compared to non-osteoporotic cells was detected, presenting a suitable candidate for antagomiR-148a transfection. Time points were set on day 3, 7 and 14. The transfection with antagomiR-148a was carried out according to the above-mentioned protocol concerning antagomiR-100 inhibition in osteoblast cells of osteoporotic and non-osteoporotic cells.

First it was necessary to determine the appropriate antagonistic concentration to receive a significant inhibition as explained in the methodic chapter. Figure 25 demonstrates the transfection success displaying similar miR-148a expression levels in untreated cells and cells treated with a negative control miRNA from Qiagen (Hilden, Germany) (=negative control). miR-148a was significantly suppressed up to 60% (p<0.0006) compared to non-transfected cells.
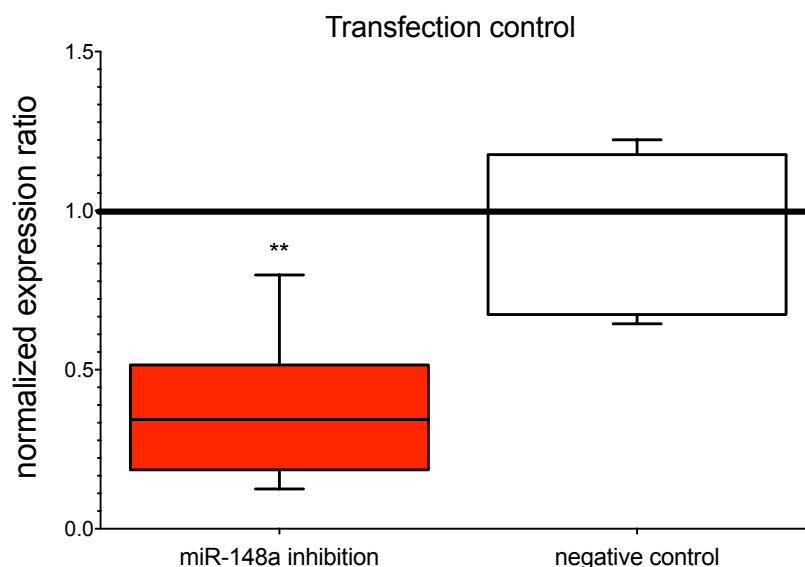

Figure 23 Transfection control with non-transfected cells and negative control miRNA from Qiagen after miR-148a inhibition. The plots contain a box bounded by the 25% quantile below and

the 75% quantile above, median is illustrated as an extra line in the box, whiskers present the value of maximum and minimum. Significant differences are defined by *p <0.05, **p <0.01, ***p <0.001, ****p <0.0001. y-axis: miR-148a expression, x-axis: antagomiR-148a transfected cells and transfection negative control. The black line represents non-transfected cells.

By applying miR-148a inhibitor on day 3, a significant 75% (p<0.05) reduced expression was detectable in osteoporotic cells, which shows a slight decrease up to 50% (p<0.05) on day 7 compared to non-transfected cells. Regarding non-osteoporotic cells, the use of antagomir-148a caused a significant 50% (p<0.05) inhibition on day 3 that seems to remains on day 7 (Figure 26).
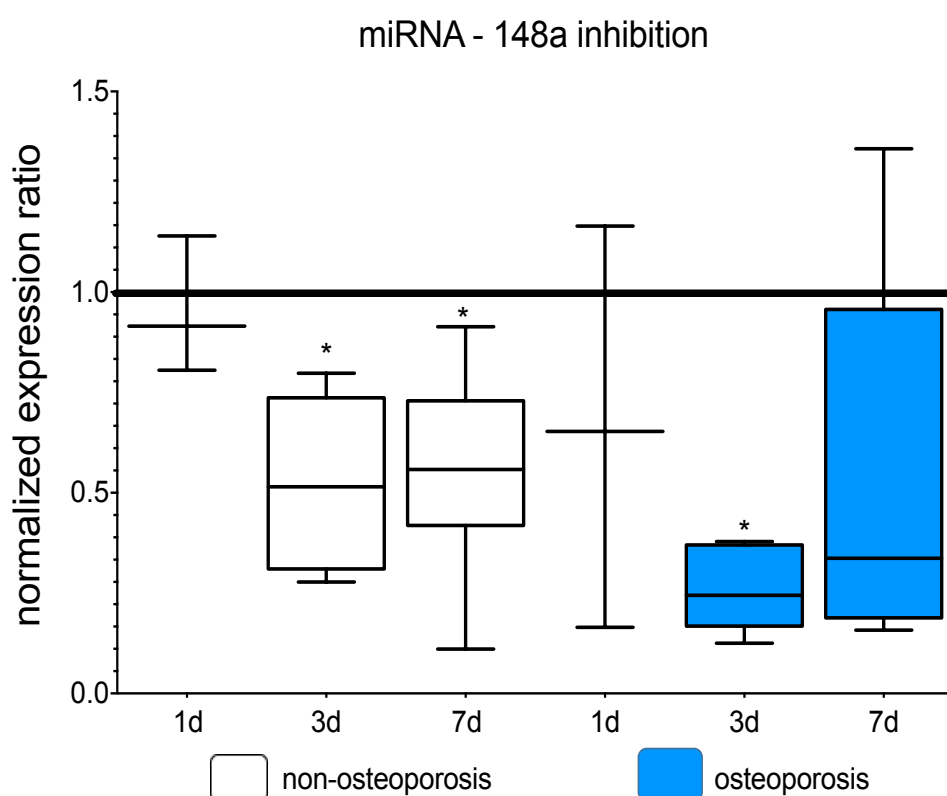

Figure 24 Normalized expression ratio of miR-148a after miR-148a inhibition in osteoporotic and non-osteoporotic osteoblasts. The plots contain a box bounded by the 25% quantile below and the 75% quantile above, median is illustrated as an extra line in the box, whiskers present the value of maximum and minimum. Significant differences are defined by *p <0.05, **p <0.01, ***p <0.001, ****p <0.0001. y-axis: miR-148a expression, x-axis: osteoblasts from non-osteoporotic patients and osteoblasts from osteoporotic patients on day 1, 3 and 7. The black line represents non-transfected cells.

3.2.5 Viability and activity assays after miR-148a transfection

MTT and Alamar Blue assay showed no toxic effects on the cell viability of primary human osteoblasts of each group (Figure 27). There was no change generated neither by one-week differentiation nor by the disease pattern. Regarding the Alamar Blue assay, no enhanced proliferation was detectable. In both viability tests, the utilized 1% triton-treated cells that served as a positive control, presented radical minimized values. Negatively transfected control showed similar values as non-transfected cells.
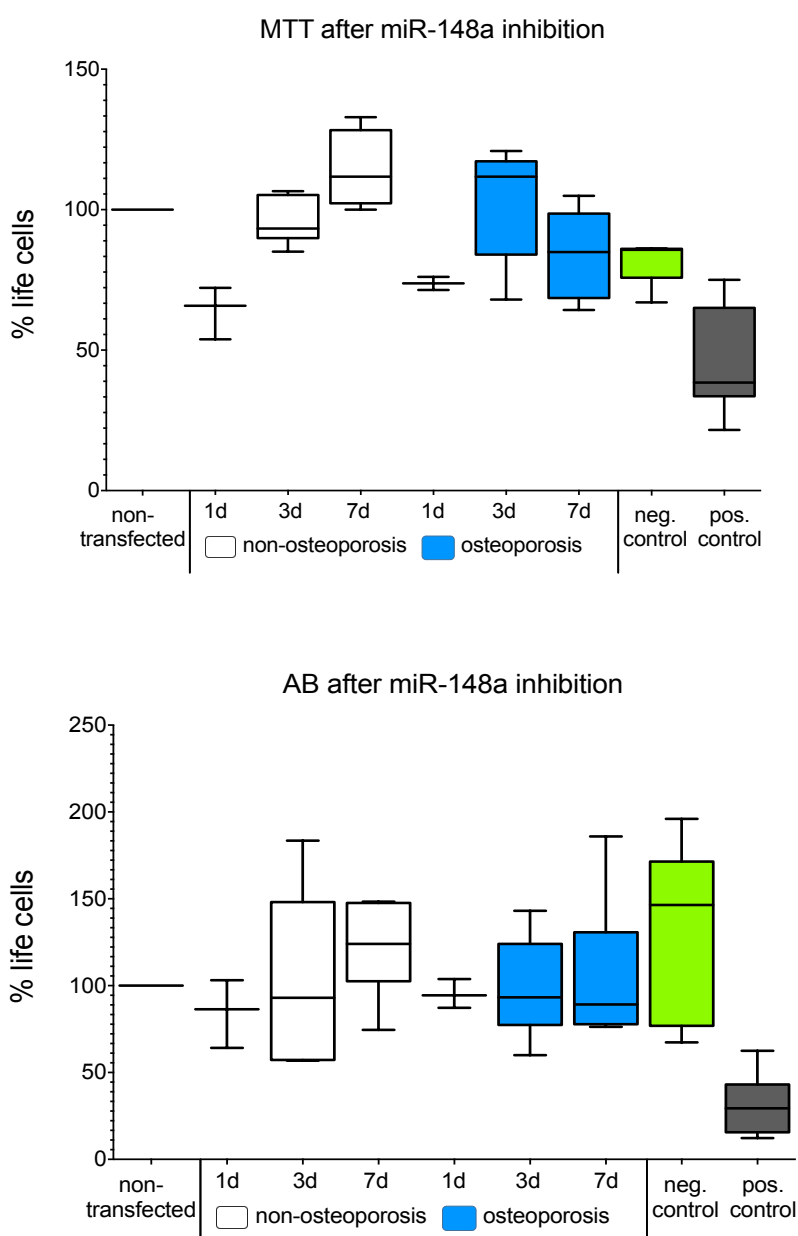
Figure 25 MTT and Alamar Blue (AB) viability tests after miR-148a transfection (percentile life of cells was calculated to control). The black line represents non-transfected cells.

AP activity assay indicated lower values in osteoporotic osteoblasts than in non-osteoporotic osteoblasts (Figure 28). AP activity showed an increase over seven days of differentiation in both groups.

Conducted AR- staining disclosed similar results as in the AP activity assay (Figure 28). In the non-osteoporotic group, a consistent increase over seven days was present. However, in the osteoporotic group, the increase was first present on day 7. The results may give the impression that the AR staining values were minimally lower in 148a-transfected cells compared to non-transfected cells.
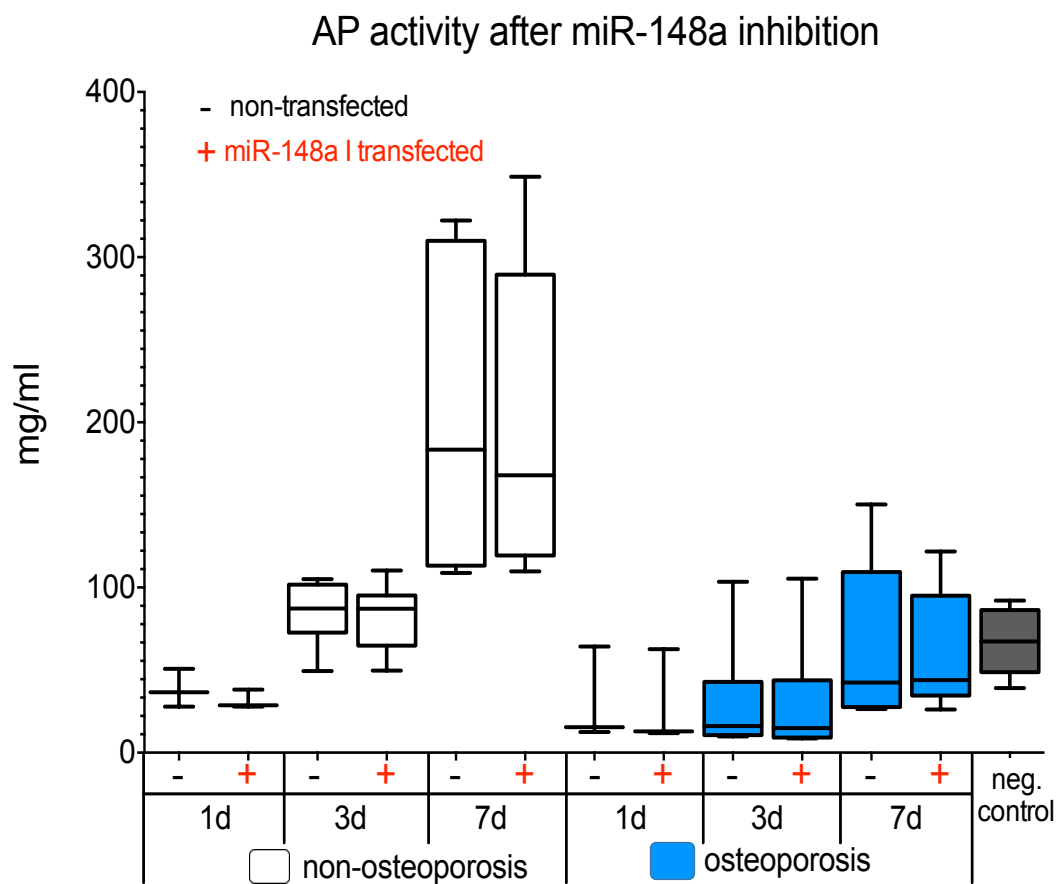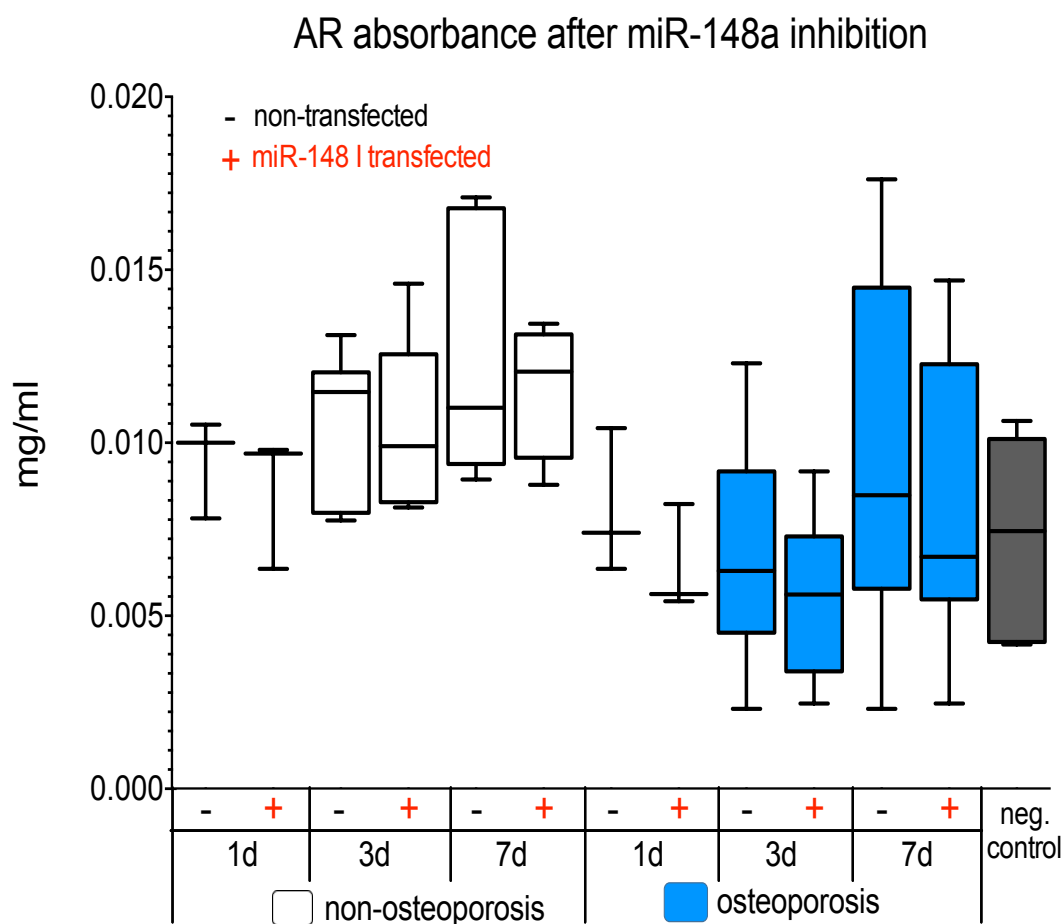
Figure 26 Alkaline phosphatase activity (AP) (y-coordinate axis: p-Nitrophenol in mg/ml) and Alizarin red staining after miR-148a (miR-148 I) inhibition. y-axis: p-Nitrophenol in mg/ml and AR in mg/ml, x-axis: - non transfected osteoblasts, + antagomiR-100 transfected osteoblasts of osteoporotic and non-osteoporotic patients on day 1, 3, 7 and negative control. Significant differences are defined by *$p <0.05$, **$p <0.01$, ***$p <0.001$, ****$p <0.0001$.

3.2.6 Osteogenic gene expression after miR-148a inhibition

Figure 29 and 30 illustrate the influence of miR-148a inhibition on RUNX2, COL1A1, AP and OPG. All negative transfection controls achieved in this various gene expression analyses showed similar values as non-transfected cells.

RUNX2 showed no influence in the expression level on day 3 in osteoporotic cells, however, this steady effect further slightly decreased on day 7. In contrast, an up to 60% (p<0.0099) reduction in the RUNX2 expression level appeared on

day 3 in non-osteoporotic cells in comparison to non-transfected cells. On day 7, an up to 40% (p<0.0099) down-regulating effect was seen in non-osteoporotic cells.

COL1A1, that is essential for coding bone matrix, displayed similar values in osteoporotic and non-osteoporotic patients. Here, no influence between miR-148a transfected osteoporotic and non-osteoporotic cells could be detected.
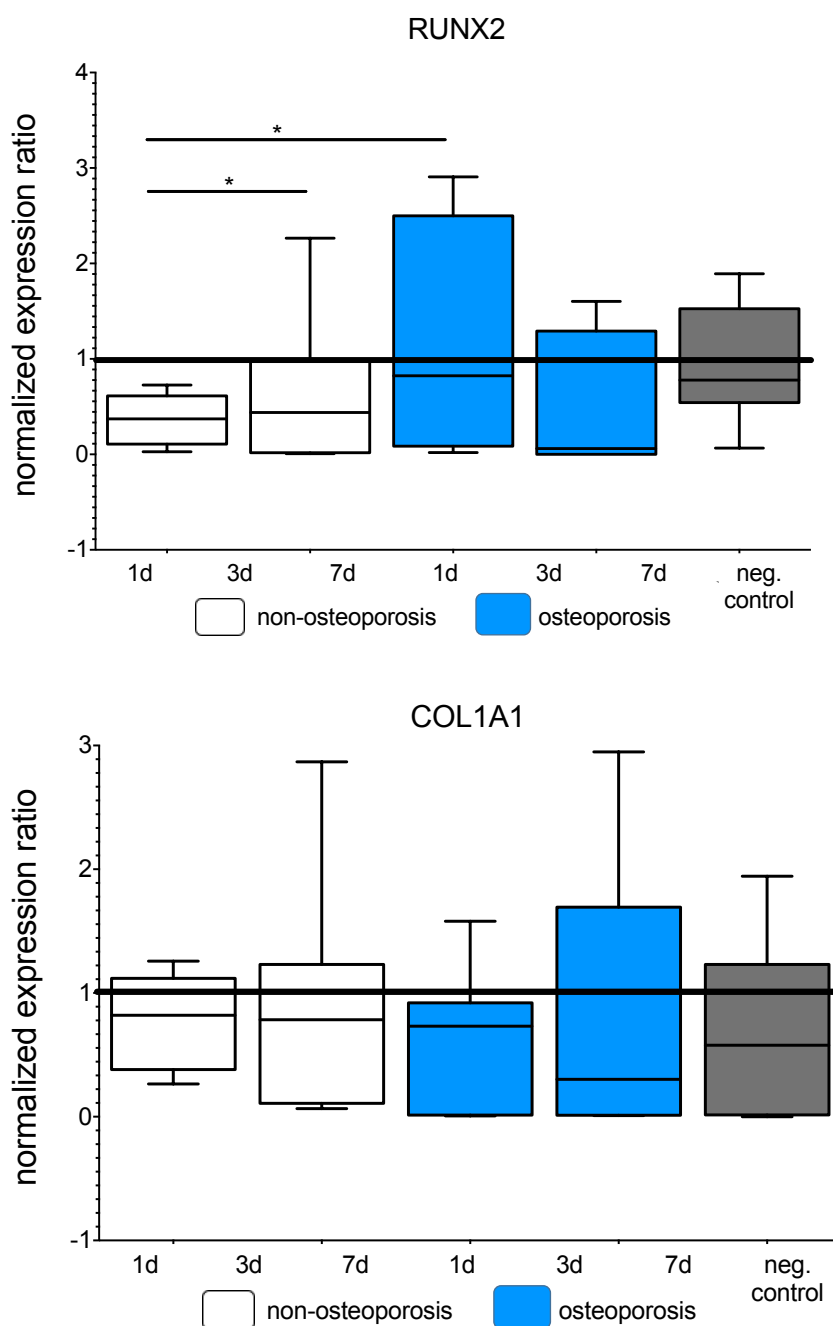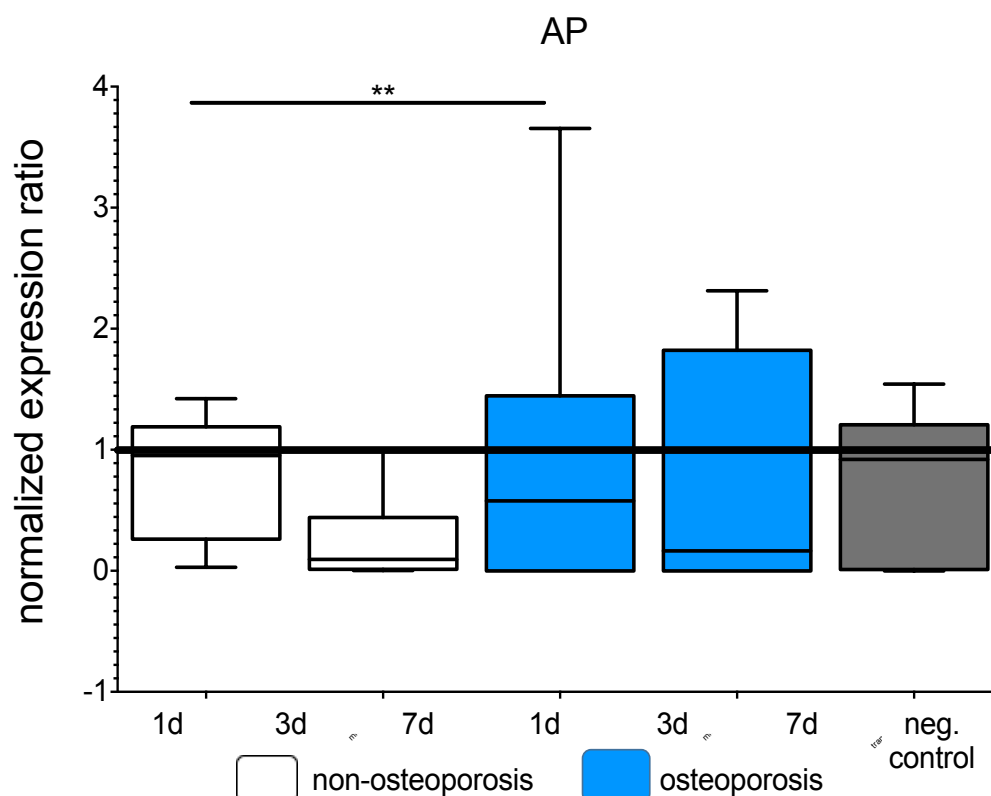
Figure 27 Normalized expression ratio of RUNX2 and COL1A1 after miR-148a inhibition. y.-axis: RUNX2 and COL1A1 expression, x-axis: transfected osteoblasts of non-osteoporotic osteoblasts, osteoporotic osteoblasts and negative control. Significant differences are defined by *p* <0.05, **p* <0.01, ***p* <0.001, ****p* <0.0001. The black line represents non-transfected cells.

Regarding bone alkaline phosphatase gene, the values displayed a steady reduction of AP expression in comparison to un-transfected cells in both groups. Notably, this decreasing expression was more pronounced in the non-osteoporotic group, whereas on day 7, we detected a 75% decreased expression (p<0.0069) (Figure 30).

OPG, the gene examined in the next step, shows a significant 57-fold up-regulation on day 7 (p<0.0087) in non-osteoporotic cells compared to day 7 in osteoporotic cells. In addition, within the non-osteoporotic group, OPG shows a significantly 26-fold (p<0.0317) increased expression on day 7 in comparison to day 3 (Figure 30). On day 3 and day 7 in osteoporotic cells, a slightly continuous decrease was detectable.
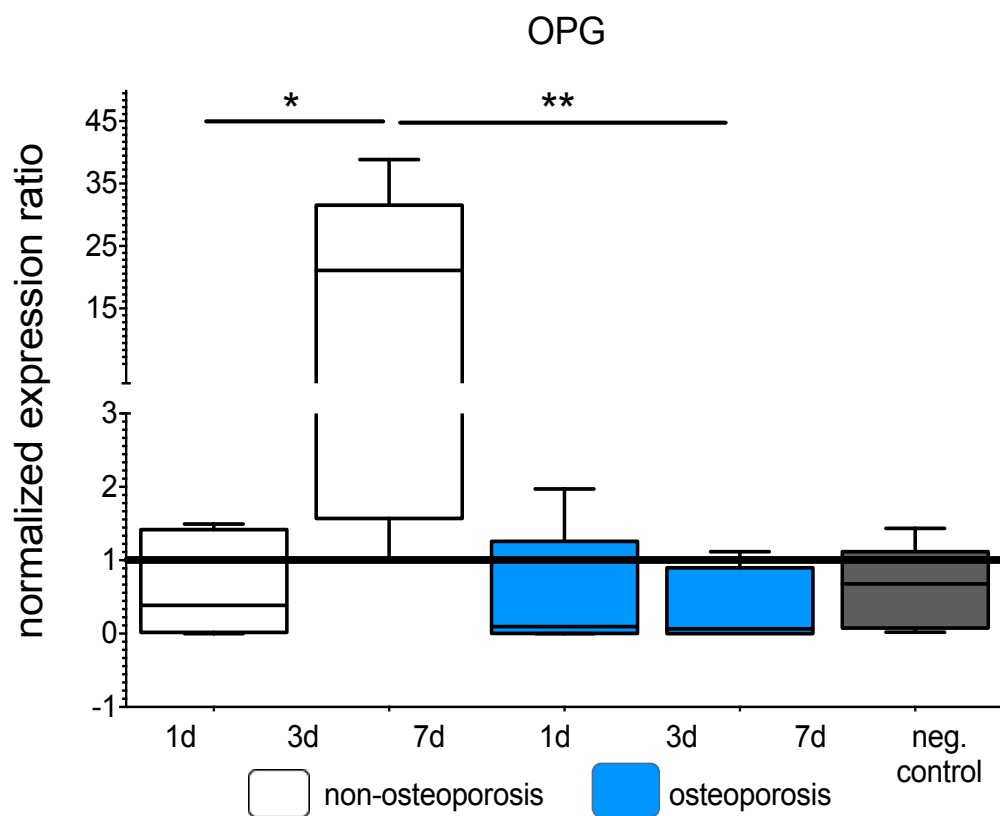
Figure 28 Normalized expression ratio of AP and OPG after miR-148a inhibition. y-axis: AP and OPG expression, x-axis: transfected osteoblasts of non-osteoporotic osteoblasts, osteoporotic osteoblasts and negative control. Significant differences are defined by *p <0.05, **p <0.01, ***p <0.001, ****p <0.0001. The black line represents non-transfected cells.

4 Discussion

4.1 Four miRNAs correlating to BMD are overexpressed and gender-independent in osteoporosis

Senescence of cells, especially of osteoblasts and osteoclasts in osteoporosis, is a sustained matter of examination and its potential impact on bone homeostasis and osteogenic gene modifications is up to date still largely obscured. Molecular cellular changes affected through miRNA signaling pathways are still not sufficiently clarified and understood. However, they would provide a new potential biomarker and target for future diagnosis, classification and treatment (Seeliger, Karpinski et al. 2014). Scientifically, it is to clarify whether expression differences of miRNAs exist depending on the gender, since in view of the fact that some studies describe a potential non-gender-dependency and since this would impact on selective miRNA therapy regimes (Mooney, Raoof et al. 2015). In this context, a previous work of Seeliger et al. registered nine significantly up-regulated circulating miRNAs in serum of osteoporotic females (Seeliger, Karpinski et al. 2014). The aim of this scientific work was to analyze the network of miRNA function, miRNA expression and the phenotype of bone cells to improve our understanding of genetic complexity in bone diseases.

In this study, therefore, it was the aim to expand our knowledge of gender-dependent miRNA transactions in serum, bone tissue, osteoblasts and osteoclasts to establish new diagnostic and therapeutic approaches in regard to the clinical picture of osteoporosis, on their base in turn further research can be build up. Especially, gender-specific expressions are crucial for the future utility of miRNAs as biomarkers. Beside therapeutic scarcities, however, there are no other significant means of radiation-free diagnosis or detection of patients at risk and complications besides DXA or qCT measurements (Statement 2000). This way, the detection of miRNAs as small non-coding RNA segments involved in the

control of bone homeostasis-related pathways, has moved basic bone research into a new era of biomarkers providing the basis for further innovation to expanse diagnostic options.

A total of 9 miRNAs was investigated in serum, bone tissue, osteoblasts and osteoclasts of osteoporotic and non-osteoporotic patients: miR-21, miR-23, miR-24, miR93, miR-100, miR-122, miR-124, miR125b and miR-148a. According to the presented outcomes, miR-21, miR-24, miR-93 and miR-100 are candidates as biomarkers for detection of osteoporosis based on serum analysis both in female and male patients due to their overexpression, while miR-125b is solely useful for serum diagnosis in females. Considering all our mature miRNA expression analyses in serum, bone tissue as well as intracellularly in osteoblasts and osteoclasts, four up-regulated and gender-independent miRNAs (miR-21, miR-24, miR-93, miR-100) exist with acceptable sensitivity and specificity.
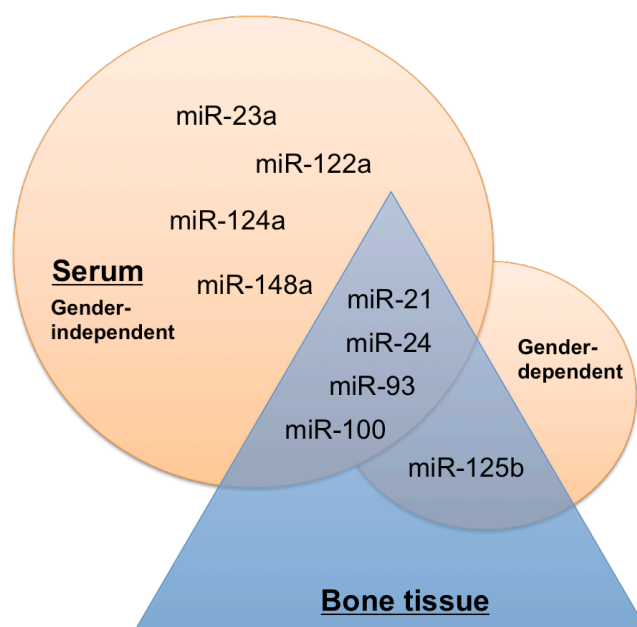

Figure 29 Depicting the significantly overexpressed miRNAs in serum and bone tissue of osteoporotic and non-osteoporotic patients, separated in gender-independency and gender-dependency.

With regard to gender differences in the expression of miRNAs in bone homoeostasis, no literature could be found that had previously examined this

context. General gender-specific differential expression of miRNAs is observed for a number of miRNAs, like the study of Mentzel et al. shows. The study investigated the gender-related differences in the expression of miRNAs in adipose tissue of male and female obese and meager pigs (Mentzel, Anthon et al. 2015).

The miRNAs miR-21, miR-24, miR-93 and miR-100 identified as gender-independent additionally correlate with bone mineral density. These miRNAs allow a targeted classification into non-osteoporosis, osteopenia and osteoporosis disease stages, providing a new approach to diagnostic detection and classification due to biological differences in concentration. Additively, overexpressed miR-125b circulates as the only gender-dependent and BMD-value-correlated miRNA in serum, bone tissue, osteoblasts and osteoclasts of female osteoporotic patients (Figure 31).

Regarding miR-21, also Li et al. described classifying correlations between miR-21 concentrations in plasma and BMD values in postmenopausal women (Li, Wang et al. 2014). Likewise, we conformingly detected these correlations of miR-21 in bone tissue and were additionally able to extend this objective fact for miR-24, miR-93, miR-100 and miR-125b (Li, Wang et al. 2014).

Based on the *in vitro* quantifications of these five listed miRNA concentrations, the disposition in non-osteoporotic patients, osteopenic patients and osteoporotic patients is possible, thereby representing a unique and innovative alternative for BMD measurements *in vitro* without using radiation techniques. The future diagnosis of osteoporosis via miRNA expression analyzes would have a significance, in particular, in countries, which do not have a permanent access to DXA and QCT measurements. Regarding the feasibility in the clinical practice, miRNA-based diagnosis of osteopenia and osteoporosis could be prospectively realized due to serum blood sampling with subsequent targeted and standardized primer analyzation by qPCR.

4.2 Intracellular miRNA overexpressions in osteoporotic osteoblasts and osteoclasts

In our study, we extended our analysis in serum and bone tissue to cell culture (osteoblasts and osteoclasts) for exposing unknown intracellular processes in order to see which cell source could be responsible for the miRNA expression in bone. The intracellular studies in the cells of bone homeostasis have shown that the expressions of miR-21, miR-23a, miR-24, miR-93, miR-100 and miR-125b increased significantly on day 7 in the osteoblast cultivation of osteoporotic patients compared to non-osteoporotic controls. Our results showed that miR-24 was solely overexpressed in osteoblasts, whereas, miR-21, miR-93 and miR-100 were similarly gender-independent and BMD-related overexpressed in both cell types (Figure 32).
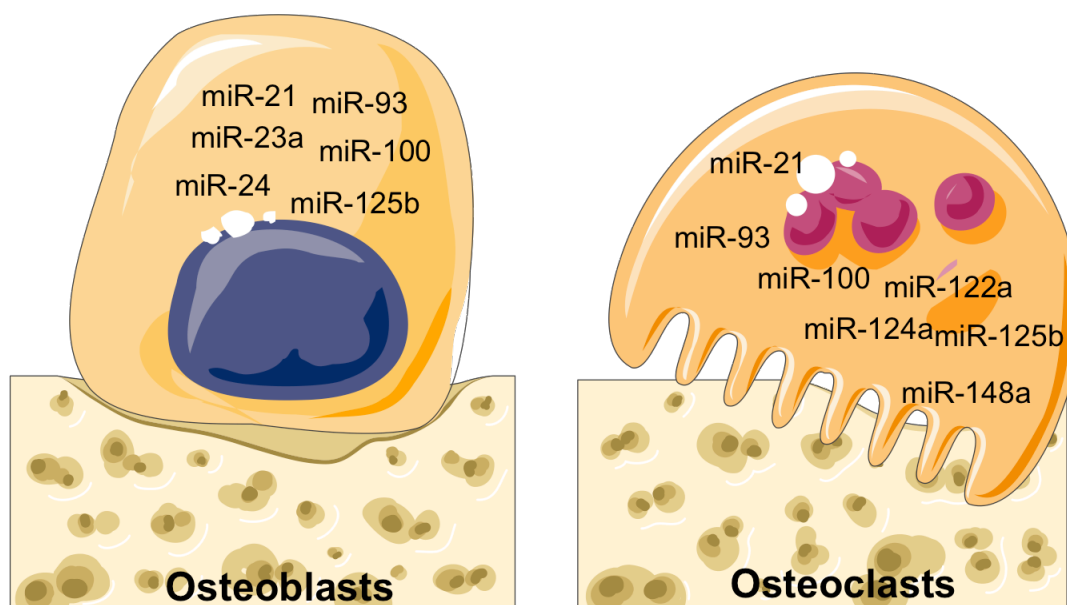

Figure 30 Significantly overexpressed miRNAs in osteoblasts and osteoclasts of osteoporotic and non-osteoporotic patients. *Designed elements were adapted from Servier Medical Art.*

The miRNAs, which can be listed as overexpressed, gender-independent and BMD-value correlated, are discussed below:

miR-21

By analogy, Sugatani et al. examined the pathomechanisms of miR-21 in osteoclasts in greater detail with the results of overexpressed signatures during osteoclastogenesis, promoting increased maturation of osteoclasts from precursor cells. They also described an increase of miR-21 concentration during estrogen deficiency, matching our increasing miR-21 values in osteoporotic patients according to the etiology of osteoporosis (Sugatani and Hruska 2013).

miR-24

The data obtained from the *in vitro* experiment with high concentrations of miR-24 in osteoblasts correspond to the outcomes of Zhao et al. These study results describe an inhibiting miR-24 influence on osteoblastogenesis through T-cell factor 1 (Tcf-1) regulation, resulting in an imbalance in bone homeostasis. AP concentration reductions, a loss of matrix mineralization and a reduction of osteogenic marker expressions visualized the disparity. Due to an *in vitro* inhibition of miR-24, an improved osteoblast differentiation could be achieved through boosting osteogenic differentiation by increasing Tcf-1 (Zhao, Wu et al. 2015). In addition, the miR-24 overexpression was described in cases of hepatocellular carcinoma. Through miR-24 inhibition by complementary strands, a cancer growth advancement and an invasive progress could be reduced, illustrating the impact of miRNA manipulation (Ma, She et al. 2014). With respect to other bone disorders, miR-24 has been shown in connection with the inflammatory osteoarthritis and the terminal differentiation of chondrocytes (Philipot, Guerit et al. 2014).

miR-93

For miR-93 and miR-100, so far only negatively regulating data on osteoblastogenesis exist, whereby their overexpression leads to a deterioration of miR-93/osterix and miR-100/BMPR2 gene signal cascade (Yang, Cheng et al. 2012, Zeng, Qu et al. 2012, Seeliger, Karpinski et al. 2014). Also, other studies describe BMPR2 to play an important role in osteoblast cytoskeletal movement

and cell invasion, being suppressed by overexpressed miR-100 concentrations (Larabee, Coia et al. 2015). For the first time in literature, high values of miR-93 and miR-100 in osteoclast cells could be constituted in this thesis.

miR-125b

Depicting miR-125b, Mizuno et al. described overexpression-induced inhibitory effects on osteoblast cells by cell proliferation impairment. By miR-125b inhibition, an increased osteoblast cell differentiation could be achieved (Mizuno, Yagi et al. 2008). In contrast, Pinto et al. identified high levels of miR-125b during osteoblast differentiation of mesenchymal stem cells, whereas in miR-125b-mimic and antagomiR-125b transfection studies, no effects on differentiation could be achieved. Considering these alluded conflicting results with our obtained data, the miR-125b expression levels are at a significantly higher level among osteoporotic patients assuming an association with a negative change in bone homeostasis. This assumption should be comparatively proven in cell culture experiments using synthetic miR-125b mimics and antagomiR agents in osteoporotic and healthy osteoblasts. Further molecular relationships, confirming our overexpressed concentration values in osteoclast cells, have not been carried out yet by other research groups.

Under consideration of all current data and our outcomes in the cells, we summarize that miR-21 overexpression is a stimulator of osteoclast cell differentiation, whereas miR-24, miR-93, miR-100 and miR-125b overexpression acts inhibitory on osteoblast cell differentiation. These facts confirm the fundamental pathophysiology of osteoporosis based on an imbalance of the two against players of the BMU, resulting in a disequilibrium of bone formation and bone resorption (N. Rucci et al. 2008).

In the literature research, studies could be found, describing the miRNA miR-31, miR-155, miR-223, miR-503 and miR-637 in the context of osteoclastogenesis (Zhang, Zhao et al. 2012, Mizoguchi, Murakami et al. 2013, Chen, Cheng et al. 2014, Xie, Zhang et al. 2015). This group of miRNAs described below, has aroused our interest in the extension of miRNA expression analysis in osteoclasts,

which play a decisive role in the development of osteoporosis:

miR-155 and miR-503

Particularly miR-155 showed a significant increase in the expression of the osteoclasts of osteoporotic patients compared to osteoclasts of non-osteoporotic patients at both observation times. In a study in 2012, Zhang et al. showed that the miR-155 potentiates the inhibitory effect of interferon-β on osteoclasts and thus represents a therapeutic target for the inhibition of osteoclast activity. Comparing both results, they appear contradictory. In this study, the miR-55 was stimulated by the addition of interferon-β (Zhang, Zhao et al. 2012). Our analysis determined the absolute expression in unstimulated cells. In this respect, further cell culture experiments and miRNA expression analyzes are necessary. miRNA-503 was the second miRNA of this selective group, which showed significant overexpression ratios in osteoclasts of osteoporotic cells compared to non-osteoporotic cells on day 21. Chen et al. additionally carried out miR-503 mimic tests with contrary results, leading to the inhibition of bone resorption in ovarectomized mice (Chen, Cheng et al. 2014).

miR-637

Interestingly, miR-637 showed a significant decrease on day 21 in osteoclasts from osteoporotic patients compared to osteoclasts from non-osteoporotic patients. According to the literature research, the expression of miR-637 in osteoclasts has never been investigated. A similar study, however, examined the expression during the cultivation of osteoblasts and adipocytes. Here, also decreased expression values were found in osteoblasts by targeting the gene Osterix while increasing expression values in the adipocytes were detected. The authors mention an intercellular balance between adipocytes and osteoblasts, which can be expanded by our results on osteoclasts (Zhang, Fu et al. 2011).

4.3 miR-100 as a suitable target for antagomiR therapy to maintain osteoblastogenesis

Our previous work stated potential correlations between up-regulated miRNA expressions and an increased risk of fractures in patients with osteoporosis. Following our first string of experiments displaying upregulated miRNA expression levels of miR-100 in serum, bone tissue, osteoblast and osteoclast cells of men and women suffering from osteoporosis, it was a consistent next step to evaluate the effects of *in vitro* suppressed miR-100 expression by use of antagomiR-100. It was our proposition to disclose adverse effects on cellular level, particularly in osteoblasts, which are responsible for bone formation. In general, at the genetic level, osteoporosis is accompanied by several changes in gene expressions resulting in bone formation diversifications. The objective of this experiment was to investigate and to understand alterations of miR-100-related gene expression by miR-100 quantity diminution as well as to rescue the osteogenic capability of osteoporotic cells. Deductively, we tried to display unacquainted interactions between early osteogenic markers and suppressed miR-100 expression levels in addition to their regulative effects on osteoblast cell cultivation of osteoporotic and non-osteoporotic patients.

Although miR-21, miR-93, miR-100 and miR-125b are overexpressed in both cells-types described above, it is yet scientifically unclear whether both cells act as donor cells forming the miRNAs or whether these miRNAs are originally formed by only one of the cells being channeled afterwards by means of the described horizontal transport mechanisms into the recipient cell (Kosaka and Ochiya 2011). In the case of miR-100, we were able to demonstrate donor cell characteristics in osteoblast cells due to an isolated cell cultivation. In future, co-culture experiments containing the BMU should be performed to realistically mimic bone homeostasis and to better assess associated miRNA regulation *in vitro*.

Due to an overexpression of miR-100, BMPR2 gene suppression is generally suppressed resulting in a reduced osteoblastogenesis (Zeng, Qu et al. 2012,

Seeliger, Karpinski et al. 2014) (Figure 33). In our study, the continuous overexpression of miR-100 during osteoblast cell culturing of osteoporotic patients was significantly suppressed by the use of antagomiR-100. Through the utilization of qPCR, we evaluated the transfection success. Via MTT assay and Alamar blue assay (Resazurin), we assessed cell viability and metabolic activity.
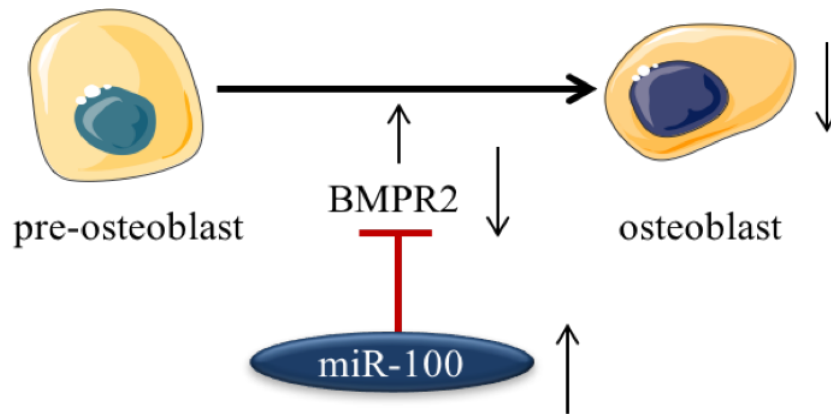

Figure 31 miR-100-regulated gene BMPR2. Overexpression of miR-100 results in a decreased osteoblastogenesis. *Designed elements were adapted from Servier Medical Art.*

Due to this induced suppression, also the expression of early osteogenic genes BMPR2, COL1A1, RUNX2, AP, has changed and increased in osteoporotic specimen samples. Overall, mineralization and proliferation revealed an increase in transfected osteoblasts over the course of our experiments. With the help of the viability tests we used, no harmful effects on osteoblast cells could be detected.

RUNX2

In general, a dose-dependent relationship between osteoblast differentiation and total amount of RUNX2 is described (Zhang, Xiao et al. 2009). By its complete absence, RUNX2 led to a missing bone formation in mice due to the non-appearance of osteoblast differentiation (Otto, Thornell et al. 1997). Li et al. discovered miR-133, which actually plays a role in myogenesis. As an inhibitor of osteogenesis, it directly regulates RUNX2 (Li, Hassan et al. 2008). Furthermore,

direct suppressing effects of miR-29b on RUNX2 could inhibit osteoblast differentiation (Li, Hassan et al. 2009). None of the above-mentioned studies investigated the effect of miR-100 inhibition on the gene RUNX2. We were able to achieve a significant increase of this gene in osteoporotic osteoblasts compared to non-osteoporotic osteoblasts by miR-100 inhibition, presenting miR-100 as an effective target for antagomiR treatment (Kaneto, Lima et al. 2014).

COL1A1

COL1A1 belongs to the genes important for the structure of collagen 1 and is essential for bone matrix (42). Cell culture experiments with antagomiR-29b showed increasing relative expressions of COL1A1 in mesenchymal stem cells. Inhibition of miR-100 showed a significant increase in concentration, which means that COL1A1 represents a target gene of miR-100. Regarding the identification of target genes, Kaneto et al. could not show any relationship between miR-29b and COL1A1. No study has described this relationship between COL1A1 and miR-100 in either non-osteoporotic osteoblasts or osteoporotic osteoblasts.

AP

AP gene, as an early osteogenic marker initializing mineralization, was significantly increased in osteoporotic cells compared to non-osteoporotic cells after miR-100 inhibition (Nakashima and de Crombrugghe 2003). Also, due to an antagomiR-138 transfection in mesenchymal stem cells, the relative AP gene expression significantly increased (Nakashima and de Crombrugghe 2003). Due to the inhibition of miR-100, it is therefore possible to increase the mineralization capacity in osteoblasts of osteoporotic patients. In addition, AP activity measurements showed an apparent increase in osteoporotic patients compared to non-osteoporotic cells.

BMPR2

miR-100 target gene BMPR2 is part of the TGF-beta superfamily-related BMPs in osteoblastogenesis (Bragdon, Moseychuk et al. 2011). In an *in vitro* model, Zeng

et al. found out that high expression of miR-100 results in an enhanced osteogenesis, while low expression due to the use of an antagomiR-100 results in a depressed osteogenesis in adipose-derived stem cells (Figure 34). The group was able to identify BMPR2 as the target miR-100 using target prediction analysis and dual luciferase report assays (Zeng, Qu et al. 2012). The results described in this thesis fit the results of Zeng et al.: suppressing miR-100 in osteoblast cell culture resulted in increased BMPR2 values in the osteoporotic and non-osteoporotic group with a tending higher value ratio in the osteoporotic group.
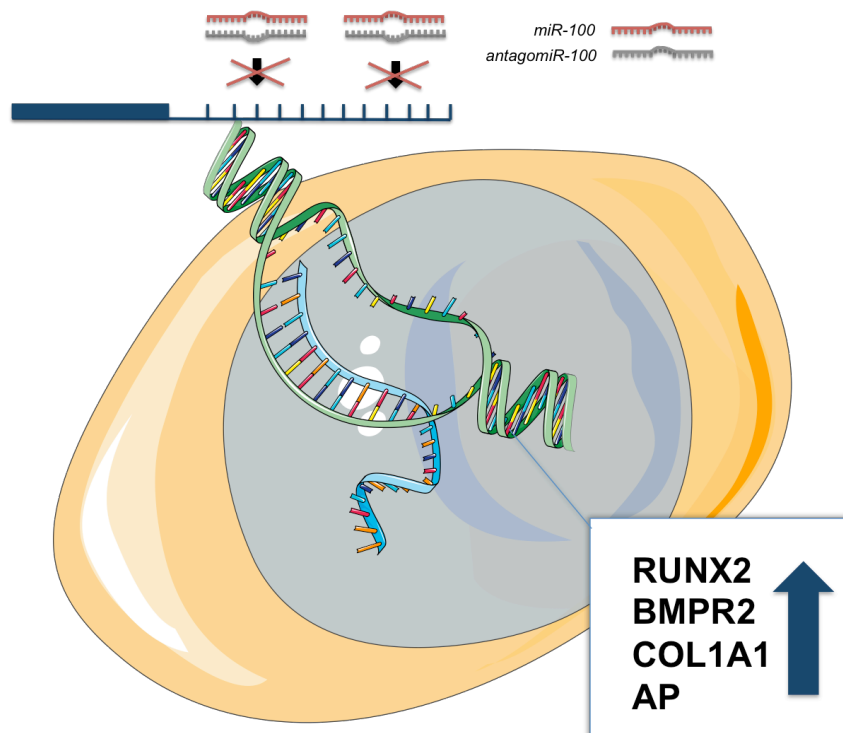

Figure 32 Significantly up-regulated early osteogenic genes after transfection with antagomiR-100 in osteoblast cells. *Designed elements were adapted from Servier Medical Art.*

To steer bone cell imbalance into the opposite direction in order to induce osteogenic differentiation of osteoblasts, our results demonstrated that lipotransfection is a successful method to insert antagomiRs intracellularly for cell culture investigations *in vitro* without exerting detrimental effects on the cells. By suppression of miR-100, which turned out to be a suitable candidate for an antagomiR therapy due to the significant gender-independent overexpression, a

better qualitative osteogenic differentiation of the osteoblast cells could be achieved. These results likewise indicate that miR-100 overexpression exerts a decisive influence on the function of osteoblast cells in osteoporosis, which in turn represents a therapeutic target for further development of anabolic osteoporosis medications. Regarding antagomiR therapy, the question arises if it is sufficient to inhibit a single miRNA, such as miR-100, to reach a significant positively regulating systemic effect on bone homeostasis *in vivo* in osteoporotic patients, as in the presented example of RG-101 in chronic hepatitis C-targeting miR-122 (Horvath 2016). It is therefore required to clarify whether a combination of different antagomiR therapeutics is necessary in order to achieve a sufficient cell modulation *in vivo* or whether another of the 5 identified miRNA inhibitions displays a more effective option for miRNA-targeted therapy. Regarding osteoporosis, it is also relevant to find out with which existing medication class the antagomiR therapy can be carried out in combination concerning clinical studies.

When debating the clinical application of our antagomiR *in vivo* organisms, one has to take into consideration that the described *in vitro* experiments took place under specific conditions, since superiorly hormonal regulations and otherwise negative influences are missing. Because various up- or downregulated miRNAs may be associated with an increased tumor growth, according to the current state of relevant studies, it is not predictable if a patient's miRNA downregulation leads to an increased risk of tumor growth (Liffers, Munding et al. 2011). Studies for example describe an association of a suppressed miR-100 expression with non-small cell lung cancer, ovarian cancer, hepatocellular carcinoma, esophageal squamous cell carcinoma, blood cancer and nasopharyngeal cancer (14-19). In contrast, there are also studies that have shown a positive benefit due to the inhibition of the miR-100, such as a better response to human glioblastoma cells on radiotherapy and a reduced risk for osteosarcoma and breast cancer diseases (Ng, Yan et al. 2010). Equally, there may be a concomitant low risk for other tumor diseases (Ge, Sun et al. 2013). Wherein, not only a risk for cancer must be considered, but also a risk for cardiovascular and infectious diseases (van Rooij and Olson 2012, Horvath 2016). Thus, a tissue-specific delivery is considered as a

goal to exclude harmful effects in other tissues and cells. This goal on the one hand could be achieved through means of a targeted nucleic acid conjugation that solely inhibits the miRNA of desired cells. On the other hand, a specific lipid-based-antagomiR formula could promote a targeted cell inclusion (van Rooij and Kauppinen 2014). In order to attain further knowledge concerning potential off-target effects and safety, further extensive preclinical studies in co-cultures and animal models are required for future miRNA-based therapeutic implementation.

4.4 miR-148 inhibition has no maintaining influence on osteoblast activity in osteoporosis

miRNAs have the property to interfere with various gene expression profiles by dis-equilibrating specific target mRNAs or respectively by inhibiting the translation (Moore and Xiao 2013).

In the presented work using qPCR, we showed that during the development of osteoblasts of osteoporotic patients, the expression of miR-148a continuously increased. This evidenced that miR-148a is part of the genetic network predicating the disease picture osteoporosis. In a next step, we proposed to investigate its intracellular role. Corresponding to high expression values in serum, miR-148a also achieved an up to threefold significant overexpression in osteoporotic osteoblasts.

Many miRNAs, comprising miR-148a, are associated with different tumor diseases. Growing evidence indicates that by an up- and down-regulation in their expression, miRNAs in general can function as classical tumor suppressor genes or oncogenes in the genesis of neoplasia and can be used to estimate prognostic clinical outcomes (Hu, Zhang et al. 2012). Depending on the kind of cancer, miR-148a showed a strongly regulated expression. Patients suffering from osteosarcoma, multiple myeloma, hepatocellular carcinoma, colorectal cancer or medulloblastoma displayed a significant up-regulation of miR-148a in plasma and cells (Gokhale, Kunder et al. 2010, Zhang, Li et al. 2011, Hu, Zhang et al. 2012,

Huang, Yu et al. 2012, Yuan, Lian et al. 2012). On the other hand, in ovarian cancer, hormone-refractory prostate cancer, pancreatic ductal adenocarcinoma, hepatoblastoma, breast cancer and in cells as well as in tissue of gastrointestinal cancers, a down-regulation of miR-148a was detectable (Magrelli, Azzalin et al. 2009, Chen, Song et al. 2010, Fujita, Kojima et al. 2010, Liffers, Munding et al. 2011, Zhou, Zhao et al. 2012, Xu, Jiang et al. 2013). In addition, down-regulation of miR-148a was correlated with several cancer prognostics through target gene expression regulation. miR-148a has also been described as a convenient biomarker in human cancer cells (Zheng, Xiong et al. 2014). For instance, a previous study defined the differential expression of miR-148a as a capable screening and prognostic factor for colorectal cancer (Cho 2011). In the case of gastrointestinal cancer, the reduced expression of miR-148a even correlated with an advanced pT stage (Chen, Song et al. 2010).

In the last few years, the significance of miRNA influences on the regulation of cellular processes has increased in importance (Patnaik, Kannisto et al. 2010). The expression of miR-148a in terms of stem cells commonly displayed a down-regulation during differentiation in both analyzed mesenchymal stem cells (MSCs) and in embryonic stem cells (Giraud-Triboult, Rochon-Beaucourt et al. 2011). Merkerova et al. detected a similar down-regulation during hematopoietic stem cell differentiation (Merkerova, Vasikova et al. 2010). Regarding bone development in osteogenically differentiated bone marrow MSCs from young donors, the miR-148a expression levels were suppressed (Gao, Yang et al. 2011). During myogenic differentiation of C2C12 myoblasts, a contrarily increased expression could be detected (Zhang, Ying et al. 2012). Additionally, in collaboration with five other miRs, a miR-148a overexpression during the differentiation of human cord lining-derived MSCs into hepatocytes was observed (Cui, Shi et al. 2013).

The differential expression of miR-148a also plays a role in non-tumor diseases. Song et al. indicated miR-148a as a direct inhibitor of the activin receptor type I gene (ACVR1) both on protein and mRNA level, which belongs to the bone morphogenetic protein (BMP) type I receptor family. This negative coherency may play a causative role in the genesis of rare congenital fibrodysplasia

ossificans progressiva (FOP), which is characterized by a progressive soft tissue ossification owing to sensitization MSCs to the differentiation into osteoblast cells and inferential formation of new bone (Song, Wang et al. 2012).

By using antagomiR-148a, a significantly decreased expression of miR-148a was found. As we conducted two independent viability tests, we were able to make sure that the lipotransfection had no destructive influence on our cells. AP activity assay that offers the possibility for the osteoblast phenotype characterization and AR staining that proves the mineralization capacity represent slight up-regulations during osteoporotic and non-osteoporotic osteoblast differentiation without displaying any discrepancy between transfected or non-transfected cells of both groups. We assume that the time window was set too short for detecting the change of the osteoblast genotype to the osteoblast phenotype or for recognizing significant influential effects regarding the mineralization status. The specified results show that the inhibition of miR-148a did not influence osteoblast activity and mineralization capacity of primary human osteoblast cells of osteoporotic and non-osteoporotic patients significantly positive or negative.

Recently, Cheng and colleagues investigated that an up-regulated miR-148a expression level promotes osteoclastogenesis by targeting the transcription factor MAFB, whereas the suppression of miR-148a extenuates osteoclastogenesis (Cheng, Chen et al. 2013). These and our results underline the wide capacity of miRNAs on different genes and cell developments. Defective molecular mechanisms in the osteogenic differentiation due to genetic or epigenetic deregulations can discontinue bone formation as well as bone remodeling with further resulting pathological consequences (Ho, Jia et al. 2000, Jensen, Gopalakrishnan et al. 2010). Additionally, since we have considerably increased our knowledge on molecular contributors to osteoblast maturation, an ascending number of studies indicates that miRNAs modulate osteoblast transcription factors and early osteogenic markers (Lian, Stein et al. 2012).

RUNX2

The osteoblastogenesis-promoting cells include genes such as RUNX2 (Moore and Xiao 2013, Komori 2010). miR-148a is predicted to target RUNX2, which operates as an essential initial master marker of the osteogenic cell lineage. At the beginning of the osteoblast differentiation, high values are described in the literature which decrease in the mature osteoblast stage (Gao, Yang et al. 2011). Patients with a mutation in RUNX2 for example suffer from cranial dysplasia (Okura, Sato et al. 2014). With our results, we could also illustrate that RUNX2 is a direct target gene of miR-148a. Due to the inhibition of miR-148a, RUNX2 expression decreased in non-osteoporotic osteoblasts more than in osteoporotic osteoblasts during one week of differentiation, without showing a significant reduction to make a statement about the initiation of the osteoblastogenesis.

COL1A1

Bone development necessitates severe control of gene expressions for gradually proceeding osteoblast progenitor cells to mature osteoblast differentiation stages in order to form extracellular matrix, especially collagen 1 (Komori 2006). In our study, we could not detect any effect of miR-148a inhibition on COL1A1. Deductively, we report that COL1A1 is no direct target gene of miR-148a in osteoblastogenesis. COL1A1, the major component of bone matrix, showed a reduced expression level during osteoblast differentiation in bone marrow stromal cells from patients being afflicted with osteogenesis imperfecta in connection with miR-29b (Kaneto, Lima et al. 2014). Li et al. demonstrated that anti-miR-29b increased expression levels of COL1A1 during osteoblast differentiation (Li, Hassan et al. 2009).

AP

We also studied the influence on the early osteogenic marker AP. Looking at the expression levels after inhibition of miR-148a, we were able to show a reduction in the AP expression of non-osteoporotic cells and a slight reduction in osteoporotic cells. These results showed that by suppressing miR-148a, the osteoblasts of non-osteoporotic patients differentiate worse compared to

osteoporotic cells, which are likely to still have a higher current level of miR-148a after inhibition at this juncture. Baglio et al. showed that an increase of miR-31 in MSCs occurred in rising transcription levels of AP that confirmed an effective osteogenic differentiation (Baglio, Devescovi et al. 2013). In comparison, Wang and colleagues could find increasesd miR-214 expression levels in osteoblasts and further identified an associated negative regulation on AP gene expression. Through the use of a complementary anti-miR-214 inhibitor, the AP expression was again excited and the osteoblastogenesis could be induced (Wang, Guo et al. 2013). Regarding these results, it is considered that AP is directly targeted by miR-148a and that a reduction of the AP gene expression caused by various miRNA deregulation leads to a reduced osteoblast differentiation.

OPG

The OPG-RANKL system expressed on pre-osteoblast cells is essential for providing an adequate initiation of osteoclast development. OPG was found to bind RANKL on pre-osteoblasts, which in turn leads to an inhibition of the binding of RANKL to RANK on osteoclasts, thereby determining the osteoclastogenesis (Khosla 2001). By this gene interaction, OPG is able to suppress NF-κB transcription factor which in turn leads to the inhibition of differentiation of osteoclast precursor to mature cells as well as consequently to the inhibition of bone resorption (Simonet, Lacey et al. 1997, Krakauer 2008, Kobayashi, Udagawa et al. 2009) (Figure 35). Pertaining to RANKL, Cheng et al. for example, identified MAFB transcription factor acting in podocyte and myeloid differentiation. The study investigated MAFB as a direct target of miR-148a through negatively regulating RANKL (Sadl, Jin et al. 2002, Bakri, Sarrazin et al. 2005, Cheng, Chen et al. 2013). Our data show a significant increase of OPG expression on day seven in non-osteoporotic osteoblast cells compared to decreasing output values in osteoporotic cells. Considering the expression decrease of OPG in osteoporotic cells, OPG cannot longer inhibit RANKL in osteoporotic cells. This mechanism inferentially induces intercellular osteoclastogenesis by osteoblast cells. To investigate the complete gene

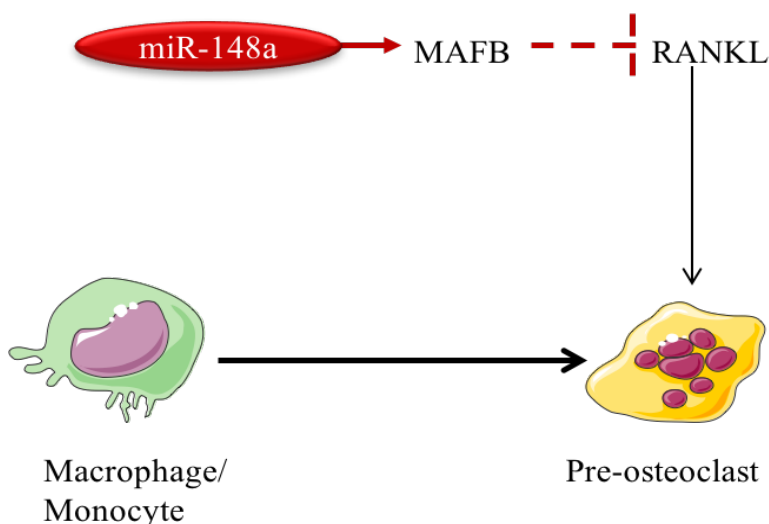correlation, further cell culture experiments regarding miR-148a and RANKL are necessary.

Figure 33 miR-148a osteogenic gene influence on osteoclast cells *Designed elements were adapted from Servier Medical Art.*

On the presented background that osteoblastogenesis is regulated by miRNAs, this study was additionally undertaken to investigate the role of miR-148a in osteoblast differentiation of osteoporotic and non-osteoporotic cells. In conclusion, all these data demonstrated that by inhibition of miR-148a the osteoblast cultivation is deteriorated considering RUNX2, COL1A1, AP and OPG in consensus with the literature (Figure 36). Interestingly, no difference to the osteoporotic cells was recognizable, except for OPG. Given that the initial concentration of miR-148a was higher in osteoporotic patients, this inhibitory effect on genes occurs not significant. Based on the results, a protective role of miR-148a in osteoblastogenesis is presentable. Definitely, it was successful to demonstrate donor cell characteristics in osteoblast cells due to an isolated cell cultivation. Here, further cell cultures are also necessary with co-cultures for the more precise evaluation of this complex genetic network.
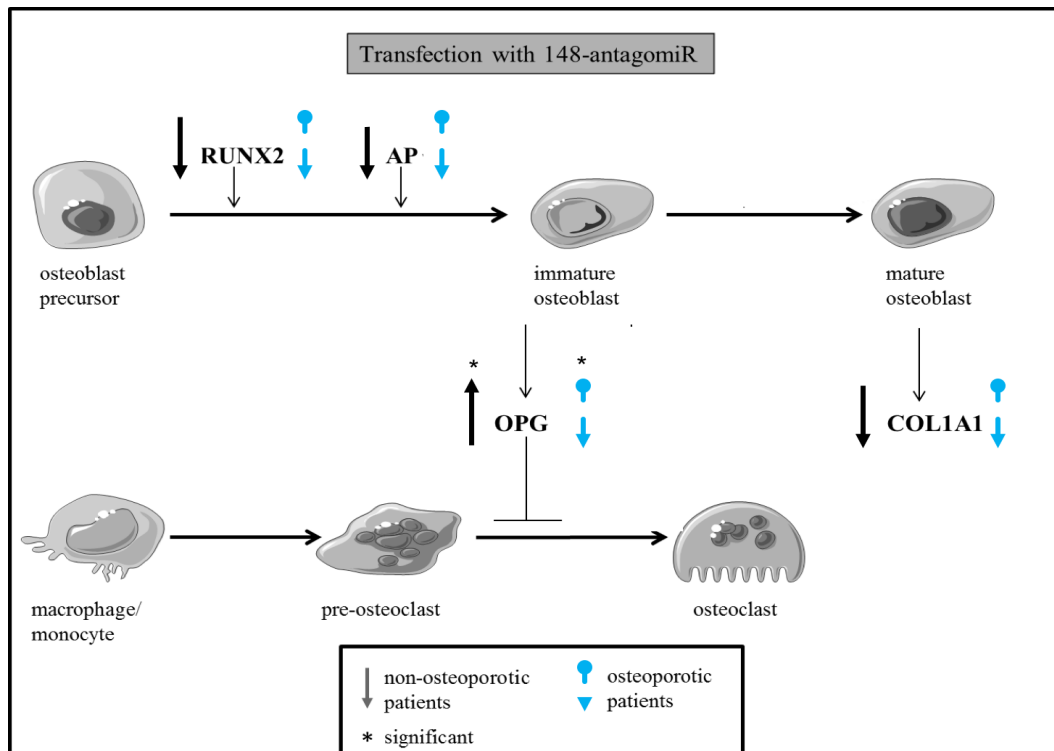
Figure 34 Osteogenic gene influences after transfection with antagomiR-148a in osteoblast cells. *Designed elements were adapted from Servier Medical Art.*

Regarding the temporal concept of our study, it can be discussed whether factors of fracture healing play a role in the identified differences of miRNA expression in osteoporotic samples due to an early sample collection. In this study, blood and bone tissue were collected 2 hours after fracture, while cells were isolated 8 hours after fracture. According to termination of fracture healing, the acute phase is not characterized by bone repair processes up to 12 hours after fracture, but by blood flow from the bone-supplying vessels resulting in hematoma (Ito and Perren 2007). The following organization of the hematoma takes place up to 48 h after fracture and inflammatory processes are initiated due to the vessel rupture. The transformation of the hematoma is then performed by differentiating cells, lasting from 2 up to 16 weeks after fracture and leading to callus formation (Schubert 2016). At this point in time, the final remodeling phase begins, being active for months to years (Ito and Perren 2007, Schubert 2016). Since the processes decisive for fracture healing occur weeks later as described above, it was of utmost priority for us to generate the sample material at an early stage.

5   Summary

The systemic skeletal disease osteoporosis defines a reduction of bone mass and is associated with a loss of bone microstructure. According to the World Health Organization (WHO), osteoporosis is one of the ten most frequent scoring diseases in the world. It has been associated with the expression of specific miRNA profiles. Various studies address the issue of miRNAs as positive or negative regulators of bone cell proliferation, differentiation and for bone-strength essential mineralization by targeting critical osteogenic factors. These studies detected a potential correlation between upregulated miRNA expression levels in serum and increased skeletal fracture risk in patients with osteoporosis. Summarizing, it is yet unclear whether miRNAs directly trigger an increased fracture risk in osteoporosis.

One aim of the research was to determine the possible cell source of miRNA expression levels; i.e. intracellularly in primary human osteoblasts and osteoclasts in an in vitro environment besides serum and bone tissue analysis. Accordingly, the next step for us was to determine whether or not there is a divergent gender-dependent circulating miRNA expression characteristic in osteoporotic and non-osteoporotic patients. Secondly, we compared miRNA expression levels from bone tissue and radiographically measured BMD values of osteoporotic and non-osteoporotic samples. In the final third step, intracellular miRNA concentrations of 9 bone-related miRNAs were examined and compared in osteoporotic and non-osteoporotic patients.

Our findings display that, in the synopsis of our miRNA expression analysis in serum, bone tissue, osteoblasts and osteoclasts, four up-regulated miRNAs (miR-21, miR-24, miR-93, miR-100) are correlated to BMD values showing a simultaneous gender independency. Irrespective of gender, these four miRNAs are associated with osteoporosis and osteopenia. Affirmatively, decreasing BMD and miRNA overexpression seem as a likely pathological interdependence for the increased fracture risk. This cognizance of gender-independent and BMD value-

correlated overexpressed miRNAs provides a commencement for a further generation of a supplemental classification disposition and new diagnostic biomarkers.

Since the regulatory influences of the overexpressed identified miRNAs in the cell culture are not yet known and in view of the lack of knowledge on the impact of an expression manipulation regarding the effects on cell differentiation, further studies were carried out in this work to reveal underlying pathomechanisms. High concentrations of miR-100 and miR-148a were correlated to osteoporosis. Therefore, the effects of their inhibition with antagomirs were investigated. They showed no major cellular toxicity. Osteogenic potential was increased in osteoporotic cells under antagomir treatment.

Our results provide the basis for possible miR-based diagnosis as well as for future therapeutic medications using antagomiRs, permitting accelerated osteoblast differentiation with increased bone formation rates. Further experimental and clinical studies are required to implement serum diagnostics and classification based on miRNA profiles in the clinical setting. Further experimental *in vitro* studies are also needed in osteoclasts and co-culture settings to adequately assess antagomiR transfection safety for prospective *in vivo* application.

6   Zusammenfassung

Die systemische Skeletterkrankung Osteoporose ist durch eine Reduktion der Knochenmasse definiert und geht mit einem ausgeprägten Mikrostrukturverlust des Knochengewebes einher. Osteoporose, die laut WHO zu den zehn häufigsten Erkrankungen weltweit zählt, wurde in Studien mit der Expression spezifischer microRNAs (miRNAs) in Verbindung gebracht. Die Identifizierung differentiell regulierter miRNAs in den an der Knochenhomöostase beteiligten Zellen ist in jüngster Zeit von großem wissenschaftlichen Interesse und in Bezug auf den Knochenstoffwechsel noch nicht ausreichend erforscht.

Diese Arbeit beschäftigte sich zunächst mit der Identifizierung von spezifischen miRNAs, welche durch Translationshemmung einen potentiellen Einfluss auf die Zellen der Knochenhomöostase nehmen. In Serum, Knochengewebe, Osteoblasten und Osteoklasten von osteoporotischen Patienten konnte eine übereinstimmende Überexpression der miR-21, miR-24, miR-93 und miR-100 festgestellt werden, die zudem eine direkte Korrelation zu gemessenen Knochedichtemessungen zeigte und in erhöhter Menge unabhängig vom Geschlecht exprimiert wird. Anhand der gemessenen Expressionsmengen konnte eine ergänzende Einteilung sowohl in die Krankheitsvorstufe der Osteopenie als auch in die manifeste Form der Osteoporose getroffen werden. Es konnte somit eine Korrelation zwischen hochregulierten miRNA Expressionsniveaus und erhöhtem Skelettbruchrisiko bei Patienten mit Osteoporose aufgezeigt werden, die eine ergänzende Säule diagnostischer und klassifizierender Möglichkeiten bildet.

In unserer Studie konnten wir spezifisch regulierte miRNAs in den beteiligten Zellen identifizieren, die bei osteoporotischen Patienten im Vergleich zu nicht-osteoporotischen Patienten differenziell reguliert waren. Da der Einfluss der genannten miRNAs positiver oder negativen Natur in Bezug auf die Proliferation und Differenzierung von Knochenzellen besonders in Hinblick auf das Krankheitsbild der Osteoporose unzureichend erforscht ist, wurde in *in vitro* Zellkulturexperimenten versucht durch Manipulation der miRNA-Expressionslevel Einfluss auf entscheidende osteogene Schlüsselgene zu nehmen

und einen innovativen Therapieansatz der Osteoporose zu generieren. Signifikant hohe Konzentrationen der miR-100 und miR-148a, die mit der Osteoporose korrelieren, präsentierten sich als geeignete Kandidaten zur Inhibition mittels komplementärer miRNAs. Die Inhibition konnte dann durch die Etablierung eines geeigneten Lipotransfektionsverfahrens verwirklicht werden. So genannte AntagomiRs zählen zu der neuen Klasse von chemisch synthetisierten Oligonukleotiden, die genutzt werden, um die zelleigenen microRNA-Moleküle stillzulegen und Einflüsse auf osteogene Zielgene zu offenbaren. Durch die Expressionsunterdrückung mittels antagomiR-100 und antagomiR-148a-Applikation konnte keine zelluläre Toxizität nachgewiesen werden. Die miR-100 Inhibition zeichnete sich durch eine Induktion osteogener Genexpressionen aus, die für die Osteoblastogenese eine entscheidende Rolle spielen. Die Zytotoxizität wurde über Alamar Blue und MTT überwacht.

Die von uns identifizierten und hochregulierten miRNAs haben das Potential, als neue Biomarker für Osteoporose zu dienen sowie eine erhebliche Rolle in der Vermeidung von osteoporoseassoziierten Frakturen zu spielen. Konsequenterweise sind weitere experimentelle Studien erforderlich, um die Diagnostik und Klassifizierung auf Basis von miRNA-Profilen im klinischen Setting durchzuführen. Weitere experimentelle In-vitro-Studien und Ko-Kulturen sind notwendig, um die antagomiR Transfektionssicherheit für die prospektive *in vivo* Anwendung adäquat zu beurteilen. Diese Studie zeigt insgesamt jedoch deutlich, dass das miRNA-Profil von Osteoporotikern offenkundig verändert ist im Vergleich zum gesunden Kontrollkollektiv und stellt somit einen innovativen Denkanstoß in der zukünftigen Diagnostik und Therapie des Knochenschwundes dar.

7   Comment

The design and provision of this project was a success of the entire team. As doctoral candidate, it was my duty to carry out the experiments and this work. The introduction to laboratory techniques by the respective specialist at our laboratory enabled me to perform the experiments by myself. The osteoblast cell isolation, following cell culture, transfection experiments, RNA isolation, functional assays, PCR and gene expression analysis were executed by myself. Owing to Assoc. Prof. Dr. Johannes Grillari, I was able to gain experience in the electrostatic transfection of cells at the University of Natural Resources and Applied Life Sciences in Vienna. It was my task to establish a successful lipotransfection protocol with the help of Claudine Seeliger and to do the transfection experiments.

8 References

http://www.ebiotrade.com/emgzf/spII200604/16-17.pdf (30.08.2017).

Aravindaram, K., S. Y. Yin and N. S. Yang (2013). "Biolistic transfection of tumor tissue samples." Methods Mol Biol **940**: 133-143.

Baglio, S. R., V. Devescovi, D. Granchi and N. Baldini (2013). "MicroRNA expression profiling of human bone marrow mesenchymal stem cells during osteogenic differentiation reveals Osterix regulation by miR-31." Gene **527**(1): 321-331.

Bakri, Y., S. Sarrazin, U. P. Mayer, S. Tillmanns, C. Nerlov, A. Boned and M. H. Sieweke (2005). "Balance of MafB and PU.1 specifies alternative macrophage or dendritic cell fate." Blood **105**(7): 2707-2716.

Behmann, M., J. Semler and U. Walter (2008). Osteoporose. Beweglich? Muskel-Skelett-Erkrankungen — Ursachen, Risikofaktoren und präventive Ansätze. Berlin, Heidelberg, Springer Berlin Heidelberg**:** 153-166.

Bhutani, G. and M. C. Gupta (2013). "Emerging therapies for the treatment of osteoporosis." J Midlife Health **4**(3): 147-152.

Bonora, M., M. R. Wieckowsk, C. Chinopoulos, O. Kepp, G. Kroemer, L. Galluzzi and P. Pinton (2015). "Molecular mechanisms of cell death: central implication of ATP synthase in mitochondrial permeability transition." Oncogene **34**(12): 1608.

Boyle, W. J., W. S. Simonet and D. L. Lacey (2003). "Osteoclast differentiation and activation." Nature **423**(6937): 337-342.

Bragdon, B., O. Moseychuk, S. Saldanha, D. King, J. Julian and A. Nohe (2011). "Bone morphogenetic proteins: a critical review." Cell Signal **23**(4): 609-620.

Bustin, S. A., V. Benes, J. A. Garson, J. Hellemans, J. Huggett, M. Kubista, R. Mueller, T. Nolan, M. W. Pfaffl, G. L. Shipley, J. Vandesompele and C. T. Wittwer (2009). "The MIQE guidelines: minimum information for publication of quantitative real-time PCR experiments." Clin Chem **55**(4): 611-622.

Care, A., D. Catalucci, F. Felicetti, D. Bonci, A. Addario, P. Gallo, M. L. Bang, P. Segnalini, Y. Gu, N. D. Dalton, L. Elia, M. V. Latronico, M. Hoydal, C. Autore, M. A. Russo, G. W. Dorn, 2nd, O. Ellingsen, P. Ruiz-Lozano, K. L. Peterson, C. M. Croce, C. Peschle and G. Condorelli (2007). "MicroRNA-133 controls cardiac hypertrophy." Nat Med **13**(5): 613-618.

Chabot, S., J. Orio, R. Castanier, E. Bellard, S. J. Nielsen, M. Golzio and J. Teissie (2012). "LNA-based oligonucleotide electrotransfer for miRNA inhibition." Mol Ther **20**(8): 1590-1598.

Chen, C., P. Cheng, H. Xie, H. D. Zhou, X. P. Wu, E. Y. Liao and X. H. Luo (2014). "MiR-503 regulates osteoclastogenesis via targeting RANK." J Bone Miner Res **29**(2): 338-347.

Chen, Y., Y. Song, Z. Wang, Z. Yue, H. Xu, C. Xing and Z. Liu (2010). "Altered expression of MiR-148a and MiR-152 in gastrointestinal cancers and its clinical significance." J Gastrointest Surg **14**(7): 1170-1179.

Cheng, C. J. and W. M. Saltzman (2012). "Polymer nanoparticle-mediated delivery of microRNA inhibition and alternative splicing." Mol Pharm **9**(5): 1481-1488.

Cheng, P., C. Chen, H. B. He, R. Hu, H. D. Zhou, H. Xie, W. Zhu, R. C. Dai, X. P. Wu, E. Y. Liao and X. H. Luo (2013). "miR-148a regulates osteoclastogenesis by targeting V-maf musculoaponeurotic fibrosarcoma oncogene homolog B." J Bone Miner Res **28**(5): 1180-1190.

Cho, W. C. (2011). "Epigenetic alteration of microRNAs in feces of colorectal cancer and its clinical significance." Expert Rev Mol Diagn **11**(7): 691-694.

Chomczynski, P. (1993). "A reagent for the single-step simultaneous isolation of RNA, DNA and proteins from cell and tissue samples." Biotechniques **15**(3): 532-534, 536-537.

Cui, L., Y. Shi, X. Zhou, X. Wang, J. Wang, Y. Lan, M. Wang, L. Zheng, H. Li, Q. Wu, J. Zhang, D. Fan and Y. Han (2013). "A set of microRNAs mediate direct conversion of human umbilical cord lining-derived mesenchymal stem cells into hepatocytes." Cell Death Dis **4**: e918.

Czech, M. P. (2006). "MicroRNAs as therapeutic targets." N Engl J Med **354**(11): 1194-1195.

Dai, L., W. Wang, S. Zhang, Q. Jiang, R. Wang, L. Dai, L. Cheng, Y. Yang, Y. Q. Wei and H. X. Deng (2012). "Vector-based miR-15a/16-1 plasmid inhibits colon cancer growth in vivo." Cell Biol Int **36**(8): 765-770.

de Pontual, L., E. Yao, P. Callier, L. Faivre, V. Drouin, S. Cariou, A. Van Haeringen, D. Genevieve, A. Goldenberg, M. Oufadem, S. Manouvrier, A. Munnich, J. A. Vidigal, M. Vekemans, S. Lyonnet, A. Henrion-Caude, A. Ventura and J. Amiel (2011). "Germline deletion of the miR-17 approximately 92 cluster causes skeletal and growth defects in humans." Nat Genet **43**(10): 1026-1030.

Ehnert S., e. a. (2011). "Mesenchymale Stammzellen aus Fettgewebe - Die bessere Alternative zu Knochenmarkszellen für das Tissue Engineering von Knochen. Regenerative Medizin. (1) p 3-9.".

Engelke, K., J. E. Adams, G. Armbrecht, P. Augat, C. E. Bogado, M. L. Bouxsein, D. Felsenberg, M. Ito, S. Prevrhal, D. B. Hans and E. M. Lewiecki (2008). "Clinical use of quantitative computed tomography and peripheral quantitative computed tomography in the management of osteoporosis in adults: the 2007 ISCD Official Positions." J Clin Densitom **11**(1): 123-162.

Farid, W. R., Q. Pan, A. J. van der Meer, P. E. de Ruiter, V. Ramakrishnaiah, J. de Jonge, J. Kwekkeboom, H. L. Janssen, H. J. Metselaar, H. W. Tilanus, G. Kazemier and L. J. van der Laan (2012). "Hepatocyte-derived microRNAs as

serum biomarkers of hepatic injury and rejection after liver transplantation." Liver Transpl **18**(3): 290-297.

Fujita, Y., K. Kojima, R. Ohhashi, N. Hamada, Y. Nozawa, A. Kitamoto, A. Sato, S. Kondo, T. Kojima, T. Deguchi and M. Ito (2010). "MiR-148a attenuates paclitaxel resistance of hormone-refractory, drug-resistant prostate cancer PC3 cells by regulating MSK1 expression." J Biol Chem **285**(25): 19076-19084.

Gallagher, J. A. (2003). Bone Research Protocols.

Gallagher, J. A. (2003). "Human osteoblast culture." Methods Mol Med **80**: 3-18.

Gao, J., T. Yang, J. Han, K. Yan, X. Qiu, Y. Zhou, Q. Fan and B. Ma (2011). "MicroRNA expression during osteogenic differentiation of human multipotent mesenchymal stromal cells from bone marrow." J Cell Biochem **112**(7): 1844-1856.

Garzon, R., G. A. Calin and C. M. Croce (2009). "MicroRNAs in Cancer." Annu Rev Med **60**: 167-179.

Gaur, T., S. Hussain, R. Mudhasani, I. Parulkar, J. L. Colby, D. Frederick, B. E. Kream, A. J. van Wijnen, J. L. Stein, G. S. Stein, S. N. Jones and J. B. Lian (2010). "Dicer inactivation in osteoprogenitor cells compromises fetal survival and bone formation, while excision in differentiated osteoblasts increases bone mass in the adult mouse." Dev Biol **340**(1): 10-21.

Ge, Y. F., J. Sun, C. J. Jin, B. Q. Cao, Z. F. Jiang and J. F. Shao (2013). "AntagomiR-27a targets FOXO3a in glioblastoma and suppresses U87 cell growth in vitro and in vivo." Asian Pac J Cancer Prev **14**(2): 963-968.

Giraud-Triboult, K., C. Rochon-Beaucourt, X. Nissan, B. Champon, S. Aubert and G. Pietu (2011). "Combined mRNA and microRNA profiling reveals that miR-148a and miR-20b control human mesenchymal stem cell phenotype via EPAS1." Physiol Genomics **43**(2): 77-86.

Gokhale, A., R. Kunder, A. Goel, R. Sarin, A. Moiyadi, A. Shenoy, C. Mamidipally, S. Noronha, S. Kannan and N. V. Shirsat (2010). "Distinctive microRNA signature of medulloblastomas associated with the WNT signaling pathway." J Cancer Res Ther **6**(4): 521-529.

Greiner, S., A. Kadow-Romacker, B. Wildemann, P. Schwabe and G. Schmidmaier (2007). "Bisphosphonates incorporated in a poly(D,L-lactide) implant coating inhibit osteoclast like cells in vitro." J Biomed Mater Res A **83**(4): 1184-1191.

Gullberg, B., O. Johnell and J. A. Kanis (1997). "World-wide projections for hip fracture." Osteoporos Int **7**(5): 407-413.

Guo, J., F. Ren, Y. Wang, S. Li, Z. Gao, X. Wang, H. Ning, J. Wu, Y. Li, Z. Wang, S. M. Chim, J. Xu and Z. Chang (2012). "miR-764-5p promotes osteoblast differentiation through inhibition of CHIP/STUB1 expression." J Bone Miner Res **27**(7): 1607-1618.

Haimes, J. (2014). "http://dharmacon.gelifesciences.com/uploadedfiles/resources/delta-cq-solaris-technote.pdf."

Han, J., Y. Lee, K. H. Yeom, Y. K. Kim, H. Jin and V. N. Kim (2004). "The Drosha-DGCR8 complex in primary microRNA processing." Genes Dev **18**(24): 3016-3027.

Harfe, B. D., M. T. McManus, J. H. Mansfield, E. Hornstein and C. J. Tabin (2005). "The RNaseIII enzyme Dicer is required for morphogenesis but not patterning of the vertebrate limb." Proc Natl Acad Sci U S A **102**(31): 10898-10903.

Hassan, M. Q., Y. Maeda, H. Taipaleenmaki, W. Zhang, M. Jafferji, J. A. Gordon, Z. Li, C. M. Croce, A. J. van Wijnen, J. L. Stein, G. S. Stein and J. B. Lian (2012). "miR-218 directs a Wnt signaling circuit to promote differentiation of osteoblasts and osteomimicry of metastatic cancer cells." J Biol Chem **287**(50): 42084-42092.

Ho, N. C., L. Jia, C. C. Driscoll, E. M. Gutter and C. A. Francomano (2000). "A skeletal gene database." J Bone Miner Res **15**(11): 2095-2122.

Horvath, G. (2016). "RG-101 in combination with 4 weeks of oral direct acting antiviral therapy achieves high virologic response rates in treatment naive genotype 1 and 4 chronic hepatitis C patients: interim results from a randomised, multi-center, phase 2 study." International Liver Congress, Barcelona, abstract GS08, 2016.

Hu, H., Y. Zhang, X. H. Cai, J. F. Huang and L. Cai (2012). "Changes in microRNA expression in the MG-63 osteosarcoma cell line compared with osteoblasts." Oncol Lett **4**(5): 1037-1042.

Huang, J. J., J. Yu, J. Y. Li, Y. T. Liu and R. Q. Zhong (2012). "Circulating microRNA expression is associated with genetic subtype and survival of multiple myeloma." Med Oncol **29**(4): 2402-2408.

Iliopoulos, D., K. N. Malizos, P. Oikonomou and A. Tsezou (2008). "Integrative microRNA and proteomic approaches identify novel osteoarthritis genes and their collaborative metabolic and inflammatory networks." PLoS One **3**(11): e3740.

Ito, K. and S. M. Perren (2007). "Biology of fracture healing." AO Principles of Fracture Management, Eds. T. P. Rüedi, R. E. Buckley and C. G. Moran. AO Publishing, Thieme, 2nd Edition, 2007. ISBN 9783131174420.

Janssen, H. L., H. W. Reesink, E. J. Lawitz, S. Zeuzem, M. Rodriguez-Torres, K. Patel, A. J. van der Meer, A. K. Patick, A. Chen, Y. Zhou, R. Persson, B. D. King, S. Kauppinen, A. A. Levin and M. R. Hodges (2013). "Treatment of HCV Infection by Targeting MicroRNA." N Engl J Med.

Jensen, E. D., R. Gopalakrishnan and J. J. Westendorf (2010). "Regulation of gene expression in osteoblasts." Biofactors **36**(1): 25-32.

Jilka, R. L. (2003). "Biology of the basic multicellular unit and the pathophysiology of osteoporosis." Med Pediatr Oncol **41**(3): 182-185.

Jilka, R. L., R. S. Weinstein, T. Bellido, P. Roberson, A. M. Parfitt and S. C. Manolagas (1999). "Increased bone formation by prevention of osteoblast apoptosis with parathyroid hormone." J Clin Invest **104**(4): 439-446.

Jing, D., J. Hao, Y. Shen, G. Tang, M. L. Li, S. H. Huang and Z. H. Zhao (2015). "The role of microRNAs in bone remodeling." Int J Oral Sci **7**(3): 131-143.

Johnell, O. and J. A. Kanis (2006). "An estimate of the worldwide prevalence and disability associated with osteoporotic fractures." Osteoporos Int **17**(12): 1726-1733.

Kadow-Romacker, A., J. E. Hoffmann, G. Duda, B. Wildemann and G. Schmidmaier (2009). "Effect of mechanical stimulation on osteoblast- and osteoclast-like cells in vitro." Cells Tissues Organs **190**(2): 61-68.

Kaneto, C. M., P. S. Lima, D. L. Zanette, K. L. Prata, J. M. Pina Neto, F. J. de Paula and W. A. Silva, Jr. (2014). "COL1A1 and miR-29b show lower expression levels during osteoblast differentiation of bone marrow stromal cells from Osteogenesis Imperfecta patients." BMC Med Genet **15**: 45.

Khosla, S. (2001). "Minireview: the OPG/RANKL/RANK system." Endocrinology **142**(12): 5050-5055.

Kim, Y. H., G. S. Kim and B. Jeong-Hwa (2002). "Inhibitory action of bisphosphonates on bone resorption does not involve the regulation of RANKL and OPG expression." Exp Mol Med **34**(2): 145-151.

Kirschner, M. B., J. J. Edelman, S. C. Kao, M. P. Vallely, N. van Zandwijk and G. Reid (2013). "The Impact of Hemolysis on Cell-Free microRNA Biomarkers." Front Genet **4**: 94.

Kobayashi, E., F. J. Hornicek and Z. Duan (2012). "MicroRNA Involvement in Osteosarcoma." Sarcoma **2012**: 359739.

Kobayashi, Y., N. Udagawa and N. Takahashi (2009). "Action of RANKL and OPG for osteoclastogenesis." Crit Rev Eukaryot Gene Expr **19**(1): 61-72.

Koberle, V., B. Kronenberger, T. Pleli, J. Trojan, E. Imelmann, J. Peveling-Oberhag, M. W. Welker, M. Elhendawy, S. Zeuzem, A. Piiper and O. Waidmann (2013). "Serum microRNA-1 and microRNA-122 are prognostic markers in patients with hepatocellular carcinoma." Eur J Cancer **49**(16): 3442-3449.

Komori, T. (2006). "Regulation of osteoblast differentiation by transcription factors." J Cell Biochem **99**(5): 1233-1239.

Komori, T. (2010). "Regulation of osteoblast differentiation by Runx2." Adv Exp Med Biol **658**: 43-49.

Kosaka, N. and T. Ochiya (2011). "Unraveling the Mystery of Cancer by Secretory microRNA: Horizontal microRNA Transfer between Living Cells." Front Genet **2**: 97.

Krakauer, T. (2008). "Nuclear factor-kappaB: fine-tuning a central integrator of diverse biologic stimuli." Int Rev Immunol **27**(5): 286-292.

Krutzfeldt, J., N. Rajewsky, R. Braich, K. G. Rajeev, T. Tuschl, M. Manoharan and M. Stoffel (2005). "Silencing of microRNAs in vivo with 'antagomirs'." Nature **438**(7068): 685-689.

Kuehn, B. M. (2009). "Long-term risks of bisphosphonates probed." <u>JAMA</u> **301**(7): 710-711.

Larabee, S. M., H. Coia, S. Jones, E. Cheung and G. I. Gallicano (2015). "miRNA-17 members that target Bmpr2 influence signaling mechanisms important for embryonic stem cell differentiation in vitro and gastrulation in embryos." <u>Stem Cells Dev</u> **24**(3): 354-371.

Lee, S. T., D. Jeon, K. Chu, K. H. Jung, J. Moon, J. Sunwoo, D. K. Park, H. Yang, J. H. Park, M. Kim, J. K. Roh and S. K. Lee (2016). "Inhibition of miR-203 Reduces Spontaneous Recurrent Seizures in Mice." <u>Mol Neurobiol</u>.

Li, H., Z. Wang, Q. Fu and J. Zhang (2014). "Plasma miRNA levels correlate with sensitivity to bone mineral density in postmenopausal osteoporosis patients." <u>Biomarkers</u> **19**(7): 553-556.

Li, Z., M. Q. Hassan, M. Jafferji, R. I. Aqeilan, R. Garzon, C. M. Croce, A. J. van Wijnen, J. L. Stein, G. S. Stein and J. B. Lian (2009). "Biological functions of miR-29b contribute to positive regulation of osteoblast differentiation." <u>J Biol Chem</u> **284**(23): 15676-15684.

Li, Z., M. Q. Hassan, S. Volinia, A. J. van Wijnen, J. L. Stein, C. M. Croce, J. B. Lian and G. S. Stein (2008). "A microRNA signature for a BMP2-induced osteoblast lineage commitment program." <u>Proc Natl Acad Sci U S A</u> **105**(37): 13906-13911.

Lian, J. B., G. S. Stein, A. J. van Wijnen, J. L. Stein, M. Q. Hassan, T. Gaur and Y. Zhang (2012). "MicroRNA control of bone formation and homeostasis." <u>Nat Rev Endocrinol</u> **8**(4): 212-227.

Liffers, S. T., J. B. Munding, M. Vogt, J. D. Kuhlmann, B. Verdoodt, S. Nambiar, A. Maghnouj, A. Mirmohammadsadegh, S. A. Hahn and A. Tannapfel (2011). "MicroRNA-148a is down-regulated in human pancreatic ductal adenocarcinomas and regulates cell survival by targeting CDC25B." <u>Lab Invest</u> **91**(10): 1472-1479.

Lin, J., L. Schyschka, R. Muhl-Benninghaus, J. Neumann, L. Hao, N. Nussler, S. Dooley, L. Liu, U. Stockle, A. K. Nussler and S. Ehnert (2012). "Comparative analysis of phase I and II enzyme activities in 5 hepatic cell lines identifies Huh-7 and HCC-T cells with the highest potential to study drug metabolism." <u>Arch Toxicol</u> **86**(1): 87-95.

Lippuner, K. (2012). "The future of osteoporosis treatment - a research update." <u>Swiss Med Wkly</u> **142**: w13624.

Lorenzo, J., M. Horowitz and Y. Choi (2008). "Osteoimmunology: interactions of the bone and immune system." <u>Endocr Rev</u> **29**(4): 403-440.

Ma, L., F. Reinhardt, E. Pan, J. Soutschek, B. Bhat, E. G. Marcusson, J. Teruya-Feldstein, G. W. Bell and R. A. Weinberg (2010). "Therapeutic silencing of miR-10b inhibits metastasis in a mouse mammary tumor model." <u>Nat Biotechnol</u> **28**(4): 341-347.

Ma, X. H., W. Zhang, Y. Wang, P. Xue and Y. K. Li (2015). "Comparison of the Spine and Hip BMD Assessments Derived from Quantitative Computed Tomography." <u>Int J Endocrinol</u> **2015**: 675340.

Ma, Y., X. G. She, Y. Z. Ming and Q. Q. Wan (2014). "miR-24 promotes the proliferation and invasion of HCC cells by targeting SOX7." Tumour Biol **35**(11): 10731-10736.

Magrelli, A., G. Azzalin, M. Salvatore, M. Viganotti, F. Tosto, T. Colombo, R. Devito, A. Di Masi, A. Antoccia, S. Lorenzetti, F. Maranghi, A. Mantovani, C. Tanzarella, G. Macino and D. Taruscio (2009). "Altered microRNA Expression Patterns in Hepatoblastoma Patients." Transl Oncol **2**(3): 157-163.

Mentzel, C. M., C. Anthon, M. J. Jacobsen, P. Karlskov-Mortensen, C. S. Bruun, C. B. Jorgensen, J. Gorodkin, S. Cirera and M. Fredholm (2015). "Gender and Obesity Specific MicroRNA Expression in Adipose Tissue from Lean and Obese Pigs." PLoS One **10**(7): e0131650.

Mercatelli, N., V. Coppola, D. Bonci, F. Miele, A. Costantini, M. Guadagnoli, E. Bonanno, G. Muto, G. V. Frajese, R. De Maria, L. G. Spagnoli, M. G. Farace and S. A. Ciafre (2008). "The inhibition of the highly expressed miR-221 and miR-222 impairs the growth of prostate carcinoma xenografts in mice." PLoS One **3**(12): e4029.

Merkerova, M., A. Vasikova, M. Belickova and H. Bruchova (2010). "MicroRNA expression profiles in umbilical cord blood cell lineages." Stem Cells Dev **19**(1): 17-26.

Mizoguchi, F., Y. Murakami, T. Saito, N. Miyasaka and H. Kohsaka (2013). "miR-31 controls osteoclast formation and bone resorption by targeting RhoA." Arthritis Res Ther **15**(5): R102.

Mizuno, Y., K. Yagi, Y. Tokuzawa, Y. Kanesaki-Yatsuka, T. Suda, T. Katagiri, T. Fukuda, M. Maruyama, A. Okuda, T. Amemiya, Y. Kondoh, H. Tashiro and Y. Okazaki (2008). "miR-125b inhibits osteoblastic differentiation by down-regulation of cell proliferation." Biochem Biophys Res Commun **368**(2): 267-272.

Moldovan, L., K. Batte, Y. Wang, J. Wisler and M. Piper (2013). "Analyzing the circulating microRNAs in exosomes/extracellular vesicles from serum or plasma by qRT-PCR." Methods Mol Biol **1024**: 129-145.

Mooney, C., R. Raoof, H. El-Naggar, A. Sanz-Rodriguez, E. M. Jimenez-Mateos and D. C. Henshall (2015). "High Throughput qPCR Expression Profiling of Circulating MicroRNAs Reveals Minimal Sex- and Sample Timing-Related Variation in Plasma of Healthy Volunteers." PLoS One **10**(12): e0145316.

Moore, B. T. and P. Xiao (2013). "MiRNAs in bone diseases." Microrna **2**(1): 20-31.

Morrow, R., F. Deyhim, B. S. Patil and B. J. Stoecker (2009). "Feeding orange pulp improved bone quality in a rat model of male osteoporosis." J Med Food **12**(2): 298-303.

Mosmann, T. (1983). "Rapid colorimetric assay for cellular growth and survival: application to proliferation and cytotoxicity assays." J Immunol Methods **65**(1-2): 55-63.

N. Rucci, M. b. o. b. r., " Clin Cases Miner Bone Metab, vol. 5, pp. 49-56, Jan 2008.

Nakashima, K. and B. de Crombrugghe (2003). "Transcriptional mechanisms in osteoblast differentiation and bone formation." Trends Genet **19**(8): 458-466.

Ng, W. L., D. Yan, X. Zhang, Y. Y. Mo and Y. Wang (2010). "Over-expression of miR-100 is responsible for the low-expression of ATM in the human glioma cell line: M059J." DNA Repair (Amst) **9**(11): 1170-1175.

Okura, H., S. Sato, S. Kishikawa, S. Kaneto, T. Nakashima, N. Yoshida, H. Takayanagi and H. Kiyono (2014). "Runx2-I isoform contributes to fetal bone formation even in the absence of specific N-terminal amino acids." PLoS One **9**(9): e108294.

Otto, F., A. P. Thornell, T. Crompton, A. Denzel, K. C. Gilmour, I. R. Rosewell, G. W. Stamp, R. S. Beddington, S. Mundlos, B. R. Olsen, P. B. Selby and M. J. Owen (1997). "Cbfa1, a candidate gene for cleidocranial dysplasia syndrome, is essential for osteoblast differentiation and bone development." Cell **89**(5): 765-771.

Papachroni, K. K., D. N. Karatzas, K. A. Papavassiliou, E. K. Basdra and A. G. Papavassiliou (2009). "Mechanotransduction in osteoblast regulation and bone disease." Trends Mol Med **15**(5): 208-216.

Papagiannakopoulos, T. and K. S. Kosik (2008). "MicroRNAs: regulators of oncogenesis and stemness." BMC Med **6**: 15.

Patnaik, S. K., E. Kannisto and S. Yendamuri (2010). "Overexpression of microRNA miR-30a or miR-191 in A549 lung cancer or BEAS-2B normal lung cell lines does not alter phenotype." PLoS One **5**(2): e9219.

Philipot, D., D. Guerit, D. Platano, P. Chuchana, E. Olivotto, F. Espinoza, A. Dorandeu, Y. M. Pers, J. Piette, R. M. Borzi, C. Jorgensen, D. Noel and J. M. Brondello (2014). "p16INK4a and its regulator miR-24 link senescence and chondrocyte terminal differentiation-associated matrix remodeling in osteoarthritis." Arthritis Res Ther **16**(1): R58.

Rayner, K. J. and E. J. Hennessy (2013). "Extracellular communication via microRNA: lipid particles have a new message." J Lipid Res **54**(5): 1174-1181.

Rey, J. R., E. V. Cervino, M. L. Rentero, E. C. Crespo, A. O. Alvaro and M. Casillas (2009). "Raloxifene: mechanism of action, effects on bone tissue, and applicability in clinical traumatology practice." Open Orthop J **3**: 14-21.

Sadl, V., F. Jin, J. Yu, S. Cui, D. Holmyard, S. Quaggin, G. Barsh and S. Cordes (2002). "The mouse Kreisler (Krml1/MafB) segmentation gene is required for differentiation of glomerular visceral epithelial cells." Dev Biol **249**(1): 16-29.

Schubert, R. (2016). "racture healing Radiology reference article in Radiopaedia encyclopedia rID 18632. 2016.".

Seeliger, C., E. R. Balmayor and M. van Griensven (2016). "miRNAs Related to Skeletal Diseases." Stem Cells Dev **25**(17): 1261-1281.

Seeliger, C., K. Karpinski, A. Haug, H. Vester, A. Schmitt, J. Bauer and M. van Griensven (2014). "Five Freely Circulating miRNAs and Bone Tissue miRNAs are Associated with Osteoporotic Fractures." J Bone Miner Res.

Simonet, W. S., D. L. Lacey, C. R. Dunstan, M. Kelley, M. S. Chang, R. Luthy, H. Q. Nguyen, S. Wooden, L. Bennett, T. Boone, G. Shimamoto, M. DeRose, R. Elliott, A. Colombero, H. L. Tan, G. Trail, J. Sullivan, E. Davy, N. Bucay, L. Renshaw-Gegg, T. M. Hughes, D. Hill, W. Pattison, P. Campbell, S. Sander, G. Van, J. Tarpley, P. Derby, R. Lee and W. J. Boyle (1997). "Osteoprotegerin: a novel secreted protein involved in the regulation of bone density." Cell **89**(2): 309-319.

Song, H., Q. Wang, J. Wen, S. Liu, X. Gao, J. Cheng and D. Zhang (2012). "ACVR1, a Therapeutic Target of Fibrodysplasia Ossificans Progressiva, Is Negatively Regulated by miR-148a." Int J Mol Sci **13**(2): 2063-2077.

Stammet, P., E. Goretti, M. Vausort, L. Zhang, D. R. Wagner and Y. Devaux (2012). "Circulating microRNAs after cardiac arrest." Crit Care Med **40**(12): 3209-3214.

Stanford, C. M., P. A. Jacobson, E. D. Eanes, L. A. Lembke and R. J. Midura (1995). "Rapidly forming apatitic mineral in an osteoblastic cell line (UMR 106-01 BSP)." J Biol Chem **270**(16): 9420-9428.

Statement, N. C. (2000). "Osteoporosis prevention, diagnosis, and therapy." ": 17(11): 11-45.

Sugatani, T. and K. A. Hruska (2009). "Impaired micro-RNA pathways diminish osteoclast differentiation and function." J Biol Chem **284**(7): 4667-4678.

Sugatani, T. and K. A. Hruska (2013). "Down-regulation of miR-21 biogenesis by estrogen action contributes to osteoclastic apoptosis." J Cell Biochem **114**(6): 1217-1222.

The world health report 2004: changing history. Geneva, W. H. O., 2004.

Thum, T., C. Gross, J. Fiedler, T. Fischer, S. Kissler, M. Bussen, P. Galuppo, S. Just, W. Rottbauer, S. Frantz, M. Castoldi, J. Soutschek, V. Koteliansky, A. Rosenwald, M. A. Basson, J. D. Licht, J. T. Pena, S. H. Rouhanifard, M. U. Muckenthaler, T. Tuschl, G. R. Martin, J. Bauersachs and S. Engelhardt (2008). "MicroRNA-21 contributes to myocardial disease by stimulating MAP kinase signalling in fibroblasts." Nature **456**(7224): 980-984.

van Rooij, E. and S. Kauppinen (2014). "Development of microRNA therapeutics is coming of age." EMBO Mol Med **6**(7): 851-864.

van Rooij, E. and E. N. Olson (2012). "MicroRNA therapeutics for cardiovascular disease: opportunities and obstacles." Nat Rev Drug Discov **11**(11): 860-872.

Wang, X., B. Guo, Q. Li, J. Peng, Z. Yang, A. Wang, D. Li, Z. Hou, K. Lv, G. Kan, H. Cao, H. Wu, J. Song, X. Pan, Q. Sun, S. Ling, Y. Li, M. Zhu, P. Zhang, S. Peng, X. Xie, T. Tang, A. Hong, Z. Bian, Y. Bai, A. Lu, F. He and G. Zhang (2013). "miR-214 targets ATF4 to inhibit bone formation." Nat Med **19**(1): 93-100.

Wiame, I., S. Remy, R. Swennen and L. Sagi (2000). "Irreversible heat inactivation of DNase I without RNA degradation." Biotechniques **29**(2): 252-254, 256.

Wildemann, B., N. Burkhardt, M. Luebberstedt, T. Vordemvenne and G. Schmidmaier (2007). "Proliferating and differentiating effects of three different growth factors on pluripotent mesenchymal cells and osteoblast like cells." J Orthop Surg Res **2**: 27.

World Health Organization: WHO scientific group on the assessment of osteoporosis at primary health care level. Summary Meeting report. Brussels, B., 20072; 5-7, May 2004.

Xie, Y., L. Zhang, Y. Gao, W. Ge and P. Tang (2015). "The Multiple Roles of Microrna-223 in Regulating Bone Metabolism." Molecules **20**(10): 19433-19448.

Xu, Q., Y. Jiang, Y. Yin, Q. Li, J. He, Y. Jing, Y. T. Qi, Q. Xu, W. Li, B. Lu, S. S. Peiper, B. H. Jiang and L. Z. Liu (2013). "A regulatory circuit of miR-148a/152 and DNMT1 in modulating cell transformation and tumor angiogenesis through IGF-IR and IRS1." J Mol Cell Biol **5**(1): 3-13.

Xu, X. H., S. S. Dong, Y. Guo, T. L. Yang, S. F. Lei, C. J. Papasian, M. Zhao and H. W. Deng (2010). "Molecular genetic studies of gene identification for osteoporosis: the 2009 update." Endocr Rev **31**(4): 447-505.

Yang, L., P. Cheng, C. Chen, H. B. He, G. Q. Xie, H. D. Zhou, H. Xie, X. P. Wu and X. H. Luo (2012). "miR-93/Sp7 function loop mediates osteoblast mineralization." J Bone Miner Res **27**(7): 1598-1606.

Yuan, K., Z. Lian, B. Sun, M. M. Clayton, I. O. Ng and M. A. Feitelson (2012). "Role of miR-148a in hepatitis B associated hepatocellular carcinoma." PLoS One **7**(4): e35331.

Zeng, Y., X. Qu, H. Li, S. Huang, S. Wang, Q. Xu, R. Lin, Q. Han, J. Li and R. C. Zhao (2012). "MicroRNA-100 regulates osteogenic differentiation of human adipose-derived mesenchymal stem cells by targeting BMPR2." FEBS Lett **586**(16): 2375-2381.

Zhang, H., Y. Li, Q. Huang, X. Ren, H. Hu, H. Sheng and M. Lai (2011). "MiR-148a promotes apoptosis by targeting Bcl-2 in colorectal cancer." Cell Death Differ **18**(11): 1702-1710.

Zhang, J., Z. Z. Ying, Z. L. Tang, L. Q. Long and K. Li (2012). "MicroRNA-148a promotes myogenic differentiation by targeting the ROCK1 gene." J Biol Chem **287**(25): 21093-21101.

Zhang, J., H. Zhao, J. Chen, B. Xia, Y. Jin, W. Wei, J. Shen and Y. Huang (2012). "Interferon-beta-induced miR-155 inhibits osteoclast differentiation by targeting SOCS1 and MITF." FEBS Lett **586**(19): 3255-3262.

Zhang, J. F., W. M. Fu, M. L. He, H. Wang, W. M. Wang, S. C. Yu, X. W. Bian, J. Zhou, M. C. Lin, G. Lu, W. S. Poon and H. F. Kung (2011). "MiR-637 maintains the balance between adipocytes and osteoblasts by directly targeting Osterix." Mol Biol Cell **22**(21): 3955-3961.

Zhang, S., Z. Xiao, J. Luo, N. He, J. Mahlios and L. D. Quarles (2009). "Dose-dependent effects of Runx2 on bone development." J Bone Miner Res **24**(11): 1889-1904.

Zhao, W., C. Wu, Y. Dong, Y. Ma, Y. Jin and Y. Ji (2015). "MicroRNA-24 Regulates Osteogenic Differentiation via Targeting T-Cell Factor-1." <u>Int J Mol Sci</u> **16**(5): 11699-11712.

Zheng, G., Y. Xiong, W. Xu, Y. Wang, F. Chen, Z. Wang and Z. Yan (2014). "A two-microRNA signature as a potential biomarker for early gastric cancer." <u>Oncol Lett</u> **7**(3): 679-684.

Zhou, X., F. Zhao, Z. N. Wang, Y. X. Song, H. Chang, Y. Chiang and H. M. Xu (2012). "Altered expression of miR-152 and miR-148a in ovarian cancer is related to cell proliferation." <u>Oncol Rep</u> **27**(2): 447-454.

9   List of figures

10 List of pre-releases

According to § 6 para. 1 sentence 2, parts of this work were written in manuscripts and submitted for review in peer-reviewed journals:

1. Gender-independent miRNA expression profiles in osteoblast and osteoclast cell differentiation as potential cellular biomarkers and targets for osteoporosis diagnosis and therapy;

Kelch S, Sonja F, Marina U, Seeliger C, Vester H, Bauer J, van Griensven M, Rosado Balmyor E   Nature Publishing Group - Scientific reports 2017; 7: 15861. Published online 2017 Nov 20. doi: 10.1038/s41598-017-16113-x

2. miR-100 inhibition regulates early osteogenic genes in osteoblasts of osteoporotic patients: potential application approach

Sarah Kelch, Elizabeth R Balmayor, Claudine Seeliger, Martijn van Griensven

Journal of Tissue Engineering and Regenerative Medicine

3. MiR-148a and its possible protective role in osteoporosis;

Kelch S, Balmayor ER, Seeliger C, Vester H, Bauer J, van Griensven M, Rosado Balmyor E

11 Acknowledgements

It is now time to thank those who have accompanied me in this challenging, but also extremely rewarding phase of my academic career.

I hereby thank Prof. Dr. Peter Biberthaler, head of the Department of Trauma Surgery at the Klinikum rechts der Isar, for giving me the opportunity to perform my research and create this dissertation at his department.

I would like to express my special appreciation and thanks to my advisor Prof. Dr. Dr. Martijn van Griensven, head of the Department of Experimental Trauma Surgery at the Klinikum rechts der Isar, for being a tremendous mentor for me. I would like to thank you for encouraging my research and for allowing me to grow as a research scientist. Your advice on both research as well as on my career have been priceless.

Likewise, I would like to thank PD Dr. Elizabeth Rosado Balmayor, Senior Postdoctoral Researcher of Experimental Trauma Surgery at the Klinikum rechts der Isar, for enabling and supervising my research projects, publications, as well as the compilation of this dissertation. She was a brilliant source of advice and was always open to discuss new ideas.

I thank Dr. Claudine Seeliger for mentoring me and supporting me in the planning and realization of all of my work. Countless times, she lent a helping hand and always had an open ear.

I would like to thank Fritz Seidl and Marina Unger for their selfless dedication to not only mine, but countless research and other projects that would not have been brought to fruition without their constant support.

Special thanks also to the entire working group for the friendly working atmosphere, many valuable suggestions and willingness to help, which have contributed significantly to the success of this work.